Developmental effects of polystyrene nanoparticles in the chicken embryo

Wang, M.

Developmental effects of polystyrene nanoparticles in the chicken embryo

Meiru Wang

王美儒

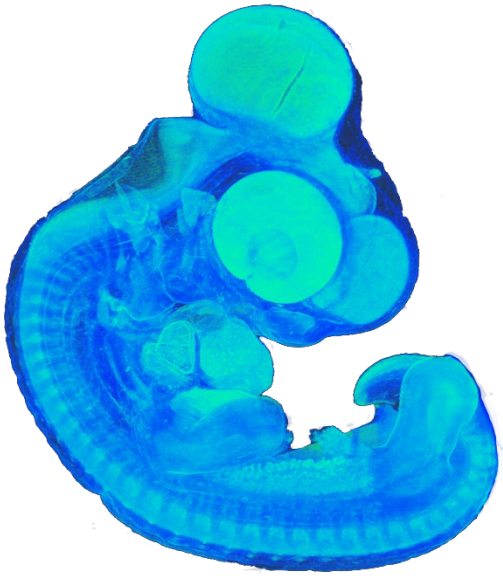

Printing: Ridderprint (www.ridderprint.nl)

Developmental effects of polystyrene nanoparticles in the chicken embryo.

Meiru Wang.

PhD. Thesis, Institute of Biology, University of Leiden, The Netherlands

Layout by Meiru Wang and Ridderprint.

Developmental effects of polystyrene nanoparticles in the chicken embryo

Proefschrift

ter verkrijging van

de graad van doctor aan de Universiteit Leiden,

op gezag van rector magnificus prof.dr.ir. H. Bijl,

volgens besluit van het college voor promoties

te verdedigen op dinsdag 16 januari 2024

klokke 13:45 uur

door

Meiru Wang

geboren te Changchun, China

in 1993

Promotores:

Prof. dr. M. K. Richardson

Prof. dr. M.G. Vijver

Promotiecommissie:

Prof. dr. A.H. Meijer

Prof. dr. M. de Ruiter (LUMC)

Dr. M. Rücklin (Naturalis)

Prof. dr. A. Briegel

Dr. K. Riebel

Prof. dr. N. Wierckx (Forschungszentrum Jülich GmbH)

Table of Contents

Chapter 1. General introduction

Problem statement

A new category of potentially harmful substances is attracting the attention of researchers. These substances are so-called nanomaterials, which are various substances in particulate form, and with a predominant particle size on the nanoscale. One group of nanomaterials are the nanoplastics (NPs). These are either intentionally manufactured for example for use as research reagents; or arise naturally in the environment from the breakdown of plastic waste (Hernandez et al., 2017; Sangkham et al., 2022). The breakdown of plastics first releases particles called microplastics (MPs) which are in the size range ≤ 5 mm (Ray et al., 2022) and these in turn can break down into smaller fragments including NPs.

NPs are widely present in the environment as pollutants in water bodies, soil or the air, and this provides a potential route for wildlife and humans (Sangkham et al., 2022). NPs are being considered as potential drug-delivery agents in the field of nanomedicine (Boehnke et al., 2022). This could open up an additional route through which humans could be exposed. The toxicity of NPs has mainly been studied using aquatic invertebrates and fish model species. In this thesis, I will use a warm-blooded vertebrate model, the chicken embryo, to investigate NP toxicity.

The origins and fate of nanoplastics

Origins of nanoplastics

Nanoplastics are small fragments of plastic — that is, polymer-based materials synthesized from petroleum products (Desai and Galage, 2015; Geyer et al., 2017). Plastics have a broad range of applications in manufacturing, the electronics, packaging and food industries, and in agriculture and medicine and surgery (Gourmelon, 2015). This is because they are durable, cheap, water-resistant, have

relatively low energy requirements for their manufacture, and are relatively light in weight (Gourmelon, 2015; Panda et al., 2010). Moreover, plastics can be significantly altered by heating (Becker and Locascio, 2002; Levine and Berman, 1995), allowing them to be molded into required shapes. Since the 1950s, the annual global growth rate in plastics production has remained at an average of 8.5% (Platt, 2003). By 2018, global plastics production reached 359 million tonnes. According to some predictions, this value will have doubled by 2025 (Gibb, 2019). This thesis is concerned with a particular form of plastics called small plastic particles. In a sense, plastics, and small plastic particles, are typical representative 'fossils' of human activity (Ng et al., 2018), that is to say, they are enduring artefacts in the environment that are **anthropogenic** (uniquely created by human activity).

Classification of small plastic particles

Small plastic particles include microplastics (MPs) whose particle size is ≤ 5 mm (Arthur et al., 2008); and nanoplastics (NPs), whose particle size is either ≤ 100 nm (Zhang and Webster, 2009) or ≤ 1000 nm (Gigault et al., 2018) depending on the opinion of the author.

Other than classifying them by their size, small plastic particles can be classified according to to their origins. Thus, MPs and NPs can be classified as being primary or secondary (Ziajahromi et al., 2017). **Primary** MPs and NPs are small plastic particles manufactured for a specific purpose, in the case of MPs: personal-use products including toothpaste, cosmetic, shampoo (Hernandez et al., 2017); and in the case of NPs as potential drug-delivery vehicles in the emerging field of nanomedicine (Galafassi et al., 2019; Patel et al., 2009). The potential route of administration of NPs to human patients might include intravenous injection or inhalation (Chai et al., 2020).

By contrast, **secondary** MPs and NPs are fragments coming from larger pieces of plastic such as plastic bags, bottles and fishing nets (Boucher and Friot, 2017). They are generated through the natural processes of physical, biological, and chemical

degradation in the environment, for example, the action of UV light, ocean waves, and wind abrasion (Stevens, 2015). Another source of MPs and NPs is the microfibers generated by laundering of synthetic textiles (Center and Wash, 2017), and the accidental discarding of plastic products during manufacturing or transport (Rezania et al., 2018). Surprisingly, even plastic teabags can release nanoplastics (Hernandez et al., 2019).

Some cosmetic products contain both primary and secondary small plastic particles. One study (Hernandez et al., 2017) analyzed commercially-available facial scrubs, and found 'microbeads' of around 200 μm diameter which were ingredients added intentionally by the manufacturer — along with nanoplastic particles of 24 ± 6 to 52 ± 14 nm. It is not clear why nanoplastics were present, because they were not part of the product formulation. It is possible that they arose from the breakdown of the larger microbeads.

Small plastic particles are also distinguished by their composition; for example they may be made of polystyrene (PS), polypropylene, polyethylene, low-density polyethylene, polyacrylates, polyvinylchloride, polyamide, polyethylene terephthalate and polyvinyl alcohol (Anderson et al., 2016; Avio et al., 2017). Finally, MPs and NPs can be categorized according to their shapes which include: beads or spheres, fibers, fragments, film, pellets and foam (Burns and Boxall, 2018).

Plastic waste as a source of small plastic particles

We mentioned above that secondary plastic particles are released from manufactured plastics when they break down (Stevens, 2015; Zhang et al., 2021). For example, at their end of usable life, plastics end up forming a large component of domestic garbage and industrial waste (Subramanian, 2000). The great majority of this plastic waste is dumped into land-fills, while some is burned and a smaller amount is recycled (Geyer et al., 2017). Dumped plastic waste can been found in freshwater bodies, oceans, soil, air, and even in remote, uninhabited islands (Bergmann et al., 2019). For these and other reasons, plastic pollution to our

environment is a matter for great concern (Chauhan and Wani, 2019). Plastic waste can persist for years in the environment due to the low speed at which plastics undergo degradation (Webb et al., 2013). One reason so much plastic is dumped rather than being recycled is that recycling technology is not currently optimal. For example, it is common practice to collect all types of recyclable plastic into one mixed batch, making it difficult to produce a high-quality recycled product (Geyer et al., 2017). Furthermore, plastics can only be recycled twice (Geyer et al., 2017). Because of the size of nanoplastics it is not practical to remove them from water by filtration, nor is not it practical to try to sort them into different plastic types for recycling (Nguyen et al., 2019). In any case, no matter how plastic wastes are disposed, of they can potentially break down and release small plastic particles into the natural environment.

Distribution of MPs and NPs in the environment

After the breakdown of waste plastic, and its release of small plastic particles into the natural environment, MPs and NPs become widely distributed in freshwater bodies, sediments, air and the sea, from the equator to the polar regions (Browne et al., 2011; Wan et al., 2019a). Furthermore, MPs and NPs persist in aquatic system because the waste-water technology to deal with these kinds of materials is lacking. Even though membrane bioreactors have been created by scientists to remove the particles, the high cost of implementation results in feasibility problems for large-scale, public application (Westphalen and Abdelrasoul, 2017). As a result, a large amount of MPs and NPs enter the ecosystem (Browne et al., 2007; Fendall and Sewell, 2009).

Trophic transfer of MPs and NPs

MPs and NPs are transferred between species that are part of food chains (Shruti and Kutralam-Muniasamy, 2019; Vom Sqaal et al., 2008). This is called trophic transfer, and is one of the most important uptake routes of MPs and NPs (Toussaint et al., 2019). MPs and NPs can be taken up by wildlife passively or actively (Vom Sqaal et al.,

2008). For instance, fish can take up MPs and NPs while feeding or drinking (passively), or when foraging by accidental ingestion (actively; (Roch et al., 2020).

Animals tend to accidently ingest plastic items in their food (de Sá et al., 2018). In Gall & Thompson's (2015) report, large pieces of plastic have been found in the digestive tract of 208 species of marine organisms worldwide including 86% (6/7) sea turtle species, 39% (122/312) of seabird species, 0.3% (50/16,754) fish species and 26% (30/115) marine mammals (Gall and Thompson, 2015). Such large pieces of plastic (plastic bottles, plastic bags etc.) can cause adverse effect to wild animals, resulting in starvation and even death (Nkwachukwu et al., 2013). In addition, animals (including sea turtles, seals and sharks) can become entangled in plastic fishing nets and fishing lines and this may impair the movement of the animals, and even cause asphyxia (Butterworth et al., 2012).

MPs and NPs are difficult to detect in terrestrial environments owing to the complex composition of soils. Fortunately, analytical methods for measuring MPs in soils have been developed (He et al., 2018). Large amounts of MPs and NPs have been found in agricultural soils and in industrial regions (Galloway et al., 2017; Zhang and Liu, 2018). The accumulation of MPs and NPs in the soil cause negative effects through altering its biophysical properties (Navarro et al., 2008; Wan et al., 2019b).

Toxicity of small plastic particles to living organisms

MPs and NPs pose a number of health threats to wildlife and humans. For example, once they have entered the natural environment, they can adsorb further toxic chemicals such as polycyclic aromatic hydrocarbons (PAHs) (Maes et al., 2017), polychlorinated biphenyls (PCBs) (Velzeboer et al., 2014) and dichlorodiphenyltrichloroethane (DDT) (Bakir et al., 2014), which can potentiate any intrinsic toxicity they may have (Souza et al., 2022; Ziccardi et al., 2016).

Any of these toxins may later get leached out and released into the environment when the plastic is degraded into particles (Burns and Boxall, 2018; de Souza Machado et al., 2018; Horton et al., 2017; Smith et al., 2018). Adsorption and leaching, respectively, are influenced by internal factors, namely: particle composition, size and shape, and external factors such as temperature, pressure and pH in the environment (Bakir et al., 2014; Frere et al., 2017). In this context, it is important to note that NPs have a very high surface-area-to-volume ratio.

Like all plastics, NPs may contain toxic plasticizers and pigments from manufacture (Unar et al., 2010). Toxic chemicals used in the manufacture of some plastics include nonylphenol, bisphenol A, and vinyl chloride, and these are able to leach from the plastics when they degrade in the environment (Gallo et al., 2018; Koelmans et al., 2014). Also, MPs and NPs can affect the food chain by transferring biocide (pesticide and herbicide) residues in agro-ecosystems (Ng et al., 2018). Other pollutants such as heavy metals and organic chemicals can also be adsorbed to the surface of the MPs and NPs (Zeng, 2018). In summary, MPs and NPs are widely distributed in biotic and abiotic matrices (Karlsson et al., 2017), and can show enhanced toxicity due to physical and chemical changes.

Toxic effects of MPs and NPs in experimental animals

The biological effects of MPs and NPs have been widely studied in aquatic organisms including crustaceans such as *Daphnia* sp. (Brun et al., 2017), and teleost fish such as the zebrafish (*Danio rerio*) (Bashirova et al., 2023), its adults or embryos/larvae (Veneman et al., 2017), reviewed by (Jiang et al., 2020). When MPs or NPs enter into the body of animals, they can accumulate and cause significant effects. These effects may be on **higher levels of the biological hierarchy**, such as changes to the populations, communities and ecosystems of animals (Eerkes-Medrano and Thompson, 2018; Galloway et al., 2017). Pollution by MPs and NPs can affect a community if a an invasive species contaminated by MPs and NPs is introduced; this

can result in alterations to the composition of species in ecosystem (Gall and Thompson, 2015; Lusher, 2015).

Effects of MPs and NPs on **lower levels in the biological hierarchy**, include deleterious effects at the molecular, cellular and organismal levels such as reproductive and development toxicity (Wang et al., 2019; Zhang et al., 2019). Such organismal effects have been seen in the common goby (*Pomatoschistus microps*) (Ferreira et al., 2016), the Pacific mole crab (*Emerita analoga*) (Horn et al., 2020) and the water flea (*Daphnia magna*) (Aljaibachi and Callaghan, 2018). Furthermore, polyethylene MPs accumulated in gill and intestine of the adult zebrafish can lead to abnormal behavior and movements, including seizures (Brun et al., 2019; Mak et al., 2019). More seriously, it has been reported that 40 nm and 200 nm polystyrene NPs can increase the risk of cardiovascular disease by disrupting the cellular components and extracellular matrix in human induced pluripotent cells (Bojic et al., 2020; Prata, 2018).

In the rainbow trout (*Oncorhynchus mykiss*), PS-Pd NPs (Palladium-doped polystyrene nanoplastics) can adhere to the gut epithelium, and can be taken up into the liver, kidney, gills and muscles (Clark et al., 2023). In another study it was found that NPs of 51 nm can be transferred into the gallbladder, liver, pancreas, heart and brain of zebrafish larvae (Pitt et al., 2018). Moreover, it has been found that MPs and NPs can cause inflammation in the liver, heart, lungs, kidney and brain in the Medaka fish (*Oryszia latipes*) (Kashiwada, 2006).

It is not clear whether they then enter the blood stream or the lymphatic system, both of which drain the gut. It is possible that MPs and NPs might be cleared from the circulation by the spleen, and some might be secreted in the urine reviewed by (Bouwmeester et al., 2015; Li et al., 2022; Zhu et al., 2022). Zhu *et al.* (2020) also found that MPs of 10 µm diameter accumulated in the gills and gut of the medaka (*Oryzias latipes*) (Zhu et al., 2020). The distribution of the NPs *in vivo* appeared to be influenced the size of the NPs. Thus, when zebrafish were exposed to 70 nm, 5 µm,

and 20 µm diameter polystyrene particles, the 5 µm particles could be found in the gills, gut, and liver whereas the 70 nm and 20 µm particles were not taken up (Lu et al., 2016). In this kind of study, it is important to realize that, with increased particle size, the number of particles decreases, for any given concentration of the plastic in the carrier vehicle (Wang et al., 2023).

A recent study in zebrafish larvae suggests that fluorescein-tagged 20 nm polystyrene NPs are able to cross the blood-brain barrier, and are subsequently accumulated in the brain itself, of the zebrafish larvae (Sökmen et al., 2020). The blood-brain barrier appears to develop in the normal zebrafish sometime between 2- and 10-days post fertilization, depending on the molecular size of the marker studied (Quiñonez-Silvero et al., 2020). The uptake, accumulation and transportation of MPs and NPs can have deleterious effects on the immune system, nervous system, and on metabolism in mammals (reviewed by (Yong et al., 2020). Another zebrafish study found that 5 µm polystyrene particles can induce inflammation and oxidative stress in the gut and changes in the metabolome and microbiome of the gut (Qiao et al., 2019).

Potential risks of MPs and NPs to humans

Relatively little has been published about the biological effects of small plastic particles on humans, not least because of the ethical difficulties in doing research on human subjects. Among their possible toxic effects on humans, are those affecting the embryo or fetus (reviewed by (Hougaard et al., 2015). Little is known about the possibility of placental transfer in any mammalian species, but one study used the BeWo cell line (which is used to model placental cells), and found that they could take up 50 nm polystyrene NPs (Dusza et al., 2022).

In addition, Ragusa *et al.* (2021) found a few fragments of MPs in human placentas including on the maternal side, the fetal side and in the chorioamniotic membrane (Ragusa et al., 2021). As a result, it has been speculated that MPs and NPs might be able to cause decreased birth weight, autoimmune lung disease, and a series of central nervous system abnormalities (Bates, 2019). Another recent study using the

perfused human placenta found that the NPs affect the gene expression related to inflammation and iron homeostasis (Chortarea et al., 2023).

MPs and NPs potentially cause effects on humans *via* various other exposure routes (Galloway, 2015; Powell et al., 2007). For example, MPs and NPs can be transferred to humans from food species (Chang et al., 2020). Thus, they have been widely found in fish, shellfish and shrimps (Garrido Gamarro et al., 2020; Li et al., 2015; Smith et al., 2018); in honey, salt and sugar (Liebezeit and Liebezeit, 2013; Yang et al., 2015); and in food and beverage packages such as teabags and soup cups (Du et al., 2020; Hernandez et al., 2019). Cox *et al.* revealed that people eat at least 50,000 MPs particles per year on average (Cox et al., 2019). Hence, there is at least the potential for humans to suffer harmful effects from exposure to MPs and NPs.

Even though the skin functions as a biological barrier, it is still another potential route of human exposure (Prata *et al.*, 2020) because MPs and NPs are commonly contained in personal products such as sun cream, toothpaste and shower gel (Sharma & Chatterjee, 2017) in many countries (except the EU, Canada and USA, where personal care products containing such plastic 'microbeads' are banned (Hernandez et al., 2017). It has been shown that other classes of nanomaterials, namely the so-called 'quantum dot' nanoparticles, can penetrate the skin of mice (Mortensen et al., 2008). There is evidence that 40 nm polystyrene NPs can enter through hair follicles in human skin (Vogt et al., 2006). Both 40 nm and 200 nm polystyrene NPs were found to be able to penetrate into mouse skin (Mahe et al., 2009). In addition, poly(l-lactide-co-glycolide) nanoparticles of 70 nm and 300 nm diameter were found to accumulate more, and penetrate deeper, in inflamed skin compared to healthy skin, in mouse and pig models (Try et al., 2016). Moreover, the degree of penetration of NPs into the skin was influenced by their size (Try et al., 2016).

The penetration and accumulation of NPs in skin can, in principle, result in the exposure of epidermal and dermal cells to the NPs. However, the epidermis does not

contain blood vessels or lymphatic vessels (Lund et al., 2016). Therefore, in order for the NPs to spread to other parts of the body, from the skin, they will have to cross the epidermal basement membrane and enter the blood vessels or lymphatic vessels in the dermis. Furthermore, it has been shown that exposure to NPs can lead to oxidative stress in human cerebral and epithelial cells *in vitro* (Schirinzi et al., 2017).

While it is difficult or impossible to perform the necessary experiments in humans with MPs and NPs, we can get insight from other warm-blooded vertebrates such as rats and birds (De Jong et al., 2008; Wang et al., 2023). We can also get indirect evidence about plastic nanoparticles from experiments with metal or other sorts of nanoparticles (De Jong et al., 2008; Yan et al., 2020; Yan et al., 2021), although great care should be used in extrapolating from one nanomaterial to the other. In summary, there is growing evidence that MPs and NPs might be a potential threat to human health.

The potential advantages of using chicken embryos in nanoplastic toxicity research

The aim of this thesis was to use a model closer to humans than the fish and invertebrates that have often been used for testing the toxicity of MPs and NPs. This model is the embryo of the chicken (*Gallus gallus*). Birds are warm-blooded, 'higher' vertebrates with a physiology quite similar to humans (Pozio, 2005). Birds share a most recent common ancestor with humans that lived approxinately 319 million years ago (Pardo et al., 2020; Rezania et al., 2018; Sánchez-Villagra, 2012; St John et al., 2012). By contrast, the most recent common ancestor of humans and the zebrafish (*Danio rerio*) lived 450 million years ago (Hedges and Kumar, 2009). Furthermore, the chicken embryo can be directly exposed experimentally to NPs *in ovo*, and then the egg returned to the incubator (Tickle, 1993). Such experiments are

not possible to perform in mammalian model species because of the placental barrier.

Other reasons for using the chicken embryo (often called the chick embryo) are that there is a genome sequenced and the chicken embryo has been for decades an important model in developmental and toxicology studies (Bryda, 2013; Davey and Tickle, 2007; Hamburger and Hamilton, 1951; Korhonen et al., 1982; Rashidi and Sottile, 2009; Romanoff, 1960). Another argument in favor of using the chick embryo model is that the chicken is a bird, and there is a need to understand the effects of pollutants on wild birds, as shown by Rachel Carson in *Silent Spring* (Carson, 1962).

Before hatching, the chicken embryo is not subject to the European Laws on animal welfare licensing (European Union (EU) directive no. 2010/63/EU). At Leiden University, we have chosen to use the embryos no further than day 14, which is ⅔ of the incubation period. Additionally, the chicken embryo is a relatively cost-effective model, and at the time of writing, in our laboratory, we buy fertilized chicken eggs costing approximately €1.00 each (including transport costs) from a commercial hatchery.

A standard series of embryonic stages has been described for the chicken (Hamburger and Hamilton, 1951) from laying to hatching (21 d). These stages allow for the standardization of research between laboratories. Duman *et al.* found that the chicken embryo model can be used to mimic human tissues and can be considered as a platform for the study of teratogen-induced malformations (Duman et al., 2019). For example, exposure of the human embryo to valproic acid (a teratogenic drug used to treat epilepsy) can harm the developing embryo, producing fetal valproate syndrome (Ornoy, 2009). The same exposure has also been shown to be teratogenic in chicken embryos, producing a pattern of defects similar to those in humans (Nanau and Neuman, 2013; Tanoshima et al., 2015). Thus, the chicken embryo is likely to act as a practical model with relevance to humans.

The chicken embryo model has been used for examining the effects of nanomaterials in a small number of studies (reviewed by (Ghimire et al., 2022). These include studies of nanoparticles made out of polystyrene (Nie et al., 2021; Wang et al., 2023), zinc oxide (Yan et al., 2020; Yan et al., 2021), titanium oxide (Patel et al., 2018), carbon (Kurantowicz et al., 2017; Samak et al., 2020), gold (Zielinska et al., 2011), platinum (Prasek et al., 2013), silver (Grodzik and Sawosz, 2006), magnetic iron oxide (Patel et al., 2019). We do not claim that the chicken embryo is a model for environmental exposure, nor do we make any claims about the uptake of particles into the bird egg in the field. We are simply using it as a convenient experimental model to unravel the cellular and molecular effects of nanoplastics in a warm-blooded, higher vertebrate model.

Outline of this thesis

The main objective of this thesis is to explore the developmental toxicity of nanoplastics and the underlying mechanisms of that toxicity. Another objective is to determine whether the chicken embryo a good model for ecotoxicology. My specific research questions are these:

- Do MPs and NPs cause developmental toxicity in chicken embryos?
- If so, what are the cellular and molecular mechanisms underlying the toxic effects?

I use a multi-technique approach in this doctoral work to: (i) unravel the effects of surface embryonic exposure to different concentration of 25 nm nanoplastics in the stage 8 chicken embryo using experimental embryological techniques; (ii) explore the teratogenic effects induced by nanoplastics in the chicken embryo using MicroCT and synchrotron x-ray tomography; (iii) determine the cellular and molecular mechanisms of toxicity of nanoplastics exposure by *in situ* hybridization in the chicken embryo.

In **Chapter 1**, I review the relevant research literature relating to nanoplastics, their origins and harmful effects, including their potential (but poorly understood) risks to humans. I also explore the literature justifying the my use of the chicken embryo as a model for this research.

In **Chapter 2**, I describe the research in which I exposed chick embryos to nanoplastics and looked at their dose-dependent and size-dependent developmental toxicity (and teratogenicity). I found that the the nanoplastics have a dose-dependent harmful effect on the neural tube, eye, tail and other organs. I could not make any conclusions about the possible size-depency of these effects because of confounding variables (surface area, number of particles) which also change with particle size.

Chapter 3 consists of a detailed analysis of the effects of polystyrene nanoparticles (PS-NPs) on the cardiovascular system of the chicken embryo. Using synchrotron scanning, I showed that 25 nm PS-NPs cause ventricular septal defects and abnormal numbers of aortic arches. Video recordings of live, exposed chicken embryos showed that PS-NPs caused bradycardia. Gene expression studies and immunochemistry showed that malformations in the cardiovascular system might be understood in terms of abnormal migration of the cardiac neural crest.

In **Chapter 4**, I conducted transcriptional profiling of neural crest marker-genes in early chick embryos. I found that exposure of chick embryos to 25 nm PS-NPs caused disrupted migration of the trunk and cranial neural crest. Using fluorescein-tagged PS-NPs I showed that the nanoparticles co-localised to the neural crest (dorsal midline of the neural tube). TUNEL staining showed that exposure to PS-NPs caused a wave of cell death in the dorsal cells of the embryo.

Chapter 5 presents a summary, discussion and perspective of my research. I conclude that PS-NPs pose a potential health risk because they bind to, and disrupt the development of, neural crest cells. I argue that more work is needed to understand the mechanism underlying these effects, and to map the biodistribution of PS-NPs in the body of animals and humans.

References

Aljaibachi, R. and Callaghan, A. (2018). Impact of Polystyrene Microplastics on *Daphnia Magna* Mortality and Reproduction in Relation to Food Availability. *PeerJ* **6**, e4601-e4601.

Anderson, J. C., Park, B. J. and Palace, V. P. (2016). Microplastics in Aquatic Environments: Implications for Canadian Ecosystems. *Environmental Pollution* **218**, 269-280.

Arthur, C., Baker, J. and Bamford, H. (2008). International Research Workshop on the Occurrence, Effects, and Fate of Microplastic Marine Debris. In *Conference Proceedings. Sept*, pp. 9-11.

Avio, C. G., Gorbi, S. and Regoli, F. (2017). Plastics and Microplastics in the Oceans: From Emerging Pollutants to Emerged Threat. *Marine Environmental Research* **128**, 2-11.

Bakir, A., Rowland, S. J. and Thompson, R. C. (2014). Enhanced Desorption of Persistent Organic Pollutants from Microplastics under Simulated Physiological Conditions. *Environmental Pollution* **185**, 16-23.

Bashirova, N., Poppitz, D., Klüver, N., Scholz, S., Matysik, J. and Alia, A. (2023). A Mechanistic Understanding of the Effects of Polyethylene Terephthalate Nanoplastics in the Zebrafish (*Danio Rerio*) Embryo. *Scientific Reports* **13**, 1891.

Bates, A. (2019). *Transforming Plastic: From Pollution to Evolution*: GroundSwell Books.

Becker, H. and Locascio, L. E. (2002). Polymer Microfluidic Devices. *Talanta* **56**, 267-287.

Bergmann, M., Mützel, S., Primpke, S., Tekman, M. B., Trachsel, J. and Gerdts, G. (2019). White and Wonderful? Microplastics Prevail in Snow from the Alps to the Arctic. *Science Advances* **5**, eaax1157-eaax1157.

Boehnke, N., Straehla, J. P., Safford, H. C., Kocak, M., Rees, M. G., Ronan, M., Rosenberg, D., Adelmann, C. H., Chivukula, R. R., Nabar, N., et al. (2022). Massively Parallel Pooled Screening Reveals Genomic Determinants of Nanoparticle Delivery. *Science* **377**, eabm5551.

Bojic, S., Falco, M. M., Stojkovic, P., Ljujic, B., Gazdic Jankovic, M., Armstrong, L., Markovic, N., Dopazo, J., Lako, M., Bauer, R., et al. (2020). Platform to Study Intracellular Polystyrene Nanoplastic Pollution and Clinical Outcomes. *Stem Cells* **38**, 1321-1325.

Boucher, J. and Friot, D. (2017). *Primary Microplastics in the Oceans: A Global Evaluation of Sources*: IUCN Gland, Switzerland.

Bouwmeester, H., Hollman, P. C. H. and Peters, R. J. B. (2015). Potential Health Impact of Environmentally Released Micro-and Nanoplastics in the Human Food Production Chain: Experiences from Nanotoxicology. *Environmental Science & Technology* **49**, 8932-8947.

Browne, M. A., Crump, P., Niven, S. J., Teuten, E., Tonkin, A., Galloway, T. and Thompson, R. (2011). Accumulation of Microplastic on Shorelines Woldwide: Sources and Sinks. *Environmental Science & Technology* **45**, 9175-9179.

Browne, M. A., Galloway, T. and Thompson, R. (2007). Microplastic—an Emerging Contaminant of Potential Concern? *Integrated Environmental Assessment and Management: An International Journal* **3**, 559-561.

Brun, N. R., Beenakker, M. M. T., Hunting, E. R., Ebert, D. and Vijver, M. G. (2017). Brood Pouch-Mediated Polystyrene Nanoparticle Uptake During Daphnia Magna Embryogenesis. *Nanotoxicology* **11**, 1059-1069.

Brun, N. R., van Hage, P., Hunting, E. R., Haramis, A. G., Vink, S. C., Vijver, M. G., Schaaf, M. J. M. and Tudorache, C. (2019). Polystyrene Nanoplastics Disrupt Glucose Metabolism and Cortisol Levels with a Possible Link to Behavioural Changes in Larval Zebrafish. *Commun Biol* **2**, 382.

Bryda, E. C. (2013). The Mighty Mouse: The Impact of Rodents on Advances in Biomedical Research. *Missouri Medicine* **110**, 207-207.

Burns, E. E. and Boxall, A. B. A. (2018). Microplastics in the Aquatic Environment: Evidence for or against Adverse Impacts and Major Knowledge Gaps. *Environmental Toxicology and Chemistry* **37**, 2776-2796.

Butterworth, A., Clegg, I. and Bass, C. (2012). Marine Debris: A Global Picture of the Impact on Animal Welfare and of Animal-Focused Solutions. *WSPA International* **222**.

Carson, R. (1962). *Silent Spring Iii*. New Yorker **23**.

Center, L. T. and Wash, O. C. (2017). Microfiber Release from Clothes after Washing: Hard Facts, Figures and Promising Solutions.

Chai, G., Hassan, A., Meng, T., Lou, L., Ma, J., Simmers, R., Zhou, L., Rubin, B. K., Zhou, Q. T., Longest, P. W., et al. (2020). Dry Powder Aerosol Containing Muco-Inert Particles for Excipient Enhanced Growth Pulmonary Drug Delivery. *Nanomedicine* **29**, 102262.

Chang, X., Xue, Y., Li, J., Zou, L. and Tang, M. (2020). Potential Health Impact of Environmental Micro-and Nanoplastics Pollution. *Journal of Applied Toxicology* **40**, 4-15.

Chauhan, G. S. and Wani, S. (2019). Plastic Pollution: A Major Environmental Threat. *Int. J. Innov. Res. Technol* **6**, 43-46.

Chortarea, S., Gupta, G., Saarimäki, L. A., Netkueakul, W., Manser, P., Aengenheister, L., Wichser, A., Fortino, V., Wick, P., Greco, D., et al. (2023). Transcriptomic Profiling Reveals Differential Cellular Response to Copper Oxide Nanoparticles and Polystyrene Nanoplastics in Perfused Human Placenta. *Environment International* **177**, 108015.

Clark, N. J., Khan, F. R., Crowther, C., Mitrano, D. M. and Thompson, R. C. (2023). Uptake, Distribution and Elimination of Palladium-Doped Polystyrene Nanoplastics in Rainbow Trout (Oncorhynchus Mykiss) Following Dietary Exposure. *Science of The Total Environment* **854**, 158765.

Cox, K. D., Covernton, G. A., Davies, H. L., Dower, J. F., Juanes, F. and Dudas, S. E. (2019). Human Consumption of Microplastics. *Environmental Science & Technology* **53**, 7068-7074.

Davey, M. G. and Tickle, C. (2007). The Chicken as a Model for Embryonic Development. *Cytogenetic and Genome Research* **117**, 231-239.

De Jong, W. H., Hagens, W. I., Krystek, P., Burger, M. C., Sips, A. J. and Geertsma, R. E. (2008). Particle Size-Dependent Organ Distribution of Gold Nanoparticles after Intravenous Administration. *Biomaterials* **29**, 1912-1919.

de Sá, L. C., Oliveira, M., Ribeiro, F., Rocha, T. L. and Futter, M. N. (2018). Studies of the Effects of Microplastics on Aquatic Organisms: What Do We Know and Where Should We Focus Our Efforts in the Future? *Science of The Total environment* **645**, 1029-1039.

de Souza Machado, A. A., Kloas, W., Zarfl, C., Hempel, S. and Rillig, M. C. (2018). Microplastics as an Emerging Threat to Terrestrial Ecosystems. *Global Change Biology* **24**, 1405-1416.

Desai, S. B. and Galage, C. K. (2015). Production and Analysis of Pyrolysis Oil from Waste Plastic in Kolhapur City. *International Journal of Engineering Research and General Science* **3**, 590-595.

Du, F., Cai, H., Zhang, Q., Chen, Q. and Shi, H. (2020). Microplastics in Take-out Food Containers. *Journal of Hazardous Materials*, 122969-122969.

Duman, R., Ertekin, T., Duman, R., Aslan, E., Sabaner, M. C. and Cetinkaya, E. (2019). The Novel Model: Experimental Optical Coherence Tomography-Guided Anterior Segment Imaging Chick Embryo Model. *Indian J Ophthalmol* **67**, 54-58.

Dusza, H. M., Katrukha, E. A., Nijmeijer, S. M., Akhmanova, A., Vethaak, A. D., Walker, D. I. and Legler, J. (2022). Uptake, Transport, and Toxicity of Pristine and Weathered Micro-and Nanoplastics in Human Placenta Cells. *Environmental Health Perspectives* **130**, 097006.

Eerkes-Medrano, D. and Thompson, R. (2018). Occurrence, Fate, and Effect of Microplastics in Freshwater Systems. In *Microplastic Contamination in Aquatic Environments*, pp. 95-132: Elsevier.

Fendall, L. S. and Sewell, M. A. (2009). Contributing to Marine Pollution by Washing Your Face: Microplastics in Facial Cleansers. *Marine Pollution Bulletin* **58**, 1225-1228.

Ferreira, P., Fonte, E., Soares, M. E., Carvalho, F. and Guilhermino, L. (2016). Effects of Multi-Stressors on Juveniles of the Marine Fish Pomatoschistus Microps: Gold Nanoparticles, Microplastics and Temperature. *Aquatic Toxicology* **170**, 89-103.

Frere, L., Paul-Pont, I., Rinnert, E., Petton, S., Jaffré, J., Bihannic, I., Soudant, P., Lambert, C. and Huvet, A. (2017). Influence of Environmental and Anthropogenic Factors on the Composition, Concentration and Spatial Distribution of Microplastics: A Case Study of the Bay of Brest (Brittany, France). *Environmental Pollution* **225**, 211-222.

Galafassi, S., Nizzetto, L. and Volta, P. (2019). Plastic Sources: A Survey across Scientific and Grey Literature for Their Inventory and Relative Contribution to Microplastics Pollution in Natural Environments, with an Emphasis on Surface Water. *Sci. Total Environ* **693**, 133499-133499.

Gall, S. C. and Thompson, R. C. (2015). The Impact of Debris on Marine Life. *Marine Pollution Bulletin* **92**, 170-179.

Gallo, F., Fossi, C., Weber, R., Santillo, D., Sousa, J., Ingram, I., Nadal, A. and Romano, D. (2018). Marine Litter Plastics and Microplastics and Their Toxic Chemicals Components: The Need for Urgent Preventive Measures. *Environmental Sciences Europe* **30**, 13-13.

Galloway, T. S. (2015). *Micro-and Nano-Plastics and Human Health*. pp. 343-366: Springer, Cham.

Galloway, T. S., Cole, M. and Lewis, C. (2017). Interactions of Microplastic Debris Throughout the Marine Ecosystem. *Nature Ecology & Evolution* **1**, 1-8.

Garrido Gamarro, E., Ryder, J., Elvevoll, E. O. and Olsen, R. L. (2020). Microplastics in Fish and Shellfish–a Threat to Seafood Safety? *Journal of Aquatic Food Product Technology* **29**, 417-425.

Geyer, R., Jambeck, J. R. and Law, K. L. (2017). Production, Use, and Fate of All Plastics Ever Made. *Sci Adv* **3**, e1700782.

Ghimire, S., Zhang, X., Zhang, J. and Wu, C. (2022). Use of Chicken Embryo Model in Toxicity Studies of Endocrine-Disrupting Chemicals and Nanoparticles. *Chemical Research in Toxicology* **35**, 550-568.

Gibb, B. C. (2019). Plastics Are Forever. *Nat Chem* **11**, 394-395.

Gigault, J., Ter Halle, A., Baudrimont, M., Pascal, P.-Y., Gauffre, F., Phi, T.-L., El Hadri, H., Grassl, B. and Reynaud, S. (2018). Current Opinion: What Is a Nanoplastic? *Environmental Pollution* **235**, 1030-1034.

Gourmelon, G. (2015). Global Plastic Production Rises, Recycling Lags. *Vital Signs* **22**, 91-95.

Grodzik, M. and Sawosz, E. (2006). The Influence of Silver Nanoparticles on Chick Embryo Development and Bursa of Fabricius Morphology. *Journal of Animal and Feed Sciences* **15**, 111.

Hamburger, V. and Hamilton, H. L. (1951). A Series of Normal Stages in the Development of the Chick Embryo. *J Morphol* **88**, 49-92.

He, D., Luo, Y., Lu, S., Liu, M., Song, Y. and Lei, L. (2018). Microplastics in Soils: Analytical Methods, Pollution Characteristics and Ecological Risks. *TrAC Trends in Analytical Chemistry* **109**, 163-172.

Hedges, S. B. and Kumar, S. (2009). *The Timetree of Life*: OUP Oxford.

Hernandez, L. M., Xu, E. G., Larsson, H. C. E., Tahara, R., Maisuria, V. B. and Tufenkji, N. (2019). Plastic Teabags Release Billions of Microparticles and Nanoparticles into Tea. *Environmental Science & Technology* **53**, 12300-12310.

Hernandez, L. M., Yousefi, N. and Tufenkji, N. (2017). Are There Nanoplastics in Your Personal Care Products? *Environmental Science & Technology Letters* **4**, 280-285.

Horn, D. A., Granek, E. F. and Steele, C. L. (2020). Effects of Environmentally Relevant Concentrations of Microplastic Fibers on Pacific Mole Crab (Emerita Analoga) Mortality and Reproduction. *Limnology and Oceanography Letters* **5**, 74-83.

Horton, A. A., Walton, A., Spurgeon, D. J., Lahive, E. and Svendsen, C. (2017). Microplastics in Freshwater and Terrestrial Environments: Evaluating the Current Understanding to Identify the Knowledge Gaps and Future Research Priorities. *Science of the Total Environment* **586**, 127-141.

Hougaard, K. S., Campagnolo, L., Chavatte-Palmer, P., Tarrade, A., Rousseau-Ralliard, D., Valentino, S., Park, M. V. D. Z., de Jong, W. H., Wolterink, G. and Piersma, A. H. (2015). A Perspective on the Developmental Toxicity of Inhaled Nanoparticles. *Reproductive Toxicology* **56**, 118-140.

Jiang, B., Kauffman, A. E., Li, L., McFee, W., Cai, B., Weinstein, J., Lead, J. R., Chatterjee, S., Scott, G. I. and Xiao, S. (2020). Health Impacts of Environmental Contamination of Micro-and Nanoplastics: A Review. *Environmental Health and Preventive Medicine* **25**, 1-15.

Karlsson, T. M., Vethaak, A. D., Almroth, B. C., Ariese, F., van Velzen, M., Hassellöv, M. and Leslie, H. A. (2017). Screening for Microplastics in Sediment, Water, Marine Invertebrates and Fish: Method Development and Microplastic Accumulation. *Marine Pollution Bulletin* **122**, 403-408.

Kashiwada, S. (2006). Distribution of Nanoparticles in the See-through Medaka (Oryzias Latipes). *Environmental Health Perspectives* **114**, 1697-1702.

Koelmans, A. A., Besseling, E. and Foekema, E. M. (2014). Leaching of Plastic Additives to Marine Organisms. *Environmental Pollution* **187**, 49-54.

Korhonen, A., Hemminki, K. and Vainio, H. (1982). Application of the Chicken Embryo in Testing for Embryotoxicity: Thiurams. *Scand J Work Environ Health* **8**, 63-69.

Kurantowicz, N., Sawosz, E., Halik, G., Strojny, B., Hotowy, A., Grodzik, M., Piast, R., Pasanphan, W. and Chwalibog, A. (2017). Toxicity Studies of Six Types of Carbon Nanoparticles in a Chicken-Embryo Model. *Int J Nanomedicine* **12**, 2887-2898.

Levine, B. and Berman, W. E. (1995). The Current Status of Expanded Polytetrafluoroethylene (Gore-Tex) in Facial Plastic Surgery. *Ear, Nose & Throat Journal* **74**, 681-684.

Li, J., Chen, C. and Xia, T. (2022). Understanding Nanomaterial–Liver Interactions to Facilitate the Development of Safer Nanoapplications. *Advanced Materials* **34**, 2106456.

Li, J., Yang, D., Li, L., Jabeen, K. and Shi, H. (2015). Microplastics in Commercial Bivalves from China. *Environmental Pollution* **207**, 190-195.

Liebezeit, G. and Liebezeit, E. (2013). Non-Pollen Particulates in Honey and Sugar. *Food Additives & Contaminants: Part A* **30**, 2136-2140.

Lu, Y., Zhang, Y., Deng, Y., Jiang, W., Zhao, Y., Geng, J., Ding, L. and Ren, H. (2016). Uptake and Accumulation of Polystyrene Microplastics in Zebrafish (Danio Rerio) and Toxic Effects in Liver. *Environmental Science & Technology* **50**, 4054-4060.

Lund, A. W., Medler, T. R., Leachman, S. A. and Coussens, L. M. (2016). Lymphatic Vessels, Inflammation, and Immunity in Skin Cancer. *Cancer Discov* **6**, 22-35.

Lusher, A. (2015). Microplastics in the Marine Environment: Distribution, Interactions and Effects, Pp. 245e307.

Maes, T., Jessop, R., Wellner, N., Haupt, K. and Mayes, A. G. (2017). A Rapid-Screening Approach to Detect and Quantify Microplastics Based on Fluorescent Tagging with Nile Red. *Scientific Reports* **7**, 44501-44501.

Mahe, B., Vogt, A., Liard, C., Duffy, D., Abadie, V., Bonduelle, O., Boissonnas, A., Sterry, W., Verrier, B., Blume-Peytavi, U., et al. (2009). Nanoparticle-Based Targeting of Vaccine Compounds to Skin Antigen-Presenting Cells by Hair Follicles and Their Transport in Mice. *Journal of Investigative Dermatology* **129**, 1156-1164.

Mak, C. W., Yeung, K. C.-F. and Chan, K. M. (2019). Acute Toxic Effects of Polyethylene Microplastic on Adult Zebrafish. *Ecotoxicology and Environmental Safety* **182**, 109442-109442.

Mortensen, L. J., Oberdörster, G., Pentland, A. P. and DeLouise, L. A. (2008). In Vivo Skin Penetration of Quantum Dot Nanoparticles in the Murine Model: The Effect of Uvr. *Nano letters* **8**, 2779-2787.

Nanau, R. M. and Neuman, M. G. (2013). Adverse Drug Reactions Induced by Valproic Acid. *Clinical Biochemistry* **46**, 1323-1338.

Navarro, E., Baun, A., Behra, R., Hartmann, N. B., Filser, J., Miao, A.-J., Quigg, A., Santschi, P. H. and Sigg, L. (2008). Environmental Behavior and Ecotoxicity of Engineered Nanoparticles to Algae, Plants, and Fungi. *Ecotoxicology* **17**, 372-386.

Ng, E.-L., Lwanga, E. H., Eldridge, S. M., Johnston, P., Hu, H.-W., Geissen, V. and Chen, D. (2018). An Overview of Microplastic and Nanoplastic Pollution in Agroecosystems. *Science of The Total Environment* **627**, 1377-1388.

Nguyen, B., Claveau-Mallet, D., Hernandez, L. M., Xu, E. G., Farner, J. M. and Tufenkji, N. (2019). Separation and Analysis of Microplastics and Nanoplastics in Complex Environmental Samples. *Accounts of Chemical Research* **52**, 858-866.

Nie, J.-h., Shen, Y., Roshdy, M., Cheng, X., Wang, G. and Yang, X. (2021). Polystyrene Nanoplastics Exposure Caused Defective Neural Tube Morphogenesis through Caveolae-Mediated Endocytosis and Faulty Apoptosis. *Nanotoxicology*, 1-20.

Nkwachukwu, O. I., Chima, C. H., Ikenna, A. O. and Albert, L. (2013). Focus on Potential Environmental Issues on Plastic World Towards a Sustainable Plastic Recycling in Developing Countries. *International Journal of Industrial Chemistry* **4**, 34-34.

Ornoy, A. (2009). Valproic Acid in Pregnancy: How Much Are We Endangering the Embryo and Fetus? *Reproductive Toxicology* **28**, 1-10.

Panda, A. K., Singh, R. K. and Mishra, D. K. (2010). Thermolysis of Waste Plastics to Liquid Fuel: A Suitable Method for Plastic Waste Management and Manufacture of Value Added Products—a World Prospective. *Renewable and Sustainable Energy Reviews* **14**, 233-248.

Pardo, J. D., Lennie, K. and Anderson, J. S. (2020). Can We Reliably Calibrate Deep Nodes in the Tetrapod Tree? Case Studies in Deep Tetrapod Divergences. *Frontiers in Genetics* **11**.

Patel, M. M., Goyal, B. R., Bhadada, S. V., Bhatt, J. S. and Amin, A. F. (2009). Getting into the Brain. *CNS Drugs* **23**, 35-58.

Patel, S., Jana, S., Chetty, R., Thakore, S., Singh, M. and Devkar, R. (2018). Tio2 Nanoparticles Induce Omphalocele in Chicken Embryo by Disrupting Wnt Signaling Pathway. *Scientific Reports* **8**, 4756.

Patel, S., Jana, S., Chetty, R., Thakore, S., Singh, M. and Devkar, R. (2019). Toxicity Evaluation of Magnetic Iron Oxide Nanoparticles Reveals Neuronal Loss in Chicken Embryo. *Drug Chem Toxicol* **42**, 1-8.

Pitt, J. A., Kozal, J. S., Jayasundara, N., Massarsky, A., Trevisan, R., Geitner, N., Wiesner, M., Levin, E. D. and Di Giulio, R. T. (2018). Uptake, Tissue Distribution, and Toxicity of Polystyrene Nanoparticles in Developing Zebrafish (*Danio Rerio*). *Aquatic Toxicology* **194**, 185-194.

Platt, D. K. (2003). *Engineering and High Performance Plastics Market Report: A Rapra Market Report*: iSmithers Rapra Publishing.

Powell, J. J., Thoree, V. and Pele, L. C. (2007). Dietary Microparticles and Their Impact on Tolerance and Immune Responsiveness of the Gastrointestinal Tract. *British Journal of Nutrition* **98**, S59-S63.

Pozio, E. (2005). The Broad Spectrum of *Trichinella* Hosts: From Cold-to Warm-Blooded Animals. *Veterinary Parasitology* **132**, 3-11.

Prasek, M., Sawosz, E., Jaworski, S., Grodzik, M., Ostaszewska, T., Kamaszewski, M., Wierzbicki, M. and Chwalibog, A. (2013). Influence of Nanoparticles of Platinum on Chicken Embryo Development and Brain Morphology. *Nanoscale Res Lett* **8**, 251.

Prata, J. C. (2018). Airborne Microplastics: Consequences to Human Health? *Environmental Pollution* **234**, 115-126.

Qiao, R., Sheng, C., Lu, Y., Zhang, Y., Ren, H. and Lemos, B. (2019). Microplastics Induce Intestinal Inflammation, Oxidative Stress, and Disorders of Metabolome and Microbiome in Zebrafish. *Science of the Total Environment* **662**, 246-253.

Quiñonez-Silvero, C., Hübner, K. and Herzog, W. (2020). Development of the Brain Vasculature and the Blood-Brain Barrier in Zebrafish. *Dev Biol* **457**, 181-190.

Ragusa, A., Svelato, A., Santacroce, C., Catalano, P., Notarstefano, V., Carnevali, O., Papa, F., Rongioletti, M. C. A., Baiocco, F., Draghi, S., et al. (2021). Plasticenta: First Evidence of Microplastics in Human Placenta. *Environ Int* **146**, 106274.

Rashidi, H. and Sottile, V. (2009). The Chick Embryo: Hatching a Model for Contemporary Biomedical Research. *Bioessays* **31**, 459-465.

Ray, S. S., Lee, H. K., Huyen, D. T. T., Chen, S.-S. and Kwon, Y.-N. (2022). Microplastics Waste in Environment: A Perspective on Recycling Issues from Ppe Kits and Face Masks During the Covid-19 Pandemic. *Environmental Technology & Innovation*, 102290.

Rezania, S., Park, J., Din, M. F. M., Taib, S. M., Talaiekhozani, A., Yadav, K. K. and Kamyab, H. (2018). Microplastics Pollution in Different Aquatic Environments and Biota: A Review of Recent Studies. *Marine Pollution Bulletin* **133**, 191-208.

Roch, S., Friedrich, C. and Brinker, A. (2020). Uptake Routes of Microplastics in Fishes: Practical and Theoretical Approaches to Test Existing Theories. *Scientific Reports* **10**, 1-12.

Romanoff, A. L. (1960). *The Avian Embryo : Structural and Functional Development*. New York: Macmillan.

Samak, D. H., El-Sayed, Y. S., Shaheen, H. M., El-Far, A. H., Abd El-Hack, M. E., Noreldin, A. E., El-Naggar, K., Abdelnour, S. A., Saied, E. M., El-Seedi, H. R., et al. (2020). Developmental Toxicity of Carbon Nanoparticles During Embryogenesis in Chicken. *Environ Sci Pollut Res Int* **27**, 19058-19072.

Sánchez-Villagra, M. (2012). *Embryos in Deep Time: The Rock Record of Biological Development*: Univ of California Press.

Sangkham, S., Faikhaw, O., Munkong, N., Sakunkoo, P., Arunlertaree, C., Chavali, M., Mousazadeh, M. and Tiwari, A. (2022). A Review on Microplastics and Nanoplastics in the Environment: Their Occurrence, Exposure Routes, Toxic Studies, and Potential Effects on Human Health. *Marine Pollution Bulletin* **181**, 113832.

Schirinzi, G. F., Pérez-Pomeda, I., Sanchís, J., Rossini, C., Farré, M. and Barceló, D. (2017). Cytotoxic Effects of Commonly Used Nanomaterials and Microplastics on Cerebral and Epithelial Human Cells. *Environmental Research* **159**, 579-587.

Shruti, V. C. and Kutralam-Muniasamy, G. (2019). Bioplastics: Missing Link in the Era of Microplastics. *Science of The Total Environment* **697**, 134139-134139.

Smith, M., Love, D. C., Rochman, C. M. and Neff, R. A. (2018). Microplastics in Seafood and the Implications for Human Health. *Current Environmental Health Reports* **5**, 375-386.

Sökmen, T. Ö., Sulukan, E., Türkoğlu, M., Baran, A., Özkaraca, M. and Ceyhun, S. B. (2020). Polystyrene Nanoplastics (20 Nm) Are Able to Bioaccumulate and Cause Oxidative DNA Damages in the Brain Tissue of Zebrafish Embryo (Danio Rerio). *NeuroToxicology* **77**, 51-59.

Souza, A. M. d., Santos, A. L., Araújo, D. S., Magalhães, R. R. d. B. and Rocha, T. L. (2022). Micro(Nano)Plastics as a Vector of Pharmaceuticals in Aquatic Ecosystem: Historical Review and Future Trends. *Journal of Hazardous Materials Advances* **6**, 100068.

St John, J. A., Braun, E. L., Isberg, S. R., Miles, L. G., Chong, A. Y., Gongora, J., Dalzell, P., Moran, C., Bed'Hom, B., Abzhanov, A., et al. (2012). Sequencing Three Crocodilian Genomes to Illuminate the Evolution of Archosaurs and Amniotes. *Genome Biology* **13**, 415.

Stevens, A. P. (2015). Tiny Plastic, Big Problem. *Science News for Students*.

Subramanian, P. M. (2000). Plastics Recycling and Waste Management in the Us. *Resources, Conservation and Recycling* **28**, 253-263.

Tanoshima, M., Kobayashi, T., Tanoshima, R., Beyene, J., Koren, G. and Ito, S. (2015). Risks of Congenital Malformations in Offspring Exposed to Valproic Acid in Utero: A Systematic Review and Cumulative Meta-Analysis. *Clinical Pharmacology & Therapeutics* **98**, 417-441.

Tickle, C. (1993). Chick Limb Buds. In *Essential Developmental Biology: A Practical Approach*, pp. 119-125: IRL Press at Oxford University Press.

Toussaint, B., Raffael, B., Angers-Loustau, A., Gilliland, D., Kestens, V., Petrillo, M., Rio-Echevarria, I. M. and Van den Eede, G. (2019). Review of Micro-and Nanoplastic Contamination in the Food Chain. *Food Additives & Contaminants: Part A* **36**, 639-673.

Try, C., Moulari, B., Béduneau, A., Fantini, O., Pin, D., Pellequer, Y. and Lamprecht, A. (2016). Size Dependent Skin Penetration of Nanoparticles in Murine and Porcine Dermatitis Models. *European Journal of Pharmaceutics and Biopharmaceutics* **100**, 101-108.

Unar, I. N., Soomro, S. A. and Aziz, S. (2010). Effect of Various Additives on the Physical Properties of Polyvinylchloride Resin. *Pakistan Journal of Analytical & Environmental Chemistry* **11**, 7-7.

Velzeboer, I., Kwadijk, C. and Koelmans, A. A. (2014). Strong Sorption of Pcbs to Nanoplastics, Microplastics, Carbon Nanotubes, and Fullerenes. *Environmental Science & Technology* **48**, 4869-4876.

Veneman, W. J., Spaink, H. P., Brun, N. R., Bosker, T. and Vijver, M. G. (2017). Pathway Analysis of Systemic Transcriptome Responses to Injected Polystyrene Particles in Zebrafish Larvae. *Aquatic Toxicology* **190**, 112-120.

Vogt, A., Combadiere, B., Hadam, S., Stieler, K. M., Lademann, J., Schaefer, H., Autran, B., Sterry, W. and Blume-Peytavi, U. (2006). 40nm, but Not 750 or 1,500nm, Nanoparticles Enter Epidermal Cd1a+ Cells after Transcutaneous Application on Human Skin. *Journal of Investigative Dermatology* **126**, 1316-1322.

Vom Sqaal, F., Parmigiani, S., Palanza, P. L., Everett, L. G. and Ragaini, R. (2008). The Plastic World: Sources, Amounts, Ecological Impacts and Effects on Development Reproduction, Brain and Behavior in Aquatic and Terrestrial Animals and Humans. *Environmental Research (New York, NY: Print)* **108**, 127-184.

Wan, J.-K., Chu, W.-L., Kok, Y.-Y. and Lee, C.-S. (2019a). Distribution of Microplastics and Nanoplastics in Aquatic Ecosystems and Their Impacts on Aquatic Organisms, with Emphasis on Microalgae. *Reviews of Environmental Contamination and Toxicology Volume 246*, 133-158.

Wan, Y., Wu, C., Xue, Q. and Hui, X. (2019b). Effects of Plastic Contamination on Water Evaporation and Desiccation Cracking in Soil. *Science of The Total Environment* **654**, 576-582.

Wang, M., Rücklin, M., Poelmann, R. E., de Mooij, C. L., Fokkema, M., Lamers, G. E. M., de Bakker, M. A. G., Chin, E., Bakos, L. J., Marone, F., et al. (2023). Nanoplastics Causes Extensive Congenital Malformations During Embryonic Development by Passively Targeting Neural Crest Cells. *Environment International* **173**, 107865.

Wang, W., Gao, H., Jin, S., Li, R. and Na, G. (2019). The Ecotoxicological Effects of Microplastics on Aquatic Food Web, from Primary Producer to Human: A Review. *Ecotoxicology and Environmental Safety* **173**, 110-117.

Webb, H. K., Arnott, J., Crawford, R. J. and Ivanova, E. P. (2013). Plastic Degradation and Its Environmental Implications with Special Reference to Poly (Ethylene Terephthalate). *Polymers* **5**, 1-18.

Westphalen, H. and Abdelrasoul, A. (2017). Challenges and Treatment of Microplastics in Water. IntechOpen.

Yan, Y., Wang, G., Huang, J., Zhang, Y., Cheng, X., Chuai, M., Brand-Saberi, B., Chen, G., Jiang, X. and Yang, X. (2020). Zinc Oxide Nanoparticles Exposure-Induced Oxidative Stress Restricts Cranial Neural Crest Development During Chicken Embryogenesis. *Ecotoxicology and Environmental Safety* **194**, 110415.

Yan, Y., Wang, G., Luo, X., Zhang, P., Peng, S., Cheng, X., Wang, M. and Yang, X. (2021). Endoplasmic Reticulum Stress-Related Calcium Imbalance Plays an Important Role on Zinc Oxide Nanoparticles-Induced Failure of Neural Tube Closure During Embryogenesis. *Environment International* **152**, 106495.

Yang, D., Shi, H., Li, L., Li, J., Jabeen, K. and Kolandhasamy, P. (2015). Microplastic Pollution in Table Salts from China. *Environmental Science & Technology* **49**, 13622-13627.

Yong, C. Q. Y., Valiyaveetill, S. and Tang, B. L. (2020). Toxicity of Microplastics and Nanoplastics in Mammalian Systems. *International Journal of Environmental Research and Public Health* **17**, 1509-1509.

Zeng, E. Y. (2018). *Microplastic Contamination in Aquatic Environments: An Emerging Matter of Environmental Urgency*: Elsevier.

Zhang, G. S. and Liu, Y. F. (2018). The Distribution of Microplastics in Soil Aggregate Fractions in Southwestern China. *Science of the Total Environment* **642**, 12-20.

Zhang, K., Hamidian, A. H., Tubić, A., Zhang, Y., Fang, J. K. H., Wu, C. and Lam, P. K. S. (2021). Understanding Plastic Degradation and Microplastic Formation in the Environment: A Review. *Environmental Pollution* **274**, 116554.

Zhang, L. and Webster, T. J. (2009). Nanotechnology and Nanomaterials: Promises for Improved Tissue Regeneration. *Nano Today* **4**, 66-80.

Zhang, S., Wang, J., Liu, X., Qu, F., Wang, X., Wang, X., Li, Y. and Sun, Y. (2019). Microplastics in the Environment: A Review of Analytical Methods, Distribution, and Biological Effects. *TrAC Trends in Analytical Chemistry* **111**, 62-72.

Zhu, G. H., Gray, A. B. C. and Patra, H. K. (2022). Nanomedicine: Controlling Nanoparticle Clearance for Translational Success. *Trends in Pharmacological Sciences* **43**, 709-711.

Zhu, M., Chernick, M., Rittschof, D. and Hinton, D. E. (2020). Chronic Dietary Exposure to Polystyrene Microplastics in Maturing Japanese Medaka (*Oryzias Latipes*). *Aquatic Toxicology* **220**, 105396-105396.

Ziajahromi, S., Neale, P. A., Rintoul, L. and Leusch, F. D. L. (2017). Wastewater Treatment Plants as a Pathway for Microplastics: Development of a New Approach to Sample Wastewater-Based Microplastics. *Water Research* **112**, 93-99.

Ziccardi, L. M., Edgington, A., Hentz, K., Kulacki, K. J. and Driscoll, S. K. (2016). Microplastics as Vectors for Bioaccumulation of Hydrophobic Organic Chemicals in the Marine Environment: A State-of-the-Science Review. *Environmental Toxicology and Chemistry* **35**, 1667-1676.

Zielinska, M., Sawosz, E., Grodzik, M., Wierzbicki, M., Gromadka, M., Hotowy, A., Sawosz, F., Lozicki, A. and Chwalibog, A. (2011). Effect of Heparan Sulfate and Gold Nanoparticles on Muscle Development During Embryogenesis. *Int J Nanomedicine* **6**, 3163-3172.

Chapter 2. Developmental toxicity of nanoplastics in the chicken embryo

Meiru Wang[1,2], Martin Rücklin[2,1], Robert E. Poelmann[1,3], Marjolein Fokkema[4], Gerda E.M. Lamers[1], Martina G. Vijver[5], Michael K. Richardson[1].*

1. Institute of Biology, Leiden University, Sylvius Laboratory, Sylviusweg 72, 2333 BE, Leiden, The Netherlands.
2. Naturalis Biodiversity Center, Darwinweg 2, 2333 CR, Leiden, The Netherlands.
3. Department of Cardiology, Leiden University Medical Center, The Netherlands.
4. Institute of Psychology, Methodology and Statistics, Pieter de la Court Building, Wassenaarseweg 52, 2333 AK, Leiden, The Netherlands.
5. Institute of Environmental Sciences, Leiden University (CML), Van Steenis Building, Einsteinweg 2, 2333 CC, Leiden, The Netherlands.

This chapter has been published as part of: Wang, M., Rücklin, M., Poelmann, R.E., de Mooij, C.L., Fokkema, M., Lamers, G.E.M., de Bakker, M.A.G., Chin, E., Bakos, L.J., Marone, F., Wisse, B.J., de Ruiter, M.C., Cheng, S., Nurhidayat, L., Vijver, M.G., Richardson, M.K. Nanoplastics causes extensive congenital malformations during embryonic development by passively targeting neural crest cells. *Environment International* **173**, 107865. https://doi.org/10.1016/j.envint.2023.107865.

Abstract

Nanoplastics and microplastics are an emerging class of pollutants which are becoming a major source of concern due to their potentially harmful effects on the biosphere. Even though the effects of nanoplastics and microplastics are well-studied in aquatic invertebrates and fish, little is known about their effects on warm-blooded animals. The aim of our research is to determine the effects of nanoplastics on the chicken embryo might model. In this chapter, we exposed stage 8 chicken embryos to 25 nm plain polystyrene nanoplastics (PSNPs). Histology, Alcian blue staining and scanning electronic microscopy were used to visualize the effects on the embryonic phenotype 24 h and 4 d post exposure. We found that 25 nm polystyrene nanoplastics caused dose-dependent mortality and malformations of 4 d post exposure chicken embryos. The highest dose (5 mg/mL) caused malformations in 5/5 embryos, and death in 15/20 embryos at 4 d post exposure. The malformations included neural tube defects, microphthalmia and tail bud hypoplasia. We also observed a significant developmental delay in embryos examined at 24 h post exposure. Together, our findings strongly suggest that PSNPs are toxic to the developing chicken embryo. These results call for an in-depth investigation of cellular and molecular mechanisms of toxicity of nanoplastics in the chicken embryo (Chapter 4).

Introduction

In recent decades, many new pollutants such as microplastics and nanoplastics (MPs and NPs) have been identified (Lim, 2021). Plastics are polymers derived from the petroleum industry. They are one of the important basic five materials of human invention which bring the greatest convenience to people's daily life (Ewen, 1997). They are durable, light, water-proof and relatively cheap compared with other materials. Therefore plastic are widely used in different including medicine, the military and high-tech industries (Abbing, 2019; Rosato and Rosato, 2011). The value of global plastic production reached 568.9 billion dollars in 2019 (Roy et al., 2021). Many plastics directly enter the environment after use by consumers (Lim, 2021). In some countries, where they are not collected and disposed of safely, plastics can become degraded in the natural environment into tiny particles called microplastics and nanoplastics (Godfrey, 2019). MPs are defined as plastic particles or fragments ≤5 mm in diameter. Among microplastics there may be even smaller particles called nanoplastics which are ≤100 nm or ≤ 1 µm (Mitrano et al., 2021). MPs and NPs can arise from the physical degradation of larger plastic items such as supermarket carrier bags, plastic bottles, etc. They are also generated during the manufacture of clothing from synthetic fabrics such as nylon or acrylic (Fuschi et al., 2022).

MPs and NPs have been widely studied in aquatic animals such as the zebrafish (Bhagat et al., 2020) and *Daphnia* (Imhof et al., 2017; Liu et al., 2019). In the zebrafish, for example, the major toxic effects of MPs and/or NPs are developmental toxicity, reproductive toxicity, neurotoxicity, immunotoxicity, genotoxicity, metabolome imbalance, behavior variation and oxidative stress (Reviewed in Ref. (Bhagat et al., 2020)). Furthermore, the type, size and surface charge of the MPs and NPs were found to potentially influence their effects (Kögel et al., 2020). The toxicity of MPs and NPs has also been investigated in *Daphnia* spp. Interestingly, MPs and NPs can be found in the offspring of zebrafish (Pitt et al., 2018) and in generations (F_1 and F_2) of *Daphnia manga* (Martins and Guilhermino, 2018). These findings give rise

to the possibility that MPs and NPs could transfer from adult to newborn. Furthermore, one study showed that MPs were present in human placentas including maternal side, fetal side and in the chorioamniotic membranes (Ragusa et al., 2021). Therefore, it is possible that MPs may be transferred to the embryo or fetus.

Knowledge of the effects of MPs and NPs on developing embryos of warm-blooded animals, including humans, is very limited. The chicken embryo is a commonly used model organism to study embryotoxicity. This is because the chicken embryo is a warm-blooded vertebrate which is more closely related to mammals than are the cold-blooded aquatic species (such as zebrafish and *Daphnia*) that are usually used for testing the toxicity of MPs and NPs (Wilson, 1978). For example, the most recent common ancestor of humans and the chicken lived approxiamtely 319 million years ago (Pardo et al., 2020; Rezania et al., 2018; Sánchez-Villagra, 2012; St John et al., 2012); of humans and the zebrafish 429 Mya; and of humans and *Daphnia*, 708 Mya (Kumar et al., 2017). Furthermore, the chicken embryo is highly sensitive to various chemicals and physical agents meaning that it is a good indicator species for toxicity studies (Hill and Hoffman, 1984). Finally, based on the large amount literature about chicken embryo development, it is an ideal model species (Stark and Ross, 2019). Among the literature are classic text books on chicken developmental anatomy (Lillie, 1952; Romanoff, 1960) developmental atlases (Bellairs and Osmond, 2014) and staging tables (Hamburger and Hamilton, 1951).

There are a few studies of the effects of nanomaterials in general on the chick embryo. For example, zinc nanoparticles cause neural crest defects in the chick embryo (Yan et al., 2020; Yan et al., 2021). Further, using various routes and stages of exposure, it has also been shown that 50 nm and 1 µm polystyrene nanoplastics cause neural tube and craniofacial defects in chicken embryos (Nie et al., 2021). The mechanism of neural tube injury was attributed to caveolae mediated endocytosis (Nie et al., 2021).

In this Chapter, we have investigated the toxicity of MPs and NPs to developing chick embryos. We also examined whether the size and concentration of the plastics particles is a determining factor of toxicity they may cause to the chick embryo. Additionally, we have looked for phenotypic effects of the nanoplastics using standard morphological and histological techniques.

Materials and Methods

Preparation and analysis of the nanoplastics

Plain (non-functionalized) polystyrene nanoplastics (PS-NPs) were purchased from Lab 261 (cat. number PST25, PST100 and PST 500, Palo Alto, U.S.), with nominal diameter of 25 nm, 100 nm, 500 nm (1% solid, 1.05 g/cm^3). As supplied by the manufacturer, the PS-NP suspension was in a vehicle of 0.03% Tween®20 in Milli-Q® water. We specifically requested the manufacture to not add azide.

In size comparison experiments, different sizes of PS-NP suspension including PST25, PST100 and PST500 were diluted with Ringer's solution (pH 7, 2.5 g/L, cat. number 1.15525, Merck Millipore, Germany), which we autoclaved before use. They were diluted two times for a final concentration of 5 mg/mL. In the concentration comparison experiments, PST25 suspension was then diluted with Ringer's solution. The dilution series in Ringer's was as follows: 2, 10, 100, and 1000 × to yield final PS-NP concentrations of 5 mg/mL, 1 mg/mL, 0.1 mg/mL, and 0.01 mg/mL, respectively.

The sterility of the PS-NPs suspensions was tested by streaking on LB agar plates (File S1). PS-NP size, shape and zeta-potential in Milli-Q® water or Ringer's solution were measured by multi angle dynamic light scattering (MADLS; Malvern Panalytical Ltd., Malvern, UK) and TEM (transmission electron microscopy using a JEOL 1400+). The suspensions were sonicated for 10 min before use using a USC200T ultrasonic cleaning bath (VWR, Amsterdam, the Netherlands).

In vivo embryo toxicity

Fertilized eggs of the White Leghorn chicken (*Gallus gallus*) strain were purchased from a commercial supplier (Drost Loosdrecht B.V., the Netherlands). They were incubated for 29 h at 38 °C on stationary shelves in a humidified, forced-draft incubator (Binder, Germany). Under aseptic conditions, the eggs were windowed and staged as described (Hamburger and Hamilton, 1951). Then, 50 µL Ringers' solution was dripped onto the dorsal side of the embryo to moisten the vitelline membrane. Next, a small hole was made in the vitelline membrane using a sharpened tungsten needle (Brady, 1965; Silver, 1960). It was made beyond the head of the embryo, avoiding the embryo itself. Next, 50 µL of either working solutions of PS-NPs or Ringer's solution as a vehicle-only control, was dripped onto the hole using a Gilson P200 Pipetman®. The egg was then sealed with Scotch® prescription label tape 800 (clear) and returned to the incubator for 24 h, 4 d. At 24 h and 4d post exposure, alive embryos were harvested by Student Vanna Spring Scissors (Cat. 91500-09, Fine Science Tool, Germany) and spoons. Meanwhile, its extra tissues were moved out carefully. Finally, embryos were harvested into cold phosphate buffered saline (PBS).

The somites of the chicken embryo at 24 h post exposure were counted and the embryo staged according to Hamburger and Hamilton (Hamburger and Hamilton, 1951). For 4 d post exposure chicken embryos, the embryos were staged (Hamburger and Hamilton, 1951) and any phenotypic abnormalities were noted.

Alcian blue wholemounts

This protocol is as previously described by us (de Bakker et al., 2013). Embryos were fixed with 5% trichloroacetic acid at 4 °C degree overnight. They were then transferred into refresh 70% ethanol for 2 h × 2 followed by acid alcohol (20% glacial acetic acid in 70% ethanol for 2 h). Embryos were then stained in 0.03% (W/V) Alcian blue in acid alcohol overnight. Then they were rinsed with acid alcohol for 2 h followed by dehydration through a graded ethanol series from 70% to 100%. Finally, embryos were cleared and stored in methyl salicylate.

Paraffin histology

We performed routine paraffin histology with haematoxylin and eosin staining according to standard protocols (Bancroft and Gamble, 2008). Embryos were fixed in 4% buffered depolymerized paraformaldehyde (pFA) for 24 h at 4 °C. They were then washed 3x with cold PBS and dehydrated in 70% ethanol overnight. Subsequently, the embryos were dehydrated through a graded ethanol series (80%, 90%, 100%), 1 h each. Embryos were cleared with Neo-Clear® (Merck, Darmstadt), 3x 1h, and embedded in paraffin (Paraclean, KP Klinipath/VWR International, Amsterdam) at 60 °C (1x overnight, 1x 1 h). Sections were cut at 7 µm. Because embryos examined at 24 h post-exposure were delicate and difficult to handle, we used a modified protocol 33. After fixing the embryos, they were embedded in a mixture of 2% agarose (Sigma-Aldrich, Zwijndrecht, A-6013) and 2.5% low melting-point agarose (super fine resolution agarose, Electron Microscopy Sciences, Hatfield, PA) at 42 °C. When the mixture had solidified at room temperature (c. 20 min), the agarose blocks containing the embedded embryos were transferred to 70% ethanol for 2 d. They were then dehydrated in graded ethanols, embedded in paraffin and sectioned. The only modification made to the embedding step was that the tissue blocks were in molten paraffin for no more than 3x 1 h.

MicroCT

This protocol for X-ray microtomography (microCT ; Refs.(Metscher, 2009)) was described previously by us (Yi et al., 2021). In brief, embryos were fixed in 4% pFA in PBS (pH 7.4) at 4 °C for 24 h. They were then rinsed 3x with PBS, 4 °C. After dehydration in a graded ethanol series (25%, 50%, 70%) they were stained with phosphotungstic acid (0.3% in 70% ethanol) for 48 h on a rotary shaker. After staining, embryos were stored in 70% ethanol. For scanning, embryos were immobilized in 1% low melting-point agarose in 1 mL pipette tips and sealed with parafilm. For scan parameters, see Table 2-1. The images were analyzed and manipulated using Avizo software (Version: 8.01; Thermo, Fisher Scientific).

Table 2-1. **MicroCT scan parameters**.

Micro-CT Xradia 520 Verda 3D X-ray microscope (Zeiss)

Embryo code	Treatment (PSNPs mg/mL)	pixel size (μm)	KV/W	exp. time (sec.)	Intensity
1	5 mg/mL	43.468	40/3	1.3	5000-6500
2	Ringer's	62.048	40/3	6	5000-6600
3	5 mg/mL	16.040	40/3	9	5000-6300
4	Ringer's	26.594	50/3	3	5000-8000
5	Ringer's	26.586	50/3	2.5	5500-7000
6	5 mg/mL	17.543	50/4	4	5000-7500

Scanning electron microscopy

The embryos were fixed in 2% glutaraldehyde (GA) and 2% PFA in sodium cacodylate buffer at room temperature for 2 h, followed by 4 °C for 22 h. After fixation, embryos were rinsed 3 × in buffered PBS, and dehydrated through a graded acetone series (25%, 50%, 75% and 100%). Then they were critical-point dried with a BAL-TEC critical point drier 030 (BalTec, Switzerland). Finally, the embryos were sputter-coated with palladium and platinum using a Q 150T S Plus Sputter Coater (Quorum, United Kingdom). The specimens were imaged using a Joel JSM-7600F field emission scanning electron microscope.

Results

Characterization of polystyrene nanoplastic particles

The plain polystyrene nanoplastics (PST25; PS-NPs) were 29.16 ± 0.23 nm in diameter and their zeta potential was 14.65 ± 4.16 mV measured in Ringer's solution. They were spherical in sterile Milli-Q water as confirmed by TEM (Fig. 2-1a). Their size distribution dispersed in Ringer's solution was monitored by MADLS (Fig. 2-1b). The

sterility of the particles, as supplied by the manufacturer was confirmed by a lack of microbial growth after streaking the particles on LB agar (File S1).

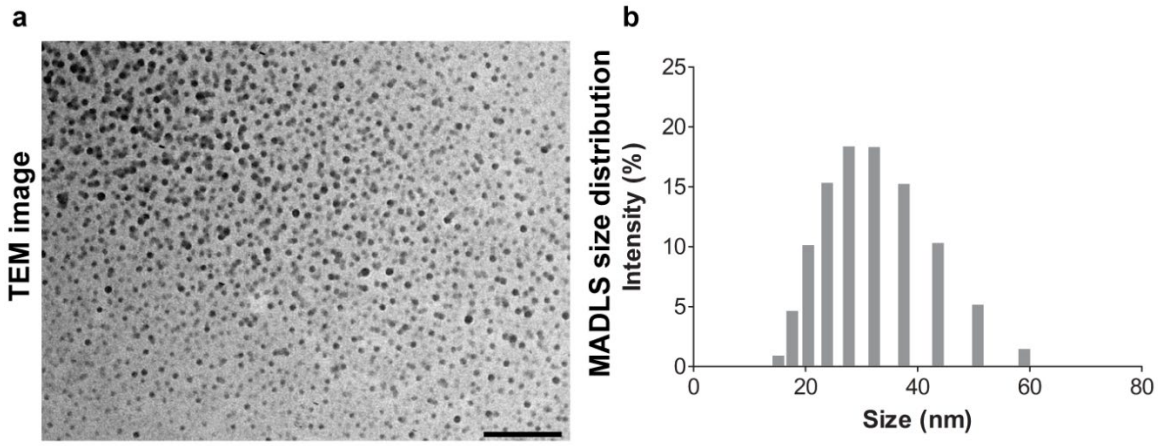

Fig. 2-1. **Characterization of 25 nm plain polystyrene nanoplastics**. (**a**), transmission electron microscopy (TEM) image. (**b**), the size distribution of 5 mg/mL 25 nm plain polystyrene nanoplastics in Ringer's solution measured by multi angle dynamic light scattering (MADLS).

PS-NPs may cause size-dependent mortality and malformations

A preliminary series of experiments was performed with 25, 100 and 500 nm plain PS-NPs. Exposure was at stage 8 and harvesting was at 4 d post-exposure (stages according to Hamburger-Hamilton (Hamburger and Hamilton, 1951)). Our statistical analyses of these data are given in File S2. We found that, using a standard exposure concertation of 5 mg/mL, the 25 nm particles produced the highest percentage of malformed embryos, and the highest mortality (File S2). Analysis suggested that the relative number of particles might provide a more reliable model than the particle size itself. There seemed to be a clear, increasing probability of malformations and mortality if the number of particles increased (File S2). But these outcomes could be a combined effect of particle size and/or the number of particles. In order to reduce the number of variables, we used 25 nm PS-NPs for all subsequent experiments. In all cases, we used plain PS-NPs except in the experiments where fluorescent particles were used to track the location of particles.

Dose-dependent mortality of 25 nm PS-NPs

The dose-response parameters of 25 nm PS-NPs were tested in chicken embryos exposed at stage 8, and examined at 4 d post-exposure. Six chicken embryos were treated for each concentration step and each experiment was repeated three times. Thus, *n* = 18 for each concentration (File S3). The mortality in the control group (Ringer's only) was 27.78 ± 5.55% (Fig. 2-2c). The fact that nearly 30% of embryos in the control group died could be due to the fact that such young embryos (stage 8) are very sensitive to manipulation. The highest concertation group (5 mg/mL) had significantly higher mortality (75 ± 4.81%; $P<0.001$) compared to the control group (Fig. 2-2c; File S3).

Dose-dependent teratogenicity of 25 nm PS-NPs

In controls (Ringer's only), the baseline teratogenicity (incidence of malformations) was 8.33 ± 8.33% (Fig. 2-2d). This baseline level of malformations could reflect the sensitively of young embryos to manipulation *in ovo* or could be due to an ageing flock (Boerjan, 2002; Pawłowska and Sosnówka-Czajka, 2019). All PS-NPs treated embryos showed excess of malformations compared to the control group. For the highest two doses in the series (1 mg/mL and 5 mg/mL) all embryos showed malformations (Fig. 2-2d; File S3).

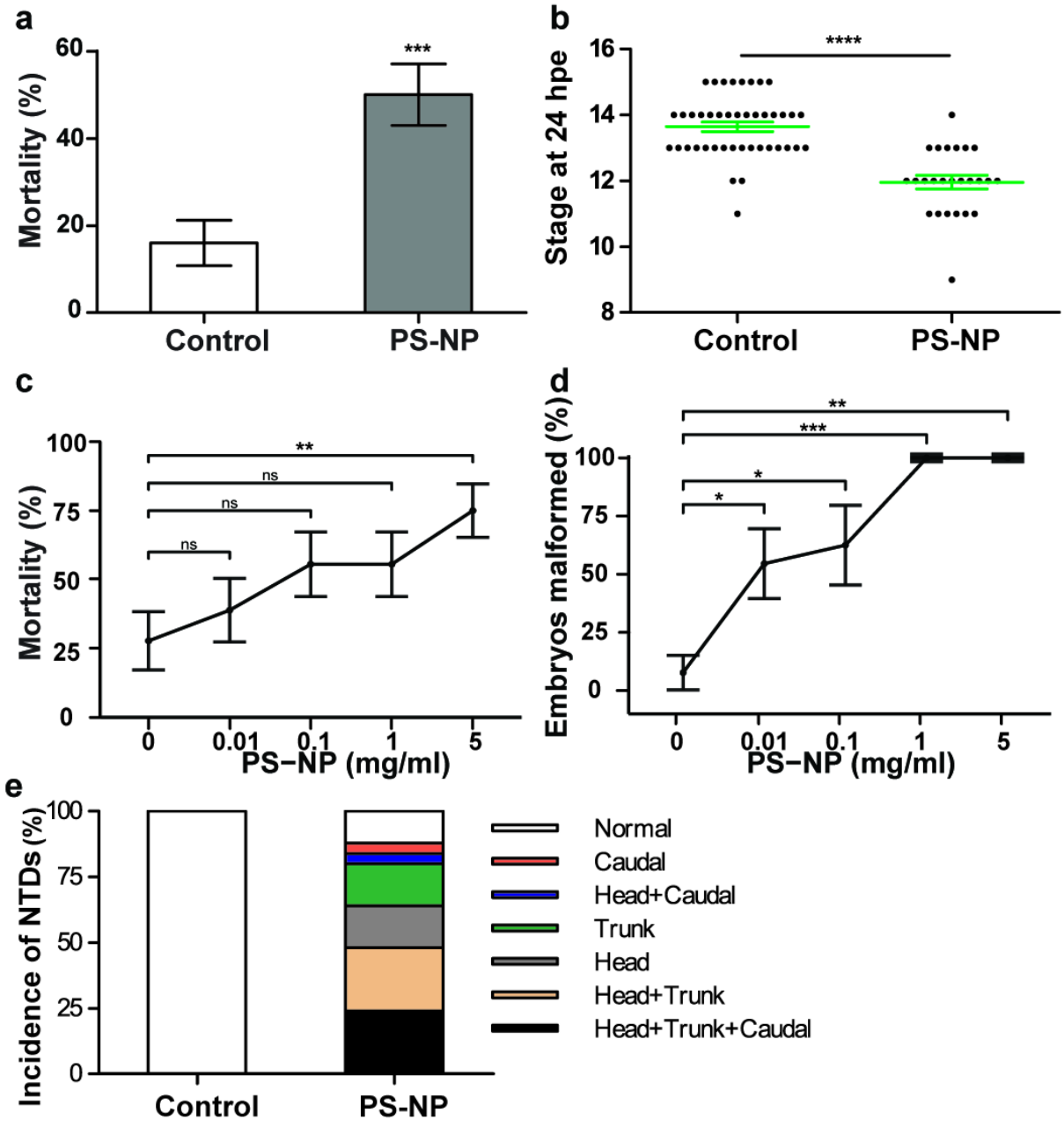

Fig. 2-2. **25 nm PS-NP exposure leads to increased mortality, developmental delay and malformations in chicken embryos.** Embryos were exposed at stage 8. **a**, **b**, 5 mg/mL PS-NP, analysed at 24 h post-exposure. **a**, mortality rate. *n* = 50 (for both control and PS-NPs-treated group) from 5 independent experiments; data are mean ± s.e.m. Chi square test, P = 0.0007. **b**, developmental delay (as expressed in stage; stages according to Ref. (Hamburger and Hamilton, 1951)). *n* = 42 for control and *n* = 25 for PS-NP-treated from 5 independent experiments; data are mean ± s.e.m. Chi square test, P < 0.0001. This delay caused by PS-NPs has also been noted by Nie and colleagues (Nie et al., 2021). **c**, **d**, dose-response series, analysed at 4 d post-exposure. **c**, mortality. *n* = 18 for 0, 0.01, 0.1 and 1 mg/mL group; *n* = 20 for 5 mg/mL group from 3 independent experiments; data are mean ± s.e.m. Chi square test, P = 0.7237 (0 mg/mL vs 0.01 mg/mL), P = 0.1763 (0 mg/mL vs 0.1 mg/mL), P = 0.1763 (0 mg/mL vs 1 mg/mL), P = 0.0097 (0 mg/mL vs 5 mg/mL PS-NPs-treated). **d**, malformation rate (all malformations). *n* = 13 (0 mg/mL), *n* = 11 (0.01 mg/mL), *n* = 8 (0.1 mg/mL), *n* = 8 (1 mg/mL), and *n* = 5 (5 mg/mL) from 3 independent experiments; data are mean ± s.e.m. Chi square test, P = 0.0387 (0 mg/mL vs 0.01 mg/mL), P = 0.0276 (0 mg/mL vs 0.1

mg/mL), P = 0.0002 (0 mg/mL vs 1 mg/mL), and P = 0.0016 (0 mg/mL vs 5 mg/mL). **e**, axial level affected by neural tube defects (per embryo), 5 mg/mL PS-NP concentration 24 h post-exposure. *n* = 42 for control and *n* = 25 for PS-NP-treated from 5 independent experiments. *Key*: NTDs, neural tube defects; hpe, hours post-exposure; PS-NP, polystyrene nanoparticles; significance of difference between control and experimental groups indicated by asterisks as follows: ****, P <0.0001; ***, P <0.001; **P <0.01; *P <0.05; ns for P >0.05.

Neural tube defects, developmental delay and mortality at 24 h post-exposure

We performed a series of experiments in which we recorded the mortality and selected malformations in embryos exposed to 25 nm PS-NPs at stage 8, then examined at 24 h post-exposure. For each experiment there 10 treated (5 mg/mL 25 nm PS-NPs) and 10 controls (Ringer's only). The experiment was repeated three times (*n* = 30, both for the control and treated groups). Our results are shown in Fig. 2-2a-b. The mortality in the treated group was 60 ± 8.16% which was significantly higher (*P* < 0.01) than in the control group (Fig. 2-2a). A significant developmental delay was seen in the surviving, treated embryos (Fig. 2-2b). The delay was based on somite count of the embryos. When we converted the somite count into Hamburger Hamilton stage, the average stage reached was 11.50 ± 1.24 for treated embryos, and 13.67 ± 1.09 for control embryos (Fig. 2-2b; Table S1). In the same experimental series, neural tube defects were never seen in the control embryos (*n* = 24/30; Fig. 2-2e; Movies S1). By contrast, all surviving embryos treated with PS-NPs (*n* = 12/30) showed neural tube defects (failure of the neural tube to close dorsally; Fig. 2-3; Movies S2; Movies S3). The defects were either in the head, trunk or tail, or in a combination of these regions (Fig. 2-2e; Fig. 2-3; Table S1). At the stages examined in this Chapter, the heart has not completed septation; we therefore reserve a detailed analysis of heart malformations for Chapter 3, where we examine older embryos.

Fig. 2-3. **Neural tube defects caused by exposure of chick embryos to 25 nm PS-NPs. a-j**, micro-CT images of control (**a**-**e**) and 25 nm PS-NPs treated embryos (**f**-**j**). *n* = 2 for both groups. **a**, stage 14, volume rendering of wholemount control chick embryo. (**b**-**e**), virtual transverse sections. f, stage 12, volume rendering of wholemount PS-NPs treated embryos. (**g**-**j**), virtual transverse sections. White arrowheads in f-j indicate neural tube abnormalities. (**k**-**u**), wholemount and histological sections of control (**k**-**n**) and 25 nm PS-NPs treated embryos (**o**-**u**). **k**, stage 13, control embryo. **l**-**n**, transverse sections, haematoxylin and eosin stain. o, stage 12, PS-NP-treated embryo. (**p**-**u**), transverse sections, haematoxylin and eosin stain; black arrowheads, neural tube abnormalities; black arrows, clumps of detached. Scale bars, 500 µm in (**a**, **f**, **k**, **o**), 200 µm in (**b**-**e**, **g**-**j**, **l**-**n**, **p**-**u**). *Key*: In figures a, f, k and o, the dashed horizontal lines indicate the plane of the associated transverse sections. PS-NP, polystyrene nanoparticles. Note that the embryos in f and o both have neural tube defects.

Phenotypic analyses of malformations caused by PS-NPs exposure at 4 d post exposure

Phenotypic analyses of embryos at 4 d post-exposure are shown in Fig. 2-4-Fig. 2-7. In all cases, the embryos were exposed to either 0.01 mg/mL, 0.1 mg/mL, 1 mg/mL or 5

mg/mL of 25 nm PS-NPs at stage 8. A consistent feature of our treated embryos was that, no matter how malformed the embryos were, they all had apparently normal limbs (wings and legs). Half of the embryos (*n* = 16/32, Table S2) showed a failure of the normal processes of flexure (dorsoventral bending of the primary axis), and/or torsion (rotation along the primary axis). These failures lead to the embryo being abnormally flat, or straight, or both (Fig. 2-4c-e and f-g). Microphthalmia was present in 8/32 embryos in the form of gross hypoplasia or dysplasia of the optic cup and lens (Fig. 2-4c and d, Fig. 2-5d-f, i and j, Table S2). The microphthalmia was unilateral in three embryos and bilateral in five (Table S2). In some embryos, the caudal neural tube showed gross dysplasia, presenting as an asymmetric mass of disorganized tissue (Fig. 2-6d-i). In other embryos, the caudal neural tube showed gross dysplasia, presenting as an asymmetric mass of disorganized tissue (Fig. 2-7d-f). The tailbud was hypoplastic or absent in 5/32 embryos at 4 dpe (Table S2).

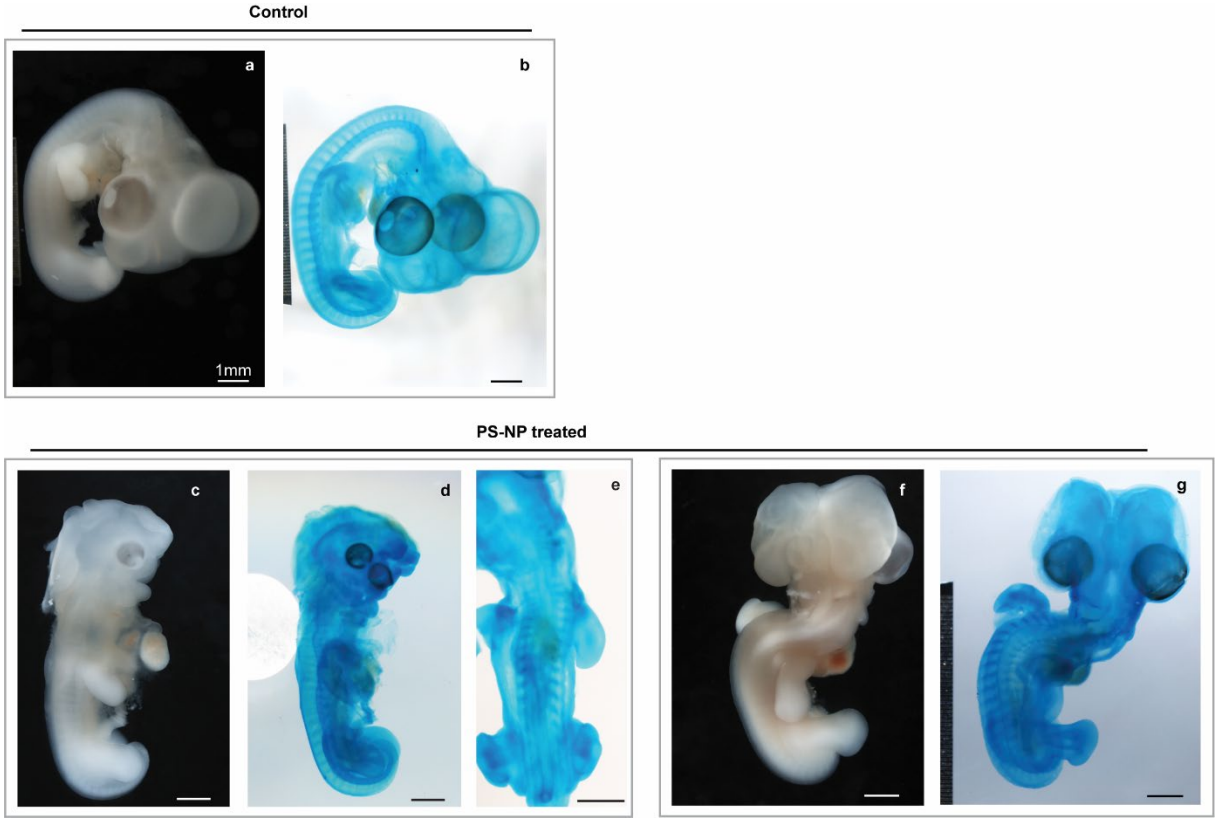

Fig. 2-4. **Phenotypic analysis of malformations 4 d after exposure to PS-NPs at stage 8. a**, **b**, the chicken embryo from the control group. **c**, **d**, **e**, PS-NPs treated chicken embryo, with microphthalmia, anencephaly and abnormal cervical flexure. **f**, **g**, PS-NPs treated chicken embryo, with exencephaly and failure of cervical flexure.

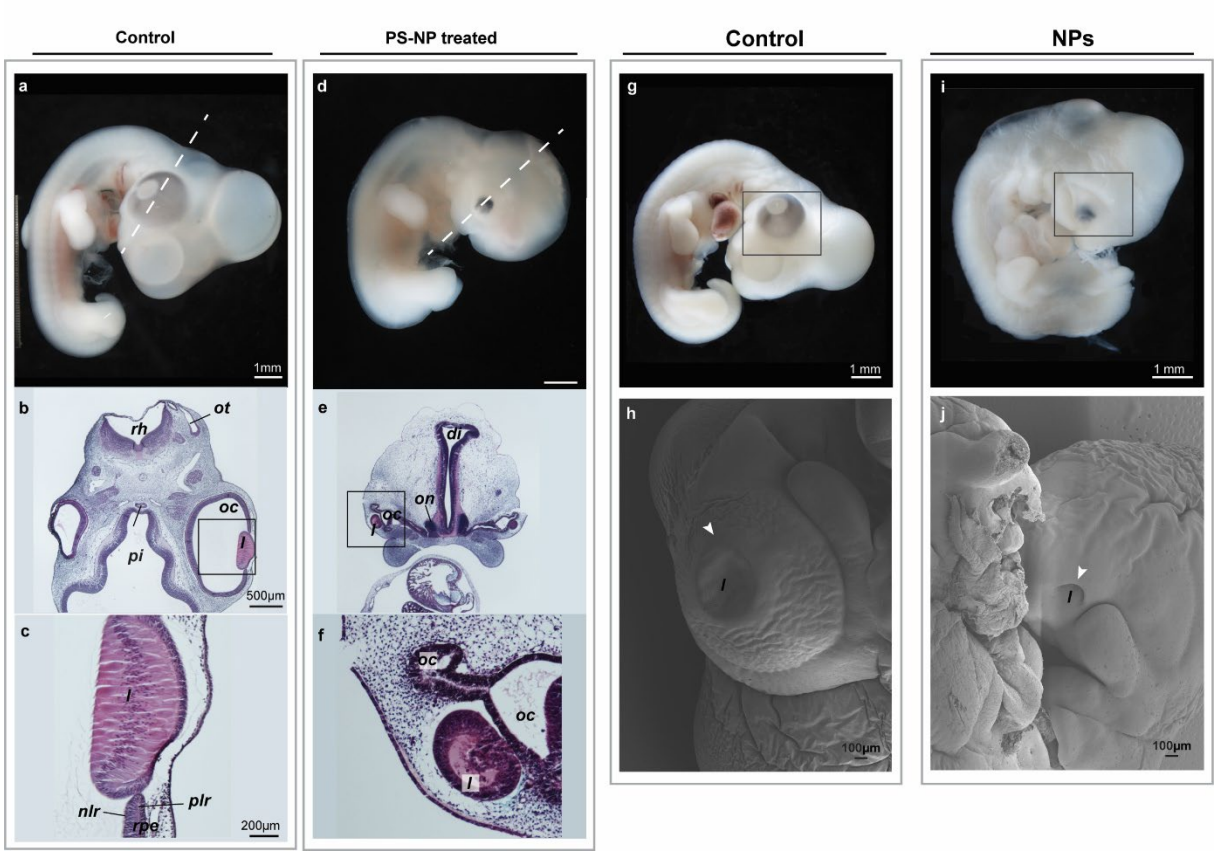

Fig. 2-5. **Phenotypic analysis of eye defects 4 d after exposure to PS-NPs at stage 8. a**, the wholemount chicken embryo from the control group, stage 25. **d**, the chicken embryo from PS-NPs treated group with microphthalmia anencephaly and caudal neural tube defect. **b**, **c**, **e** and **f** histological examinations od HE staining. **g**, the chick embryo from the control group, stage 25. **i**, the chick embryo from the PS-NPs group with microphthalmia, stage 24. **h** and **j**, the scanning of the eye from control and PS-NPs treated embryos; white arrowheads, the normal (**h**) and abnormal eye (**j**). **j**, the chick embryo with small lens. *Key*: di, diencephalon; l, lens; nc, notochord; nlr, neural layer of retina; on, otocyst; pi, pituitary; rpe, retinal pigment epithelium; rh, rhombencephalon; te, telencephalon.

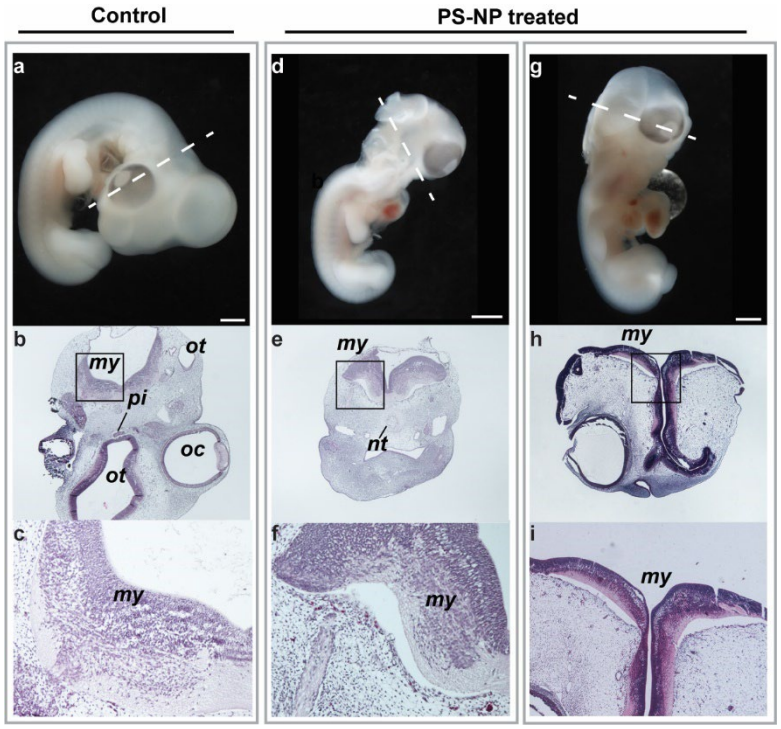

Fig. 2-6. **Phenotypic analysis of neural tube defects at 4 d after exposure to PS-NPs at stage 8. a**, the chicken embryo from the control group, stage 25. **d** and **g**, the chicken embryo from the PS-NPs treated group with anencephaly and abnormal cervical flexure. my, myelencephalon; nc, notochord; nt, neural tube; on, otocyst; pi, pituitary.

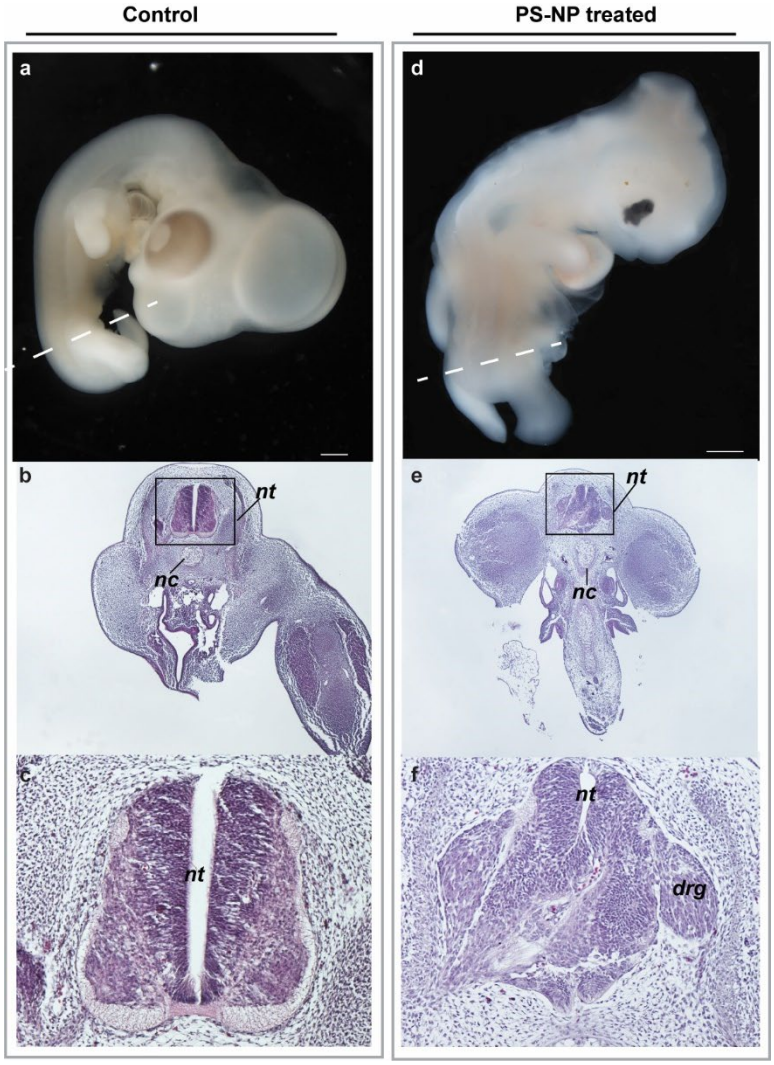

Fig. 2-7. **Phenotypic analysis of neural tube defects 4 d after exposure to PS-NPs at stage 8. m**, the chick embryo from the control group. **n**, the chick embryo from PS-NPs treated group with caudal neural tube defects, microphthalmia, anencephaly and abnormal cervical flexure. *Key*: drg, dorsal root ganglia; nc, notochord; nt, neural tube.

Discussion

We exposed chicken embryos, of Hamburger-Hamilton stage 8, to 25 nm PS-NPs; we then returned the eggs to the incubator and analyzed them 24 h or 4 d post exposure. In a first series, we examined the effect of PS-NP size. This examination showed the highest mortality and malformation rate in the chicken embryos exposed to the smallest (25 nm) PS-NPs. In a recent study , Nie et al found that 60 nm polystyrene nanoparticles cause more cases of serious malformation in chicken embryos at 24 hpe than did 900 nm nanoparticles (Nie et al., 2021). Furthermore,

smaller polystyrene nanoplastics (0.05 μm) produce higher mortality in the copeopod *Tigriopus japonicus* than larger-sized nanoplastics (0.5 μm) (Lee et al., 2013).

In some species, the situation appears to be reversed. This, when embryonic and larval stages of the sea urchin *Sphaerechinus granularis* were exposed to different sizes of PS-NP (10 nm, 80 nm and 230 nm); the larger size particles caused higher incidence of malformations than did the smaller (Trifuoggi et al., 2019). Therefore, it is possible that the relationship between nanoplastics size and toxicity is species-specific (Kögel et al., 2020).

There are other reasons why the relationship between particle size and toxicity is not straightforward (Wang et al., 2023). Thus, particles of different sizes will have different surface areas at the same mass. Therefore, the size-dependent toxicity may be caused by the combination of these characterizations of particles. In this Chapter, after we had completed the preliminary experiments, we then maintained a fixed concentration (5 mg/mL) in all subsequent experiments. This meant that we could not disentangle the effects of particle size and particle number. Therefore, the higher mortality and malformation rates at the smaller particle size (25 nm) might be due, in part, to the correspondingly higher number of particles, and their higher total surface area.

We also found that 25 nm plain polystyrene nanoplastics cause dose-response toxic effects on mortality and malformation rate of 4 dpe chicken embryos. In one study, the toxicity of three different types of 50 nm PS-NP nanoplastic particle were tested on oysters (Tallec et al., 2018). The particles tested were plain, carboxyl-modified or amine modified. Each type of particle had a different dose-response effect on fertilization yield of the oyster gametes (Tallec et al., 2018). In a study on chicken embryos, there was a dose-dependent increase in the frequency of exomphalos or omphalocele (exposure of abdominal viscera through the ventral body wall), and in the mortality (Nie et al., 2021). In summary, there is evidence of a relationship

between nanoplastic dose, and the incidence of mortality and malformations caused in exposed embryos.

In this chapter, we observed that exposure of chicken embryos to PS-NPs caused a developmental delay. Developmental delay is a typical consequence of exposure of embryos to teratogens (Harnett et al., 2021; Teixidó et al., 2013). Development delay has been reported after the exposure of chicken embryos to NPs (Nie et al., 2021) and the exposure of zebrafish embryos/larvae to 35 nm gold nanorods (Mesquita et al., 2017). Overall, our results are aligned with previous findings which confirm that nanoplastics could be considered as a teratogen in the early stages of embryos. In additional to developmental delay, Nie et al have shown that the exposure of chicken embryos to various sized PS-NPs can cause major malformations of the neural tube (Nie et al., 2021). The mechanism proposed by Nie et al was that PS-NPs are taken up by neural tube cells by endocytosis; this in turn led to led to cell damage and cell death through the increased production of reactive oxygen species (Nie et al., 2021).

In this chapter, we found neural tube defects in the head, trunk, tail, or a combination of these sites. This variation in location of the neural tube defects could be because of differences in the distribution of PS-NPs between individual treated embryos; or could be a result of multiple neural tube closure sites in one embryo, as has been postulated for human malformations (Seller, 1995). Neural tube defects result from a failure of the neural folds to meet and close (Copp and Greene, 2013; Copp et al., 2013). In one previous study, mouse embryos exposed to 6.5 nm titanium dioxide (TiO_2) particles showed neural tube defects (Hong et al., 2017).

Results similar to those in this chapter were also seen in a previous study (Nie et al., 2021) in which chicken embryos at early stages were exposed to 60 and 900 nm PS-NPs *in vitro*. Specifically, defects were noted in the cranial and truncal neural tube at 36 hpe (Nie et al., 2021). One difference with that study is that we observed in this chapter, neural tube defects in caudal regions, which were not reported in the chicken embryo before (Wang et al., 2023). There is a junction between regions of

primary and secondary neurulation (Dady et al., 2014). The secondary neurulation starts around stage 8 which suggest that PS-NPs may affect the process (Dady et al., 2014). This could explain the neural tube defects in the caudal region seen in this chapter. Furthermore the caudal region of the embryo develops later than the truncal and cranial regions and so that study (Nie et al., 2021) may have exposed the embryos too early.

Another new observation of this chapter is the presence of microphthalmia in the PS-NPs treated group at 4 dpe, something not reported in a previous study of chick embryo exposure to PS-NPs (Nie et al., 2021). Microphthalmia is a birth defect in which the newborn have abnormally small eyes. The occurrence of microphthalmia was differ between individuals. Specifically, either one or both eyes was abnormally small (Verma and FitzPatrick, 2007). In humans and mice, microphthalmia can have a genetic or environmental causes (Verma and FitzPatrick, 2007). We cannot be sure that nanoplastics directly impair affect eye development. However, it has been demonstrated that nanogold functionalized with a cationic ligand, N,N,N-trimethylammoniumethanethiol, can disrupt eye development in the zebrafish, leading to microphthalmia (Kim et al., 2013). In addition, copper nanoparticles have been found to reduce the size of eyes by decreasing the cell number of ganglion cell layer of the retina in zebrafish embryos (Zhao et al., 2020). Microphthalmia has also been reported in zebrafish embryos exposed to PS-NPs and polybrominated diphenyl ethers (Wang et al., 2022).

Skeletal abnormalities were observed among the PS-NPs-treated embryos analyzed at 4 dpe. These abnormalities included an abnormally curved vertebral column, and an absent or short tail-bud. Similar results have been found in other studies in which different species were exposed to various types of nanoparticles at early developmental stages. For instance, zebrafish embryos exposed at 6 hours post fertilization to polyethylene terephthalate nanoparticles, showed abnormal curvature of the vertebral column and tail (Bashirova et al., 2023). In mouse embryos, exposure

to 6.5 nm titanium dioxide (TiO_2) particles caused skeletal abnormalities associated with abnormal cartilage development (Hong et al., 2017).

In conclusion, we have confirmed the results of previous studies in vertebrate model species, showing that nanoparticles can cause defects of the neural tube, vertebral column and, in zebrafish, in the tail. In addition, we have shown for the first time that PS-NPS can cause microphthalmia and tail abnormalities in the chicken embryo. In Chapter 3, we will look at defects in later-developing organ systems, particularly the heart and facial region; and in Chapter 4 will explore the cellular mechanisms underlying the malformations caused by PS-NPs.

References

Abbing, M. R. (2019). *Plastic Soup: An Atlas of Ocean Pollution*: Island Press.

Bancroft, J. D. and Gamble, M. (2008). *Theory and Practice of Histological Techniques*: Elsevier health sciences.

Bashirova, N., Poppitz, D., Klüver, N., Scholz, S., Matysik, J. and Alia, A. (2023). A Mechanistic Understanding of the Effects of Polyethylene Terephthalate Nanoplastics in the Zebrafish (*Danio Rerio*) Embryo. *Scientific Reports* **13**, 1891.

Bellairs, R. and Osmond, M. (2014). *The Atlas of Chick Development*. Amsterdam: Academic Press.

Bhagat, J., Zang, L., Nishimura, N. and Shimada, Y. (2020). Zebrafish: An Emerging Model to Study Microplastic and Nanoplastic Toxicity. *Science of The Total Environment* **728**, 138707.

Boerjan, M. L. (2002). Programs for Single Stage Incubation and Chick Quality. *Avian and Poultry Biology Reviews* **13**, 237-237.

Brady, J. (1965). A Simple Technique for Making Very Fine, Durable Dissecting Needles by Sharpening Tungsten Wire Electrolytically. *Bulletin of the World Health Organization* **32**, 143.

Copp, A. J. and Greene, N. D. (2013). Neural Tube Defects—Disorders of Neurulation and Related Embryonic Processes. *Wiley Interdisciplinary Reviews: Developmental Biology* **2**, 213-227.

Copp, A. J., Stanier, P. and Greene, N. D. (2013). Neural Tube Defects: Recent Advances, Unsolved Questions, and Controversies. *The Lancet Neurology* **12**, 799-810.

Dady, A., Havis, E., Escriou, V., Catala, M. and Duband, J. L. (2014). Junctional Neurulation: A Unique Developmental Program Shaping a Discrete Region of the Spinal Cord Highly Susceptible to Neural Tube Defects. *Journal of Neuroscience* **34**, 13208-13221.

de Bakker, M. A. G., Fowler, D. A., Oude, K. d., Dondorp, E. M., Navas, M. C. G., Horbanczuk, J. O., Sire, J.-Y., Szczerbińska, D. and Richardson, M. K. (2013). Digit Loss in Archosaur Evolution and the Interplay between Selection and Constraints. *Nature* **500**, 445-448.

Ewen, J. A. (1997). New Chemical Tools to Create Plastics. *Scientific American* **276**, 86-91.

Fuschi, C., Pu, H., MacDonell, M., Picel, K., Negri, M. and Chen, J. (2022). Microplastics in the Great Lakes: Environmental, Health, and Socioeconomic Implications and Future Directions. *ACS Sustainable Chemistry & Engineering* **10**, 14074-14091.

Godfrey, L. (2019). Waste Plastic, the Challenge Facing Developing Countries—Ban It, Change It, Collect It? *Recycling* **4**, 3.

Hamburger, V. and Hamilton, H. L. (1951). A Series of Normal Stages in the Development of the Chick Embryo. *Journal of Morphology* **88**, 49-92.

Harnett, K. G., Moore, L. G., Chin, A., Cohen, I. C., Lautrup, R. R. and Schuh, S. M. (2021). Teratogenicity and Toxicity of the New Bpa Alternative Tmbpf, and Bpa, Bps, and Bpaf in Chick Embryonic Development. *Current Research in Toxicology* **2**, 399-410.

Hill, E. F. and Hoffman, D. J. (1984). Avian Models for Toxicity Testing. *Journal of the American College of Toxicology* **3**, 357-376.

Hong, F., Zhou, Y., Zhao, X., Sheng, L. and Wang, L. (2017). Maternal Exposure to Nanosized Titanium Dioxide Suppresses Embryonic Development in Mice. *International Journal of Nanomedicine* **12**, 6197-6204.

Imhof, H. K., Rusek, J., Thiel, M., Wolinska, J. and Laforsch, C. (2017). Do Microplastic Particles Affect Daphnia Magna at the Morphological, Life History and Molecular Level? *PloS One* **12**, e0187590-e0187590.

Kim, K. T., Zaikova, T., Hutchison, J. E. and Tanguay, R. L. (2013). Gold Nanoparticles Disrupt Zebrafish Eye Development and Pigmentation. *Toxicol Sci* **133**, 275-288.

Kögel, T., Bjorøy, Ø., Toto, B., Bienfait, A. M. and Sanden, M. (2020). Micro-and Nanoplastic Toxicity on Aquatic Life: Determining Factors. *Science of The Total Environment* **709**, 136050-136050.

Kumar, S., Stecher, G., Suleski, M. and Hedges, S. B. (2017). Timetree: A Resource for Timelines, Timetrees, and Divergence Times. *Molecular Biology and Evolution* **34**, 1812-1819.

Lee, K.-W., Shim, W. J., Kwon, O. Y. and Kang, J.-H. (2013). Size-Dependent Effects of Micro Polystyrene Particles in the Marine Copepod Tigriopus Japonicus. *Environmental Science & Technology* **47**, 11278-11283.

Lillie, F. R. (1952). *Lillie's Development of the Chick*. New York: Holt, Renehart and Winston.

Lim, X. (2021). Microplastics Are Everywhere—but Are They Harmful. *Nature* **593**, 22-25.

Liu, Z., Yu, P., Cai, M., Wu, D., Zhang, M., Huang, Y. and Zhao, Y. (2019). Polystyrene Nanoplastic Exposure Induces Immobilization, Reproduction, and Stress Defense in the Freshwater Cladoceran *Daphnia Pulex*. *Chemosphere* **215**, 74-81.

Martins, A. and Guilhermino, L. (2018). Transgenerational Effects and Recovery of Microplastics Exposure in Model Populations of the Freshwater Cladoceran Daphnia Magna Straus. *Science of the Total Environment* **631**, 421-428.

Mesquita, B., Lopes, I., Silva, S., Bessa, M. J., Starykevich, M., Carneiro, J., Galvão, T. L. P., Ferreira, M. G. S., Tedim, J. and Teixeira, J. P. (2017). Gold Nanorods Induce Early Embryonic Developmental Delay and Lethality in Zebrafish (Danio Rerio). *Journal of Toxicology and Environmental Health, Part A* **80**, 672-687.

Metscher, B. D. (2009). Microct for Developmental Biology: A Versatile Tool for High-Contrast 3d Imaging at Histological Resolutions. *Developmental dynamics: an official publication of the American Association of Anatomists* **238**, 632-640.

Mitrano, D. M., Wick, P. and Nowack, B. (2021). Placing Nanoplastics in the Context of Global Plastic Pollution. *Nature Nanotechnology* **16**, 491-500.

Nie, J.-h., Shen, Y., Roshdy, M., Cheng, X., Wang, G. and Yang, X. (2021). Polystyrene Nanoplastics Exposure Caused Defective Neural Tube Morphogenesis through Caveolae-Mediated Endocytosis and Faulty Apoptosis. *Nanotoxicology*, 1-20.

Pardo, J. D., Lennie, K. and Anderson, J. S. (2020). Can We Reliably Calibrate Deep Nodes in the Tetrapod Tree? Case Studies in Deep Tetrapod Divergences. *Frontiers in Genetics* **11**.

Pawłowska, J. and Sosnówka-Czajka, E. (2019). Factors Affecting Chick Quality in Poland. *World's Poultry Science Journal* **75**, 621-632.

Pitt, J. A., Trevisan, R., Massarsky, A., Kozal, J. S., Levin, E. D. and Di Giulio, R. T. (2018). Maternal Transfer of Nanoplastics to Offspring in Zebrafish (Danio Rerio): A Case Study with Nanopolystyrene. *Science of the Total Environment* **643**, 324-334.

Ragusa, A., Svelato, A., Santacroce, C., Catalano, P., Notarstefano, V., Carnevali, O., Papa, F., Rongioletti, M. C. A., Baiocco, F., Draghi, S., et al. (2021). Plasticenta: First Evidence of Microplastics in Human Placenta. *Environ Int* **146**, 106274.

Rezania, S., Park, J., Din, M. F. M., Taib, S. M., Talaiekhozani, A., Yadav, K. K. and Kamyab, H. (2018). Microplastics Pollution in Different Aquatic Environments and Biota: A Review of Recent Studies. *Marine Pollution Bulletin* **133**, 191-208.

Romanoff, A. L. (1960). *The Avian Embryo : Structural and Functional Development*. New York: Macmillan.

Rosato, D. V. and Rosato, D. V. (2011). Plastics End Use Application Fundamentals. *Plastics End Use Applications*, 11-18.

Roy, P., Ashton, L., Wang, T., Corradini, M. G., Fraser, E. D., Thimmanagari, M., Tiessan, M., Bali, A., Saharan, K. M. and Mohanty, A. K. (2021). Evolution of Drinking Straws and Their Environmental, Economic and Societal Implications. *Journal of Cleaner Production* **316**, 128234.

Sánchez-Villagra, M. (2012). *Embryos in Deep Time: The Rock Record of Biological Development*: Univ of California Press.

Seller, M. J. (1995). Sex, Neural Tube Defects, and Multisite Closure of the Human Neural Tube. *American Journal of Medical Genetics* **58**, 332-336.

Silver, P. (1960). Special Problems of Experimenting in Ovo on the Early Chick Embryo, and a Solution.

St John, J. A., Braun, E. L., Isberg, S. R., Miles, L. G., Chong, A. Y., Gongora, J., Dalzell, P., Moran, C., Bed'Hom, B., Abzhanov, A., et al. (2012). Sequencing Three Crocodilian Genomes to Illuminate the Evolution of Archosaurs and Amniotes. *Genome Biology* **13**, 415.

Stark, M. R. and Ross, M. M. (2019). The Chicken Embryo as a Model in Developmental Toxicology. In *Developmental Toxicology: Methods and Protocols* (ed. J. M. Hansen & L. M. Winn), pp. 155-171. New York, NY: Springer New York.

Tallec, K., Huvet, A., Di Poi, C., González-Fernández, C., Lambert, C., Petton, B., Le Goïc, N., Berchel, M., Soudant, P. and Paul-Pont, I. (2018). Nanoplastics Impaired Oyster Free Living Stages, Gametes and Embryos. *Environmental Pollution* **242**, 1226-1235.

Teixidó, E., Piqué, E., Gómez-Catalán, J. and Llobet, J. M. (2013). Assessment of Developmental Delay in the Zebrafish Embryo Teratogenicity Assay. *Toxicol In Vitro* **27**, 469-478.

Trifuoggi, M., Pagano, G., Oral, R., Pavičić-Hamer, D., Burić, P., Kovačić, I., Siciliano, A., Toscanesi, M., Thomas, P. J., Paduano, L., et al. (2019). Microplastic-Induced Damage in Early Embryonal Development of Sea Urchin Sphaerechinus Granularis. *Environmental Research* **179**, 108815.

Verma, A. S. and FitzPatrick, D. R. (2007). Anophthalmia and Microphthalmia. *Orphanet Journal of Rare Diseases* **2**, 1-8.

Wang, M., Rücklin, M., Poelmann, R. E., de Mooij, C. L., Fokkema, M., Lamers, G. E. M., de Bakker, M. A. G., Chin, E., Bakos, L. J., Marone, F., et al. (2023). Nanoplastics Causes Extensive Congenital

Malformations During Embryonic Development by Passively Targeting Neural Crest Cells. *Environment International*, 107865.

Wang, Q., Li, Y., Chen, Y., Tian, L., Gao, D., Liao, H., Kong, C., Chen, X., Junaid, M. and Wang, J. (2022). Toxic Effects of Polystyrene Nanoplastics and Polybrominated Diphenyl Ethers to Zebrafish (Danio Rerio). *Fish & Shellfish Immunology* **126**, 21-33.

Wilson, J. G. (1978). Survey of in Vitro Systems: Their Potential Use in Teratogenicity Screening. In *Research Procedures and Data Analysis*, pp. 135-153: Springer.

Yan, Y., Wang, G., Huang, J., Zhang, Y., Cheng, X., Chuai, M., Brand-Saberi, B., Chen, G., Jiang, X. and Yang, X. (2020). Zinc Oxide Nanoparticles Exposure-Induced Oxidative Stress Restricts Cranial Neural Crest Development During Chicken Embryogenesis. *Ecotoxicology and Environmental Safety* **194**, 110415.

Yan, Y., Wang, G., Luo, X., Zhang, P., Peng, S., Cheng, X., Wang, M. and Yang, X. (2021). Endoplasmic Reticulum Stress-Related Calcium Imbalance Plays an Important Role on Zinc Oxide Nanoparticles-Induced Failure of Neural Tube Closure During Embryogenesis. *Environment International* **152**, 106495.

Yi, W., Rücklin, M., Poelmann, R. E., Aldridge, D. C. and Richardson, M. K. (2021). Normal Stages of Embryonic Development of a Brood Parasite, the Rosy Bitterling Rhodeus Ocellatus (Teleostei: Cypriniformes). *Journal of Morphology* **282**, 783-819.

Zhao, G., Sun, H., Zhang, T. and Liu, J.-X. (2020). Copper Induce Zebrafish Retinal Developmental Defects Via Triggering Stresses and Apoptosis. *Cell Communication and Signaling* **18**, 1-14.

Chapter 3. Nanoplastics cause cardiac malformations and abnormal circulation in chicken embryos

Meiru Wang[1,2], Robert E. Poelmann[1,3], Martin Rücklin[2,1], Carmen L. de Mooij[1], Gerda E.M. Lamers[1], Ernest Chin[1], Lilla J. Bakos[1], Federica Marone[4], Bert J. Wisse[5], Marco C. de Ruiter[5], Martina G. Vijver[6], Michael K. Richardson[1].*

1. Institute of Biology, Leiden University, Sylvius Laboratory, Sylviusweg 72, 2333 BE, Leiden, The Netherlands.
2. Naturalis Biodiversity Center, Darwinweg 2, 2333 CR, Leiden, The Netherlands.
3. Department of Cardiology, Leiden University Medical Center, The Netherlands.
4. Swiss Light Source, Paul Scherrer Institut, Photon Science Department, Forschungsstrasse 111, CH-5232 Villigen, Switzerland.
5. Department of Anatomy & Embryology, Leiden University Medical Center, The Netherlands.
6. Institute of Environmental Sciences, Leiden University (CML), Van Steenis Building, Einsteinweg 2, 2333 CC, Leiden, The Netherlands.

This chapter has been published as part of: Wang, M., Rücklin, M., Poelmann, R.E., de Mooij, C.L., Fokkema, M., Lamers, G.E.M., de Bakker, M.A.G., Chin, E., Bakos, L.J., Marone, F., Wisse, B.J., de Ruiter, M.C., Cheng, S., Nurhidayat, L., Vijver, M.G., Richardson, M.K. Nanoplastics causes extensive congenital malformations during embryonic development by passively targeting neural crest cells. *Environment International* **173**, 107865. https://doi.org/10.1016/j.envint.2023.107865.

Abstract

Plastic waste has become a major environmental pollutant due to the poor management of plastic waste, and its limited recyclability. Among plastic waste, there are small plastic particles, defined as microplastics (≤ 5mm diameter) and nanoplastics (≤ 1 μm diameter). It has been previously reported in the literature, and here in Chapter 2, that nanoplastics can cause malformations in the nervous system and eye. Here, we explore the range of malformations produced by nanoplastics in more depth. We exposed stage 8 chicken embryos to 25 nm plain polystyrene nanoplastics and examined these embryos at a wider range of stages than in previous studies. We find that the polystyrene nanoparticles can cause severe malformations in craniofacial and cardiovascular systems. These include major heart defects and impaired cardiac function. In addition, the severe dysplasia of the palatine, maxillary and premaxillary cartilages was observed in embryos treated with nanoplastics. Furthermore, we found abnormal expression patterns of the genes TFAP2A, TNNI and NKX2-5 in treated embryos. Combining these data with the fact that nanoplastics also cause neural tube defects (Chapter 2) we suggest that nanoplastics disrupt the cardiocraniofacial module of the developing embryo, possibly by an effect on neural crest cells. Our hypotheses will be further explored in Chapter 4.

Introduction

Microplastics and nanoplastics (MPs and NPs) are small plastic particles with relevance to human health. Both types of particle are widely present in air and drinking water (Cox et al., 2019; Koelmans et al., 2019). A further potential source of exposure, at least for humans, is that NPs are being considered as new drug delivery vehicles for use in human medicine (Boehnke et al., 2022). They are also found in house dust (Zhang et al., 2020), and are added by the manufacturer to some household and personal hygiene products (Anagnosti et al., 2021; Vighi et al., 2021). Note that some European Union member states are considering the banning of nanoplastics as components of these products (European_Commission, 2022).

Strikingly, these plastics particles have been found in the human body. For example, there were 12 different types of MPs (PP, PET etc.) detected in the tissue of human lungs from 13 volunteers (Jenner et al., 2022). Another study detected MPs in blood samples of 22 healthy human volunteers at an average concentration of 1.6 μg/mL (Leslie et al., 2022). Furthermore, NPs ranging from 50 – 500 nm have been found in human feces (Schwabl et al., 2019). These and other studies have raised public concerns about the potential health-risk that MPs and NPs may pose (Mitrano et al., 2021).

The effects of MPs and NPs have mostly been studied on aquatic organisms including crustaceans (e.g. *Daphnia*), gastropods, and fish (e.g. zebrafish) (Kögel et al., 2020). As we discussed in more detail in Chapter 1, those studies have shown that MPs and NPs can produce a range of toxic effects including growth delays, reproductive effects, developmental toxicity, behavioral abnormalities and bradycardia (Pitt et al., 2018; Wan et al., 2018).

In Chapter 2 we reported that exposure of chicken embryos to 25 nm NPs produced neural tube defects, vertebral column abnormalities and tail bud defects. These phenotypic effects were at 24 hpe – 4 dpe. In this chapter, we analyze the effects of

PS-NPs on the embryo at a wider range of stages including later ones. We chose to do this in order to look for effects on the heart and face. These are organ systems in which it is easier to detect malformations at stages later than 4 d. They are also relatively commonly affected by malformations in humans (Mai et al., 2019) and are therefore of interest if we want to understand the implications of NPs to human health, using the chick embryo model. Relatively little is known about potential effects of PS-NPs on cardiac development (Zhu et al., 2023). For example, PS-NPs cause bradycardia in zebrafish (*Danio rerio*) embryos (Feng et al., 2022; Pitt et al., 2018). Also, 20 nm PS-NPs affect the development of zebrafish embryos, resulting in pericardial edema (Sulukan et al., 2022). In addition, the exposure of chicken embryonic myocardial cells *in vitro* to PS-NPs produces oxidative stress in those cells (Zhang et al., 2022).

In Chapter 2, we showed that 25 nm plain PS-NPs are teratogenic to developing chicken embryos. We found malformations in the neural tube, eye, vertebral column and tail bud of early stage chicken embryos. In this chapter, we have investigated the longer-term effects of PS-NPs on chick embryo development. In particular, we were interested to see if there were effects on the heart and limbs, for example, by examining the PS-NPs-treated chick embryos at later stages of development. To study heart development in more depth, we used the markers cardiac troponin I (TNNI) which is expressed in the cytoplasm of cardiac muscle, or myocardium (Abd-Elgaliel and Tung, 2012); and the homeobox gene NKX2-5 which is expressed in the nuclei of precardiac as well as myocardial cells (McCulley and Black, 2012). Furthermore, we also examined the expression of TFAP2A (transcription factor AP-2 alpha; AP-2α) which is essential for cardiac morphogenesis (in the mouse model) (Bamforth et al., 2001; Brewer et al., 2002).

Materials and Methods

In ovo embryo toxicity experiments

We have described in Chapter 2 the detailed protocol for introducing PS-NPs into the chicken egg. After the PS-NPs were introduced, the eggs were then sealed with Scotch® prescription label tape 800 (clear) and returned to the incubator for an additional 3, 4, or 8 d (post exposure). Embryos were harvested from the egg into cold phosphate buffered saline (PBS) for further analysis.

Heart-rate recordings and analysis

The embryos were exposed *in ovo* as described in the previous section. After 2–3 d of further exposure, the embryos were placed, still in the egg, in a cradle of crumpled aluminum foil in a digitally controlled heat block (38 °C). Video recordings were made of the live embryo *in ovo* using a Nikon SMZ800 stereo microscope fitted with a Dino-Eye eyepiece camera (Dino-Lite Europe, Almere).

To determine the heart rate of chicken embryos, 27 videos were analyzed using ImageJ (v. 1.53q Java 1.8.0_322, National Institutes of Health, USA) with a custom script written by Joost Willemse (institute of Biology, University of Leiden). Videos were assembled into an image stack. Then, an area of the heart was selected using the rectangle tool in ImageJ so that the heartbeat would be registered by a change in color. The mean grey value of the selected area was calculated for each frame of the video.

Alcian blue wholemounts

This protocol is as previously described by us (de Bakker et al., 2013). Embryos were fixed with 5% trichloroacetic acid at 4 °C degree overnight. They were then transferred into refresh 70% ethanol for 2 h × 2 followed by acid alcohol (20% glacial acetic acid in 70% ethanol for 2 h). Embryos were then stained in 0.03% (W/V) Alcian blue in acid alcohol overnight. Then they were rinsed with acid alcohol for 2 h

followed by dehydration through a graded ethanol series from 70% to 100%. Finally, embryos were cleared and stored in methyl salicylate.

Histology

Paraffin histology with haematoxylin and eosin staining

We performed routine paraffin histology with haematoxylin and eosin staining according to standard protocols (Bancroft and Gamble, 2008). Embryos were fixed in 4% buffered depolymerized paraformaldehyde (pFA) for 24 h at 4 °C. They were then were washed 3x with cold PBS and dehydrated in 70% ethanol overnight. Subsequently, the embryos were dehydrated through a graded ethanol series (80%, 90%, 100%), 1 h each. Embryos were cleared with Neo-Clear® (Merck, Darmstadt), 3x 1h, and embedded in paraffin (Paraclean, KP Klinipath/VWR International, Amsterdam) at 60 °C (1x overnight, 1x 1 h). Serial sections were cut at 7 µm. Because embryos examined at 24 h post-exposure were delicate and difficult to handle, we used a modified protocol (McClelland et al., 2016). After fixing the embryos, they were embedded in a mixture of 2% agarose (Sigma-Aldrich, Zwijndrecht, A-6013) and 2.5% low melting-point agarose (super fine resolution agarose, Electron Microscopy Sciences, Hatfield, PA) at 42 °C. When the mixture had solidified at room temperature (c. 20 min), the agarose blocks containing the embedded embryos were transferred to 70% ethanol for 2 d. They were then dehydrated in graded ethanols, embedded in paraffin and sectioned. The only modification made to the embedding step was that the tissue blocks were in molten paraffin for no more than 3x 1 h.

Paraffin histology with haematoxylin, eosin and Alcian blue triple-staining

This technique helped us to visualize cartilage and the also cardiac jelly in the endocardial cushions of the heart. The protocol was done using standard haematoxylin and eosin staining with some modifications. Briefly, the 7 µm section paraffin sections were mounted on slides. They were then dewaxed in refresh xylene 3 × 5 min. Then sections were then rehydrated through 100%, 90%, 80%, 70%

ethanol. Sections were stained with Alcian blue for 10 min, followed by rinsing in tap water for 10 min. The rest of the processes is the same as with standard as haematoxylin and eosin staining (Chapter 2). The sections were subsequently stained with haematoxylin and eosin. Finally, the stained sections were cleared with xylene and mounted by Eukitt® Mounting Medium (Agar Scientific, UK).

Synchrotron X-ray tomographic microscopy

For synchrotron X-ray tomographic microscopy (synchrotron scanning) embryos were harvested and fixed in a mixture of 2.5% paraformaldehyde (pFA), 1.5% glutaraldehyde in 0.1 M sodium cacodylate buffer (pH 7.4) at 4° C for 24 h as previously described (Cotti et al., 2020). They were then dehydrated in a graded ethanol series (25%, 50%, 70%). The hearts were dissected and stored in 0.2 mL PCR tubes in 70% ethanol at 4°C. Synchrotron scanning was performed at the TOMCAT (tomographic microscopy and coherent radiology experiments) beamline (Stampanoni et al., 2006), Swiss Light Source, Paul Scherrer Institute, Villigen, Switzerland. The samples were fixed to scanning electron microscopy stubs with beeswax. The X-ray beam energy was 17 keV. For the overview scans, the microscope (Optique Peter, Lentilly, France) magnification was set to 4x. To be able to laterally cover the entire sample, the rotation axis was displaced to the side of the field of view and 2,501 projections, equiangularly distributed over 360° , were acquired with a sCMOS camera (PCO.edge, Kehlheim, Germany). To fully cover the sample in the vertical direction, a sequence of 3–4 scans was necessary. The exposure time per projection was 50 ms and the X-rays were converted into visible light with a 100 µm thick Ce doped LuAG (lutetium aluminium garnet) scintillator screen (Crytur, Turnov, Czech Republic). The effective pixel size was 1.625 µm and the sample-detector distance 20 cm. For the higher resolution scans of specific details, a 10x objective with a thinner (20 µm) scintillator of the same material was used, resulting in a pixel size of 0.65 µm. The rotation axis was positioned in the middle of the field of view, and 1,501 projections, equiangularly distributed over 180 °, were acquired with an exposure time per view of 200 ms. Prior to tomographic reconstruction (Marone et

al., 2017), all projections were dark- and flat-field corrected as well as phase-retrieved (Paganin et al., 2002). The images were analyzed and manipulated using Avizo software (Version: 8.01; Thermo, Fisher Scientific).

RNA extraction and cDNA synthesis

The RNA was isolated from stage 13-16 chick embryos by TRIzol™ Reagent (Thermo Fisher Scientific, USA) in house followed by purification with RNeasy Mini Kit (50; Qiagen, Venlo, Netherlands). The concentration of purified RNA was measured by Nanodrop. To generate first strand cDNA, we performed two-step reverse transcription polymerase chain reaction (RT-PCR) using SuperScript III (Invitrogen™, USA). The cDNA was diluted 10 × with DNA- and RNA-free water and stored at -20 °C (Sigma).

Probe synthesis

This protocol is as previously described by us (de Bakker et al., 2013). In brief, we isolated total RNA from an embryo using TRIzol (Invitrogen) and carried out reverse transcription using SuperScript III (Invitrogen). PCR was performed on these templates using specific primers (Supplementary Data Table 1), and the PCR products were cloned in the TOPOTA-PCRII vector (Invitrogen™). The inserted amplicons were checked by a PCR with M13-pUC primers located on the TOPOTA-PCRII plasmid and checked on an agarose gel. When they were of the right size, they were sent for Sanger sequencing (BaseClear B.V., Leiden). After checking the sequence by BLAST searching, the positive results were used as templates for making the digoxigenin labelled antisense RNA probes. See Supplementary Data Table S4 for accession numbers.

Wholemount *in situ* hybridization

In this study, all gene names are according to Ensembl for *Homo sapiens* (https://www.ensembl.org/). This wholemount protocol is as previously described by us (de Bakker et al., 2013). In brief, embryos were fixed in 2% buffered

depolymerized pPFA for 24 h at 4 °C. They were then washed 3 × with cold PBS and dehydrated through a graded methanol series (25%, 50%, 75% and 100%) and stored at -20 °C . Embryos were rehydrated through a graded methanol series, lightly digested with proteinase K (10 mg/mL in PBS) for 5 min and postfixed in 4% buffered pFA in PBS after several washes in PBST (PBS pH 7.2 with 0.1% Tween-20). This was followed by a prehybridization step at 60 °C for at least 3 h or until the embryo had sunk. The hybridization mixture consisted of: 50% formamide, 2% Boehringer blocking powder, 5 × SSC (from 20× standard sodium citrate buffer, 3M sodium chloride, 0.3M sodium citrate, pH 7), 1mg/mL total RNA, 50 µg/mL heparin, 0.1% Triton X-100, 0.1% CHAPS (3-[(3-cholamidopropyl) dimethylammonio]-1-propanesulfonate) and 5mM ethylenediaminetetraacetic acid (EDTA). After the prehybridization mix was removed, we added 400 ng/mL specific probe to fresh hybridization mixture preheated to 60 °C. The embryos were incubated in this mix at 60 °C overnight with slow shaking. The next day, the specific probe mixture was removed, collected and stored at -20 °C for re-use. Several stringent washes were done at 60 ° C to remove non-specifically bound probe [2× SSC, 0.1% CHAPS, 50% formamide]; [2× SSC 0.1% CHAPS]; [0.2× SSC, 0.1% CHAPS]. After washing several times at room temperature with TBST (0.1M tris [tris (hydroxymethyl)aminomethane] buffered saline, pH 7.5, 0.1% Tween-20) the embryos were preincubated with heat-inactivated 10% sheep serum in TBST for 90 min at room temperature followed by overnight incubation with sheep anti-digoxigenin conjugated to alkaline phosphatase (Roche; 1:5,000 dilution in 10% sheep serum in TBST at 4 °C overnight).

The next day, the non-specifically bound antibodies were washed away by several washes with TBST of which the last one was overnight at 4 °C. The embryos were brought to a higher pH by washing 3x 10 min in NTT buffer (0.1M sodium chloride, 0.1M Tris/HCl, 0.1% Tween-20, pH 9.5). The enzyme reaction of alkaline phosphate with BM purple (Roche) as substrate results in a blue precipitate. The development of the stain was checked regularly and stopped by washing several times in TBST, removing the substrate and chromogens, and lowering the pH.

Sectioning of wholemount *in situ* hybridized embryos

The protocol had been described in Ref. (Xu and Wilkinson, 1998). In order to get better results, we modified some steps. Chick embryos treated as described above under the subheading 'Wholemount *in situ* hybridization' were fixed in 2% PFA in PBS overnight, and the next day washed 3x 10 min with TBST on shakers at low speed. Then, the embryos were dehydrated through a graded methanol series (25%, 50%, 75%, 100%), and washed 3x in isopropanol (purity ≥ 99.5%, Sigma-Aldrich Cat.190764-1L) before being put into xylene as the intermediate reagent.

Immunochemistry

Chicken embryos (3 dpe) were fixed and dehydrated as described above under 'Wholemount *in situ* hybridization'. They were then processed for paraffin histology using standard protocols (Bancroft and Gamble, 2008). Immunochemistry was performed on 7 µm sections mounted on silane-coated slides (VWR International B.V, Amsterdam). Slides were rehydrated through 2x xylene, a graded ethanol series (100%, 90%, 80%, 70%), and demi water. Slides were then transferred to a container with 0.01 M sodium citrate buffer and heated in a microwave oven to 97 °C. When the slides cooled to room temperature, they were rinsed in PBST. We purchased all first antibodies from the same company (Santa Cruz Biotechnology in California, USA). The first antibody mix including Troponin I (H-170; cat. number ab087; dilution 1:500), anti-AP-2α (3B5; cat. number sc-12726, dilution 1:200), and Nkx.2.5 (N-19; cat number ab0266; 1:2000) was diluted in 1% bovine serum albumin (BSA) in PBST. The first antibody mix was added to the slides simultaneously. Then the slides were returned to a humidified chamber inside an incubator and incubated overnight.

The slides were rinsed in PBST. The second antibody mix contained: Alexa Fluor® 488 (Donkey anti-rabbit; cat. number AB0941, dilution: 1:200), Alexa Fluor® Plus 555 (Donkey anti-Mouse; cat. number AB1661, dilution: 1:200) and Alexa Fluor® Plus 647 (Donkey anti-Goat; cat. number ab1424) was added to the slides. All second antibodies were purchased from Thermo, Fisher Scientific USA. After rinsing with

PBST, the slides were then stained with DAPI (1:1000) for 5 min. Finally, they were washed 3x with PBST and mounted with ProLong Gold antifade reagent (Invitrogen, USA). The slides were scanned using a Zeiss Axio Scan.Z1 microscope slide scanner. High magnification views were made using a Nikon AX confocal microscope.

Results

Nanoplastics cause malformations in multiple organ systems

In treated embryos analyzed at 8 dpe, 2/6 had craniofacial dysplasia, 2/6 had cleft primary palate, 1/6 had both, and 1/6 had no craniofacial malformations (Fig. 3-1 and Table S3). The embryos with craniofacial dysplasia lacked the palatine, maxillary and premaxillary cartilages. In three cases, Meckel's cartilage was present, but not fused in the midline. There were no craniofacial malformations in the controls (*n* = 6). Embryos with neural tube defects showed concomitant vertebral defects (spina bifida; Fig. 3-1).

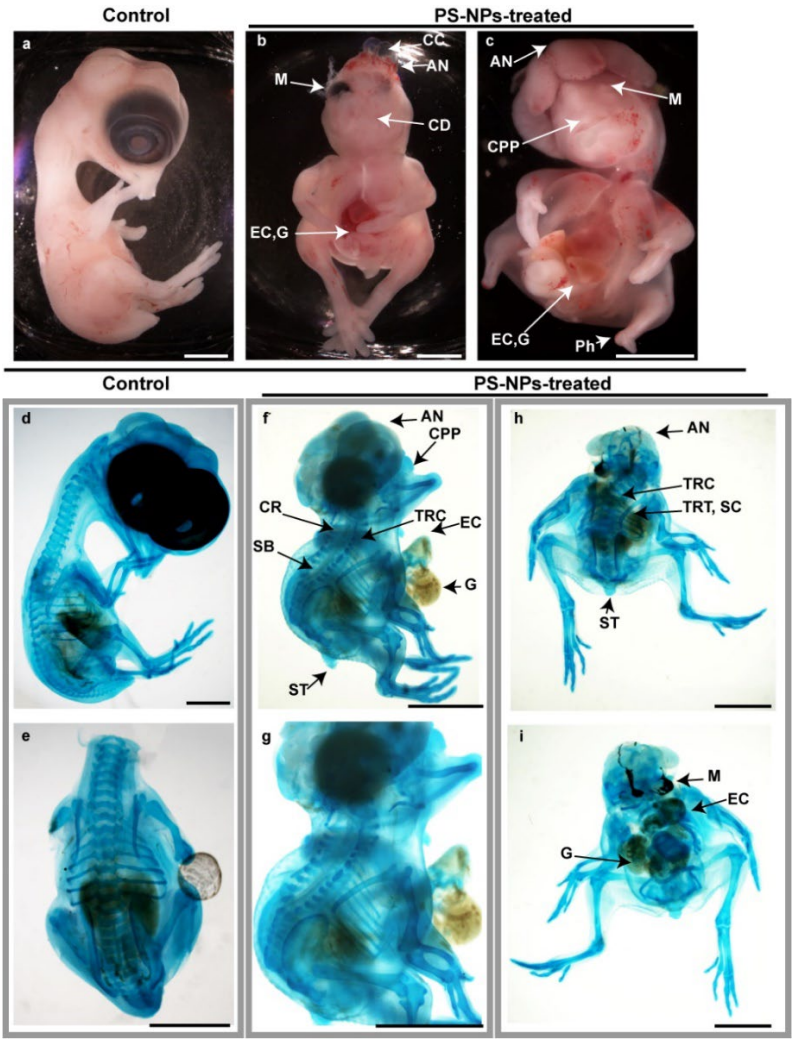

Fig. 3-1. **Gross appearance of chicken embryos examined at 8 day post exposure**. Gross appearance of embryos in control (**a**, **d**, **e**) and PS-NPs-treated group (**b**, **c**, **f**-**i**) all chicken embryos at stage 35. *Key*: AN, Anencephaly; CD, Craniofacial Dysplasia; CPP, Cleft Primary Palate; CR, Craniorachischisis; EC, Ectopia Cordis; M, Microphthalmia; Ph, Phocomelia; Sc, Scoliosis, TRC, Truncated Cervical Vertebrae; TRT, Truncated Thoracic vertebrae; ST, Short Tail, SB, Spina bifida. Scale bars are all 5 mm.

Nanoplastics cause abnormal circulatory function

When we examined living embryos *in ovo*, we found that PS-NP treated embryos showed a significant decrease in heart rate (bradycardia) at 3 dpe (Fig. 3-2). There was no significant effect on heart rate in embryos at 2 dpe.

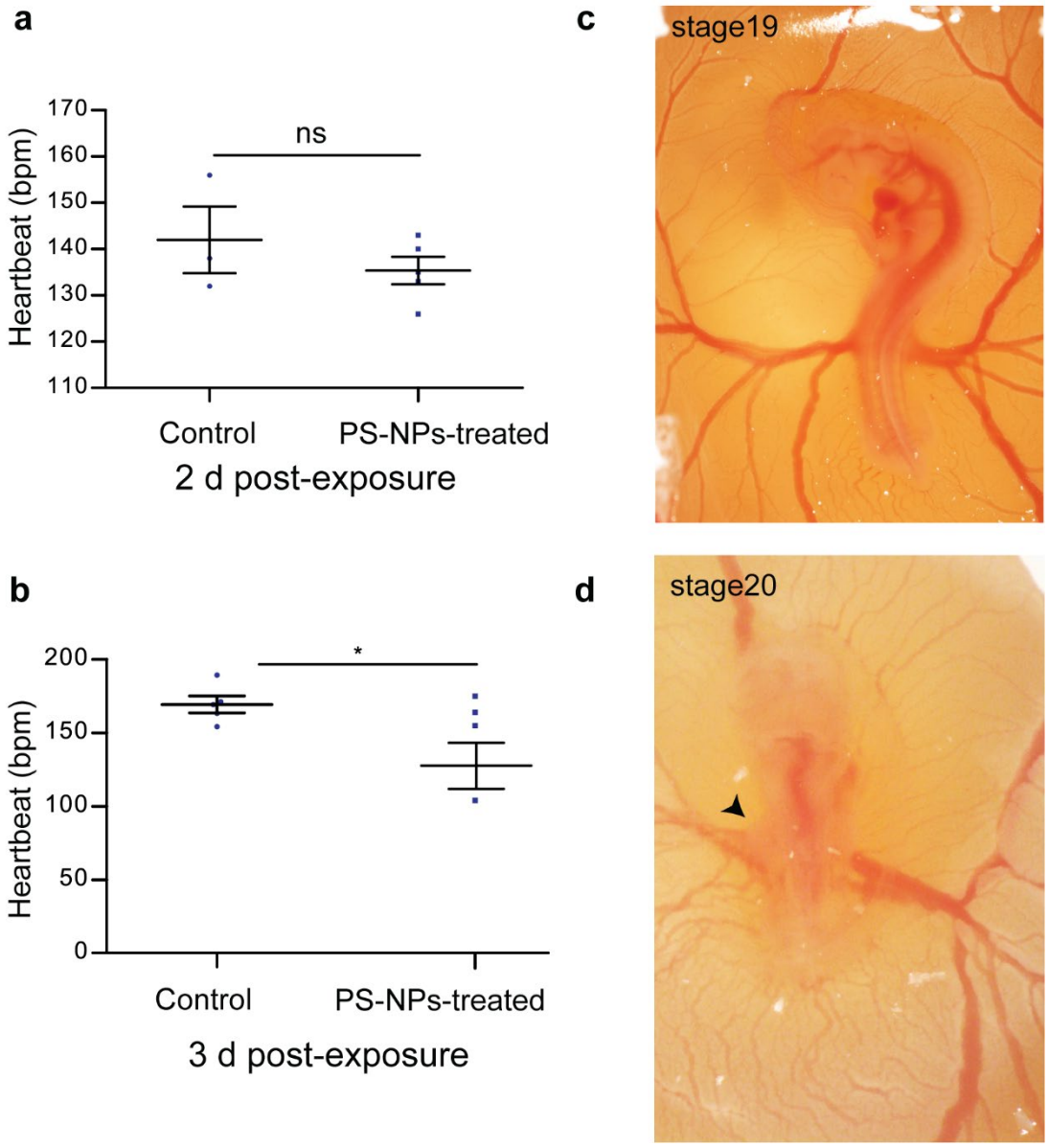

Fig. 3-2. **Heart rate and blood vessels abnormalities**. Heart rate (bpm) of 2 dpe (**a**) and 3 dpe (**b**) chick embryos, based on videos in ovo. **a**, 2 dpe chick embryos (*n* = 3 for control and *n* = 5 for PS-NP-treated). **b**, 3 dpe chick embryos (*n* = 5 for control and *n* = 4 for PS-NP-treated). **a** and **b**, data are mean ± s.e.m. Welch's t-test, P = 0.1148 for 2 dpe and P = 0.0458 for 3 dpe. **b** and **d**, chicken embryos at 2 dpe of control (**c**) and PS-NPs-treated (**d**). **c**, stage 19. **d**, stage 20, the symmetric vitelline (arrowhead) of the embryo, the left branches (arrowhead) are smaller.

Heart malformations in nanoplastic-treated embryos

One abnormality noted in PS-NPs treated embryos was an abnormal widening of vitelline blood vessels (Fig. 3-2). In some of the PS-NP treated embryos, the two dorsal aortae fuse ectopically. PS-NP treated embryos also show signs of cardiac defects when examined alive, *in ovo*, at 2 and 3 dpe. There was an abnormal abundance of cardiac jelly which continued into the apex of the heart in treated

embryos. Furthermore, the cardiac jelly appeared to be less cellularized (Fig. 3-3), most likely because of a diminished endothelial-mesenchymal transition in the endocardial lining. The myocardium also showed signs of being abnormally thin in the treated embryos (Fig. 3-3). We could not quantify any of these features in the live animals because of the rapid heartbeat.

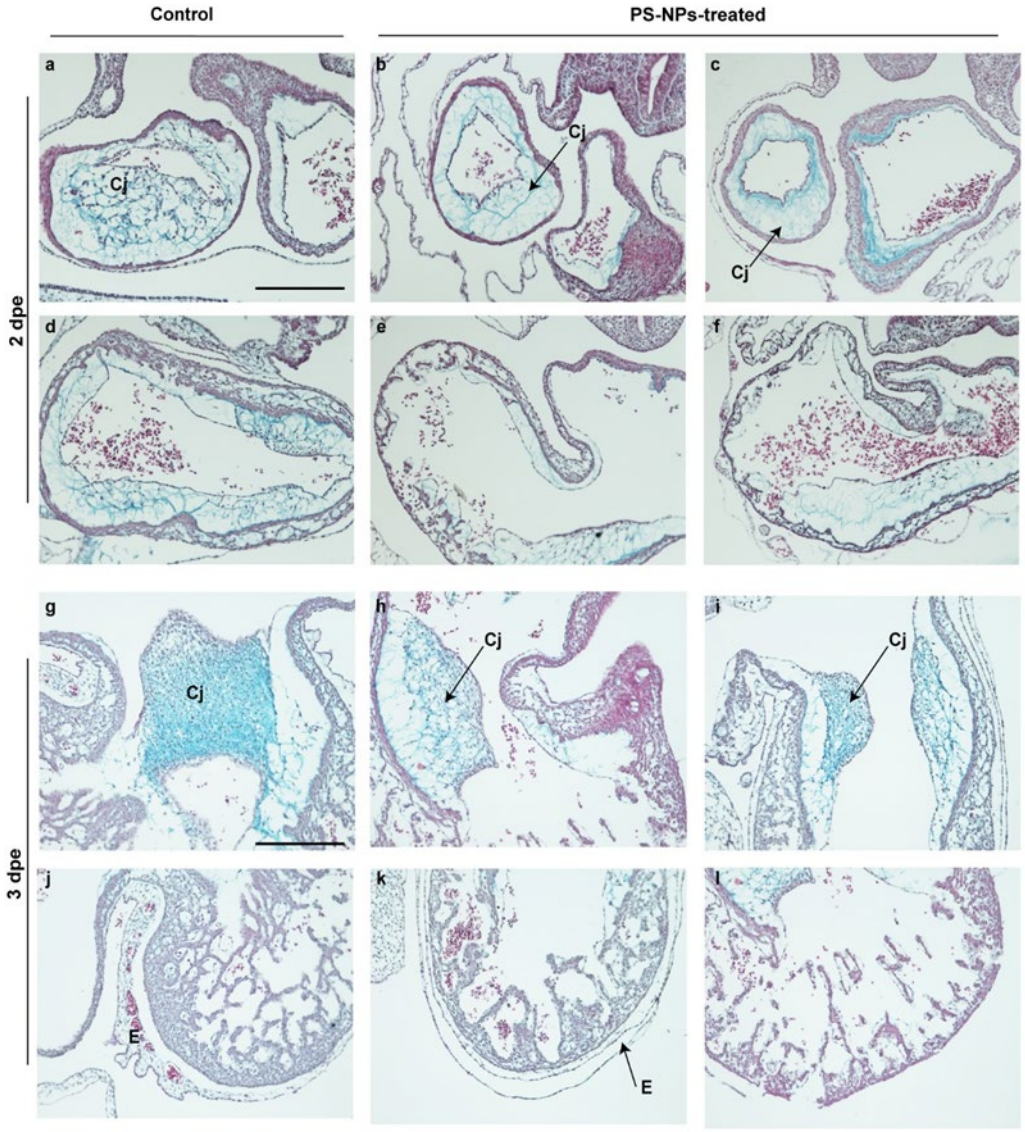

Fig. 3-3. **Heart malformation at 2 dpe and 3 dpe**. **a**-**l**, Transverse section stained with H&E and Alcian blue of **a**-**f** 2 dpe and **g**-**l** 3 dpe chick embryos. **a** and **d** control embryo, dark-stained nuclei in the cardiac jelly. **b** and **c**, PS-NPs-treated embryos, the lack of dark nuclei in the cardiac jelly is obvious. **e** and **f**, PS-NPs-treated embryos, the myocardium is thinner compared to the control embryo. **g** and **j**, heart of control embryo, note the amount of dark-stained nuclei in the cushions otherwise filled with proteoglycan-rich matrix (blue). **h** and **i**, heart of NPs treated embryo, lacking nuclei in the cushions particularly near the endocardial lining. The myocardial face of the cushion is relatively poor in matrix reflecting a defect in synthesis of the myocardium. **n**, heart of control embryo, the epicardium on the outside of the heart contains epicardium-derived cells (EPDCs) and small blood vessels. **k** and **l**, PS-

NPs-treated hearts, note the absent (**l**) or thin epicardium on the outside of the heart lacking EPDCs and blood vessels, and a thin less-trabeculated myocardium (**k**). *Key*: dpe, days post-exposure; PS-NPs Treated, polystyrene nanoparticles (5 mg/mL) treated; Cj, cardiac jelly; E, Epicardium; Scale bars are 250 µm. error bars, mean ± s.e.m.; significance of difference between control and experimental groups indicated by asterisks, *P <0.05.

Synchrotron scanning and histological sections at 8 dpe show malformations of the heart and great arteries (Fig. 3-4, Fig. 3-5, Table S3) in treated embryos. Of seven PS-NP treated embryos, three had a ventricular septal defect (Fig. 3-4h-j and n, Table S3), two had persistent or extra pharyngeal arch arteries (Fig. 3-5e-h, Table S3), one had persistent truncus arteriosus (Fig. 3-5j, Table S3) and two had aortopulmonary septal defects (Fig. 3-4o, Table S3).

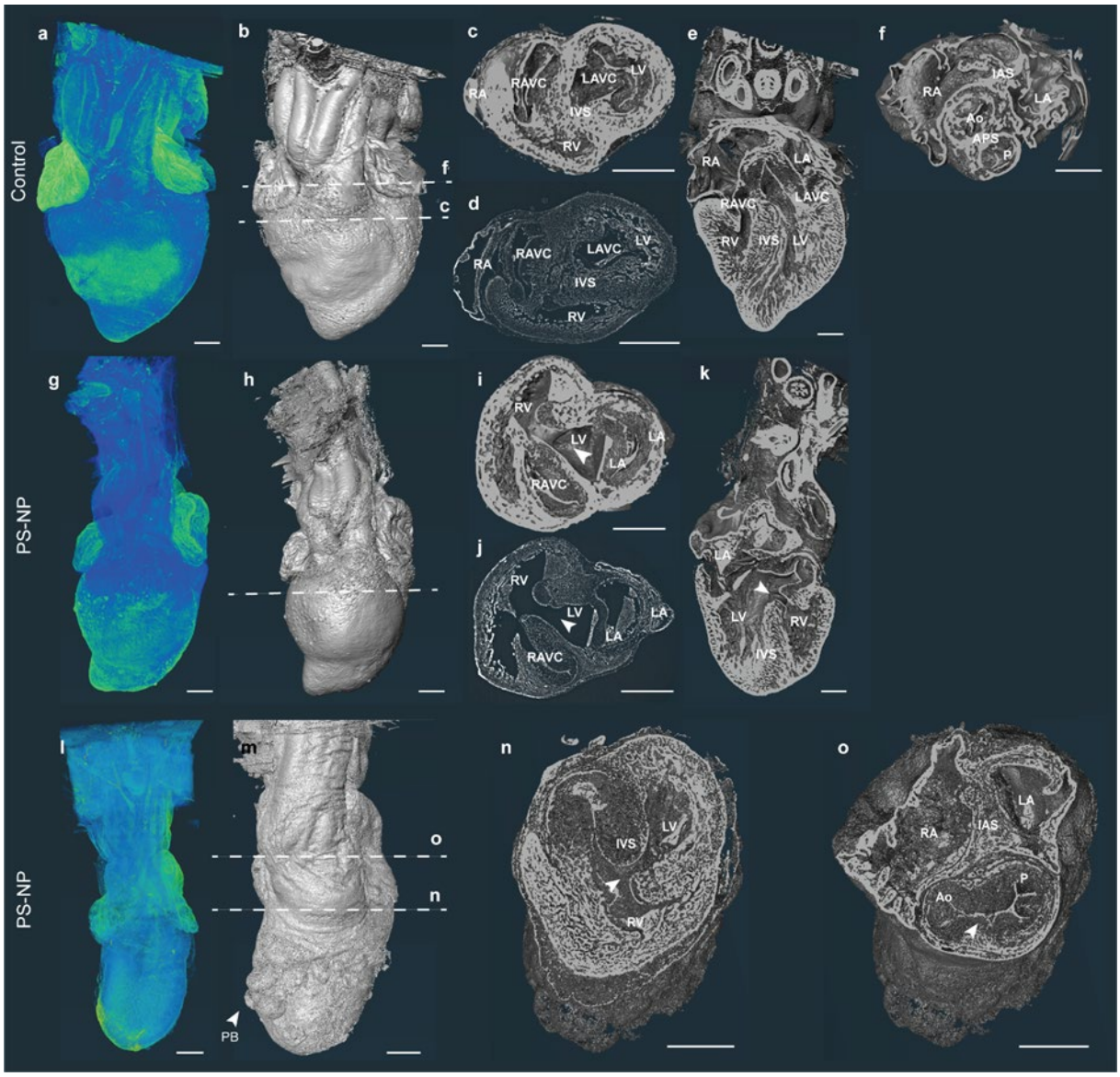

Fig. 3-4: **Synchrotron tomographic scans of hearts at 8 dpe**. **a**-**f**, control embryo, stage 35. *n* = 2. **g**-**o**, PS-NPs-treated embryos, both are stage 35. *n* = 2. (**b**, **c**, **d**, **f**), virtual sections of control embryo. (**i**, **j**, **n**, **o**), virtual transverse sections of PS-NPs-treated embryos. (**i**, **j**, **n**), virtual section at the top of the interventricular septum, with VSD (white arrow). **k**, **o**, virtual sections of the base of the outflow tract, showing APSD (white arrowhead). *Note*, treated heart in **l**-**o** both have aorticopulmonary septal defect (white arrowhead) and ventricular septal defect (white arrowhead). Key: Ao, Aorta; APS, Aorticopulmonary Septum; APSD, Aorticopulmonary Septal Defect; PB, Pericardial Blebbing; IAS, Interatrial Septum; IVS, Interventricular Septum; P, Pulmonary; LA, Left Atrium; LV, Left Ventricle; LAVC, Left Atrioventricular Canal; RA, Right Atrium; RV, Right Ventricle; RAVC, Right Atrioventricular Canal; VSD, Ventricle Septal Defect. Scale bars, 200 μm in **a**-**b**, **g**-**h**, **l**-**m** and 500 μm in **c**-**f**, **i**-**k** and **n**-**o**.

Effects of PS-NPs on expression of AP-2α and NKX2-5 genes

The analysis of 2 dpe chick embryos

We compared the wholemount *in situ* hybridization expression pattern of TFAP2A between control and NP-PS-treated embryos. In the control embryo (Fig. 3-6a), strong expression is seen in the telencephalon, in and around the eyes and in the pharyngeal arches, while less staining is observed in the area of the olfactory pit. All of the pharyngeal arches (maxilla, mandibular, hyoid, and arches 3, 4 and 6) show expression. TFAP2A is also expressed in the isthmus between the mesencephalon and the metencephalon. In contrast, we found a different expression pattern in the NP-PS-treated chick embryos (Fig. 3-6b-d). We noticed expression of TFAP2A was reduced in pharyngeal arches 3, 4 and/or 6 (Fig. 3-6b-d). Furthermore, the expression was observed to persist in the dorsal middle line or on the edges of neural folds (Fig. 3-6b and c), instead of disappearing as it did in the controls (Fig. 3-6a).

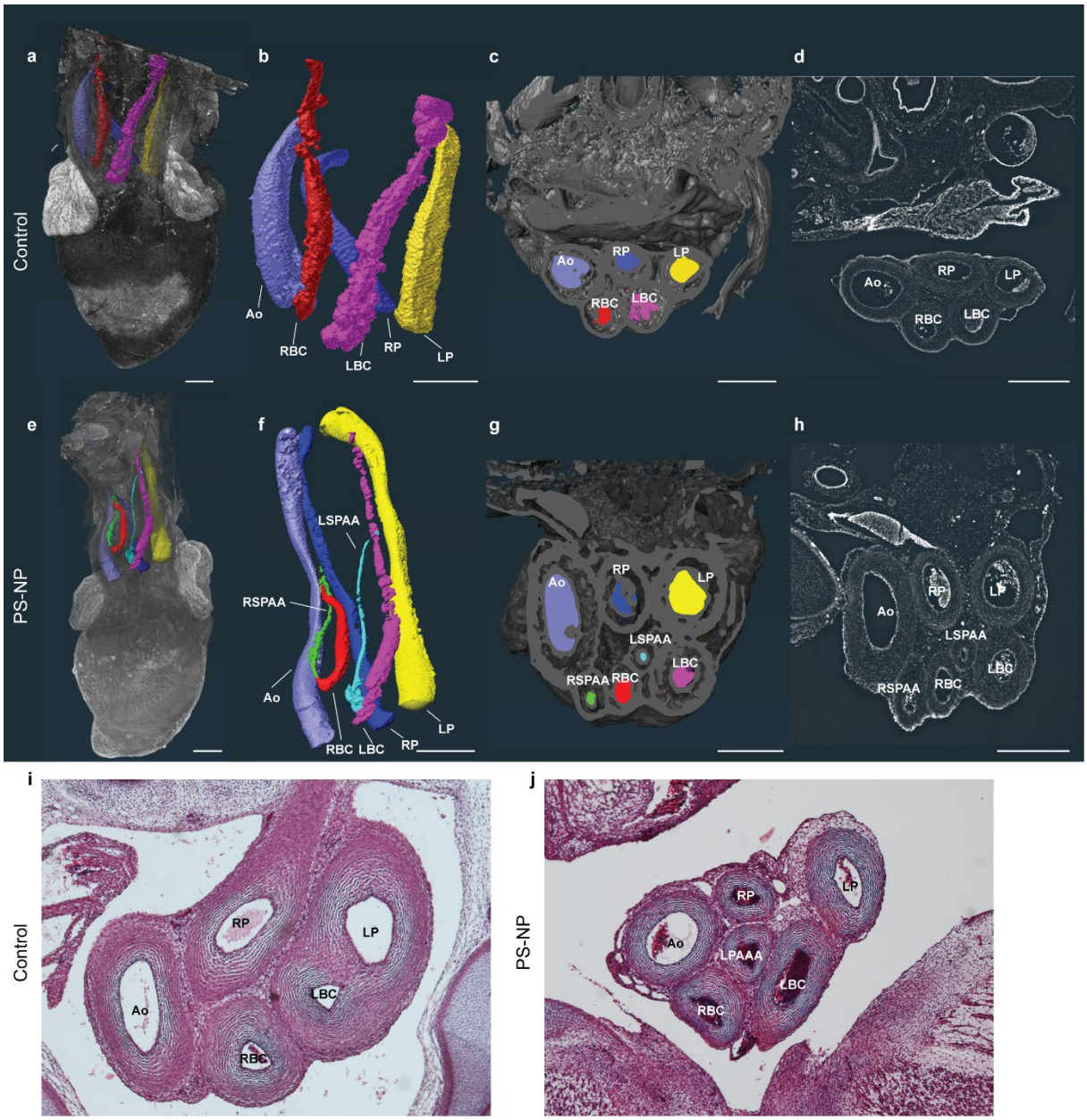

Fig. 3-5. **Synchrotron tomographic scans and transverse section of hearts at 8 dpe**. **a**-**h**, synchrotron tomographic scans of hearts and great vessels at 8 dpe. **a**-**d**, control embryo, stage 35. **e**-**h**, PS-NP treated, stage 35. **a** and **e**, volume rendering of heart and vessels. **b** and **f**, three-dimensional (3-D) model of great vessels produced by manual tracing. **c** and **g**, three-dimensional (3-D) view of virtual transverse sections. **d** and **h**, two-dimensional (2-D) view of virtual transverse sections. Transverse paraffin sections stained with H&E and Alcian blue of 8 dpe control (**i**) and PS-NPs-treated (**j**) chicken embryos. Key: Ao, Aorta; LAA, Persistent Left (4th) Aortic Arch Artery; LBC, Left Brachiocephalic Artery; LP, Left Pulmonary Artery; LSPAA, Left Supernumerary Pharyngeal Arch Arteries; RBC, Right Brachiocephalic Artery; RP, Right Pulmonary Artery; RSPAA, Right Supernumerary Pharyngeal Arch Artery.

In the case of the protein (AP-2α) of the gene TFAP2Athe expression pattern also differed between control and NP-PS-treated chick embryos. The location of AP-2α protein in pharyngeal arches is asymmetric. Particularly, in the Fig. 3-6g we see AP-2α

expression in the endoderm on one side of the arches, but barely in the other side. However, the AP-2α expression was found in ectoderm on both sides Fig. 3-6g. Interestingly, we found a cluster of cells expressing AP-2α appearing to be 'trapped' on the top of neural folds (Fig. 3-6g and h), as though they had not migrated out normally.

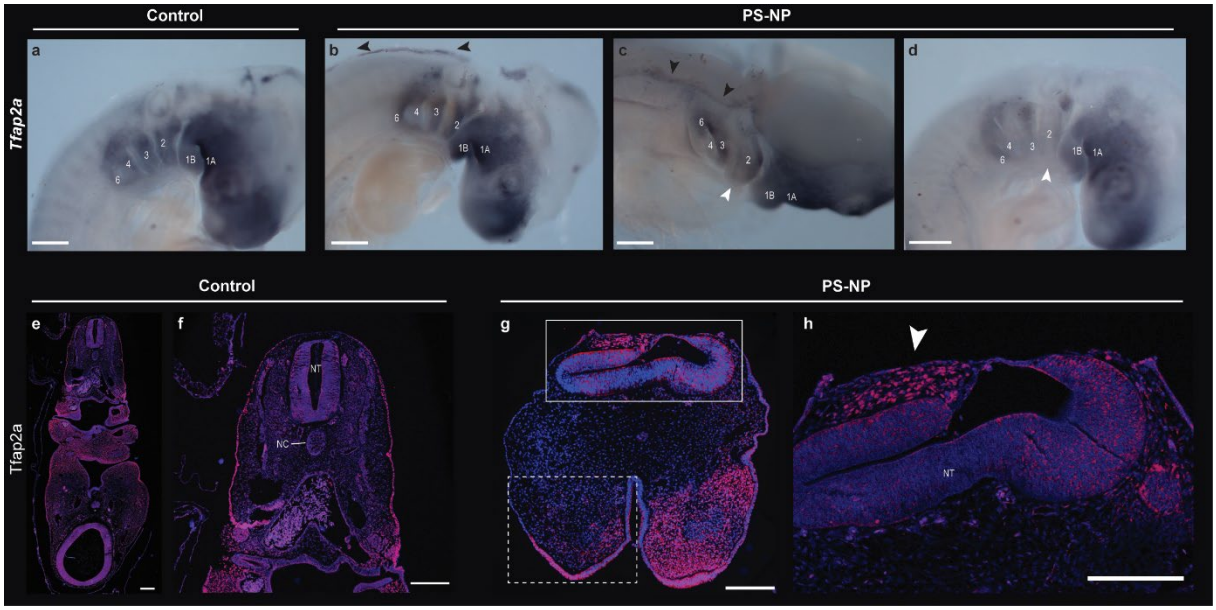

Fig. 3-6. **PS-NPs disrupt cardiac neural crest cell development in chicken embryos**. **a**-**d**, wholemount in situ hybridization for TFAP2A. **a**, control embryo, stage 19. *n* = 2. **b**-**d**, PS-NPs treated embryos, stage 18. **e**-**h**, immunochemistry showing TFAP2A (AP-2α protein; red channel) and DAPI (blue channel), transverse sections. *n* = 2 for control and *n* = 5 for PS-NPs-treated group. **e** and **f**, control chicken embryo, stage 19. **g** and **h**, PS-NPs treated embryo, stage 17. Key: black arrowhead in **b** and **c**, crest cells that apparently failed to migrate from the neural tube; white arrow in **c** and **d**, weaker expression of TFAP2A compared to control embryos. White dashed box in **g**, lack of AP-2α expression in one side of the arches. White arrowhead in **h**, some crest cells never leave the neural tube. Key: 1A, maxilla; 1B, mandible; 2, hyoid arch; 3, pharyngeal arch III; 4, pharyngeal arch IV; 6, pharyngeal arch VI; NT, neural tube; NC, notochord. Scale bars in **a**-**d**, 300 µm; in **s**-**v,** 200 µm. Blue, DAPI nuclear staining. Red, TFAP2A protein staining.

Both cardiac TNNI and NKX2-5 protein expression was compared between control and PS-NPs-treated embryos at 2 dpe (Fig. 3-7). The heart tube of the PS-NPs-treated embryos was less differentiated than that of control embryos, making it harder to distinguish the atrium from the ventricle. In the myocardium of the atrium and ventricle, similar expression patterns of cardiac TNNI and NKX2-5 are observed (Fig. 3-7a-d). DAPI staining showed that there are almost no nuclei present in the endocardial cushions of the heart (Fig. 3-7c and d).

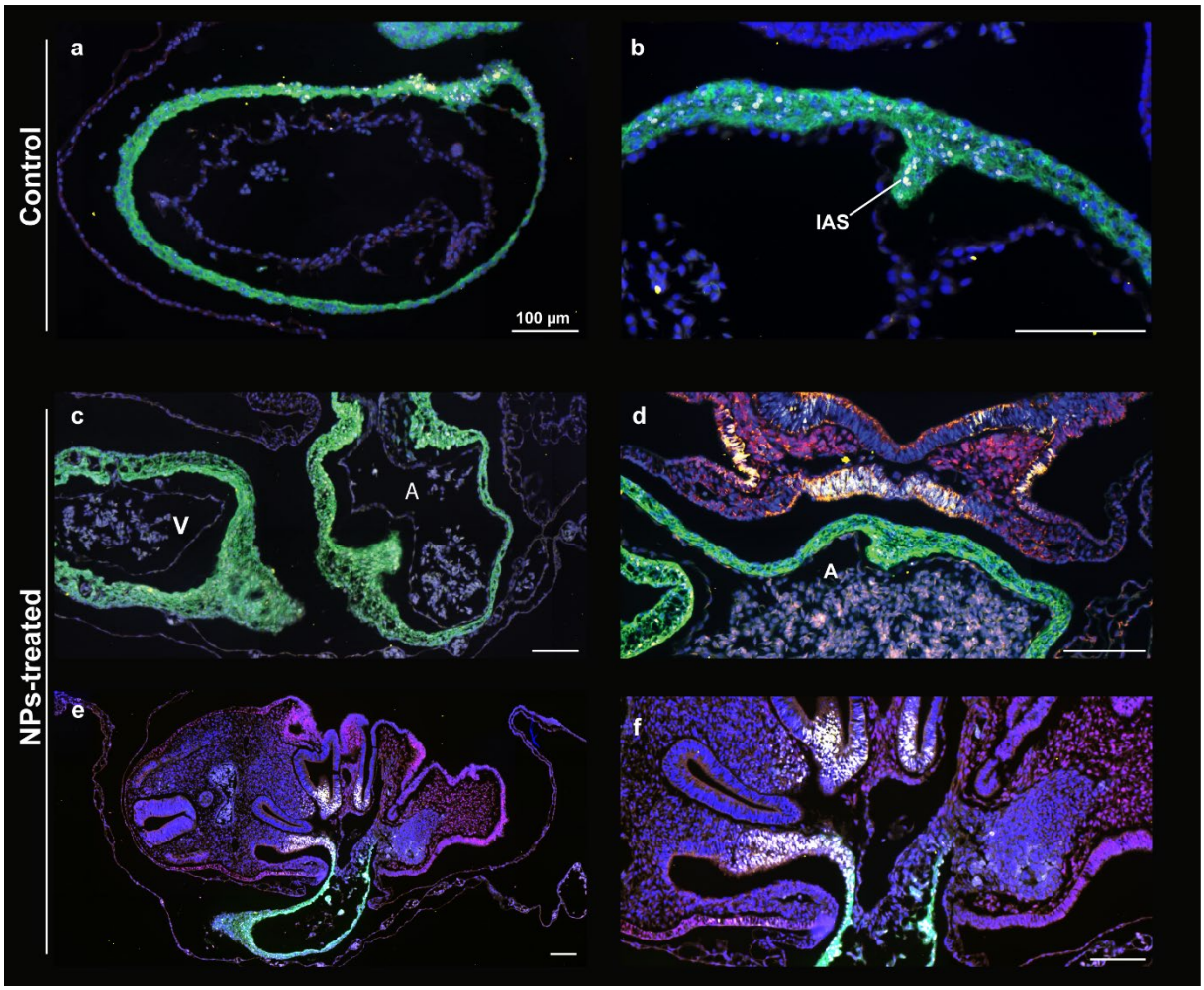

Fig. 3-7. **PS-NPs disrupt the development of the endocardial cushions of the heart in PS-NPs-treated chicken embryo at 2 dpe**. Immunochemistry for TFAP2A protein (AP-2α), NKX2-5 and cardiac TNNI performed on transverse sections of control and PS-NPs-treated chicken embryos at 2 dpe. **a** and **b**, control embryo, stage 18, *n* = 2, note the green staining TNNI in the cytoplasm and the NKX2-5 (yellow channel) in the nuclei of cells in the myocardium and inter-atrial septum. (**b**). **c**-**f**, PS-NPs-treated embryos, *n* = 5. **c**, stage 17. **d**, stage 20. **e** and **f**, both are stage 17. In **c** and **d**, the same staining has been observed in the myocardium of the PS-NPs-treated embryos. In **d**-**f**, note the NKX2-5 expression (yellow channel) in the endoderm and nuclei of the splanchnic mesoderm and myocardium. *Key*: A, atrium; IAS, inter-atrial septum; V, ventricle. Scale bars are all 100 µm. Blue, DAPI nuclear staining. Yellow, NKX2-5 protein staining. Red, TFAP2A protein staining. Green, TNNI protein staining.

The analysis of 3 dpe chick embryos

We found expression of NKX2-5 only in the PS-NPs-treated embryos, but less in control embryos (Fig. 3-8). It is highly likely that the weak staining was caused by technical problem, since that NKX2-5 play an essential role in the development of

cardiomyocytes and in cardiac precursors (Jamali et al., 2001; Paffett-Lugassy et al., 2013). We think the concentration of antibodies we used in the control embryos were relatively low. Among the PS-NP-treated embryos, the expression of NKX2-5 was located in the in the middle of the flow divider (Fig. 3-8e). In addition, the flow divider was unusually massive in some of the PS-NP-treated embryos (Fig. 3-8f). NKX2-5 expression was also observed at in the inflow end of the heart tube, continuing into the myocardium (Fig. 3-8g). Moreover, NKX2-5 staining was also observed in the ventricular wall (Fig. 3-8h). This expression was in the nuclei of the cells, most likely the excitatory cells of the heart muscle (Fig. 3-8h).

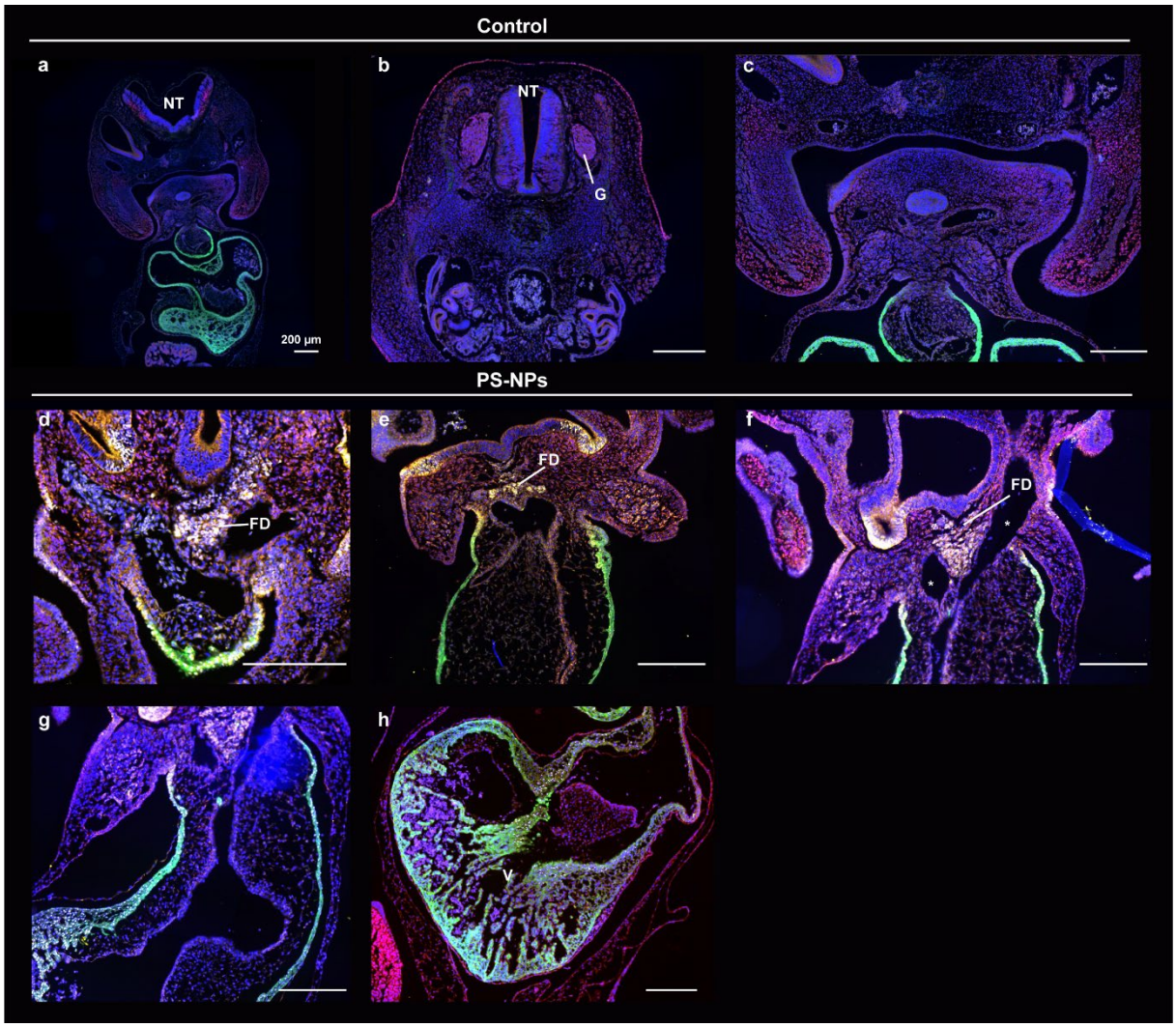

Fig. 3-8. **PS-NPs disrupt the development of the second heart field in the chicken embryos at 3 dpe**. **a**-**c**, control embryo, stage 23. **d**-**f**, PS-NPs-treated embryos. **d**, stage 24, **e**, stage 22, **f**-**h**, stage 21. Note the red staining in the ectoderm in (**a**), ganglia (**b**) and pharyngeal arches (**c**). Little or no NKX2-5 expression is seen in control embryos, but strong expression is seen in PS-NPs-treated embryos.

NKX2-5 expression (yellow channel) was observed in nuclei of the flow divider (**d**-**f**). Yellow staining was also observed at the start of the heart tube, continuing into the myocardium (**f**-**h**). Key: Asterisk (*), double outflow tract; FD, flow divider; G, ganglion; NT, neural tube; V, Ventricle. Blue, DAPI nuclear staining. Yellow, NKX2-5 protein staining. Red, TFAP2A protein staining. Green, TNNI protein staining.

Discussion

We have described a wide spectrum of severe malformations in chicken embryos exposed *in ovo* to 25 nm PS-NPs. The malformations include neural tube and craniofacial defects, as noted previously (Nie et al., 2021). In addition to those reported before, we found heart malformations, bradycardia, persistent or extra pharyngeal arch arteries, maxillary hypoplasia, axial defects, tail aplasia and, in one specimen, bilateral phocomelia of the hindlimbs. We also found that treated embryos showed defective cellularization of the cardiac jelly, thinned myocardium and reduced diameter of some blood vessels. This is a much wider spectrum of malformations than previously reported, and the congenital heart defects are reported here for the first time.

It has previously been shown that such malformations can also be produced in the chicken embryo by surgical ablation of the cardiac neural crest (Keyte and Hutson, 2012; Kirby and Waldo, 1995), that is, the crest cells at the axial level between the otocyst and somite three (Hutson and Kirby, 2007). The early-stage cardiovascular abnormalities, including altered hemodynamics that we observed have also been reported in other studies in which pre-migratory cardiac neural crest were surgically ablated (Kirby and Waldo, 1990; Waldo et al., 1999). At later stages, treated embryos showed instances of abnormal branching of the pharyngeal arch arteries, ventricular septal defects and aortopulmonary septal defects. These malformations likely arise because of damage to the neural crest, which is essential for normal development of the aortopulmonary septal complex of the heart and the wall of the great vessels (Erhardt et al., 2021; Hutson and Kirby, 2007; Kirby and Waldo, 1995; Newbern et al., 2008; Poelmann et al., 1998; Porras and Brown, 2008). We also observed epicardial

blebbing, probably caused by disturbed fluid handling of the developing coronary system that showed scant arterial development and no ingrowth into the neural crest-dependent aortic root (Gittenberger-de Groot et al., 2012). We also noted ectopia cordis, a phenotype associated with congenital cardiac malformations in human such as double outlet right ventricle (Malik et al., 2015).

In addition, we have observed thinner myocardium in the outflow tract compared to the ventricle in PS-NPs-treated embryo. This suggests that either the migration of the neural crest cells is arrested, or perhaps their signaling is affected. It could be that PS-NPs affect the development of the second heart field. The presence of neural crest cells is needed for normal second heart field development (Waldo et al., 2005). The second heart field is a population of cells located around the ventral caudal pharynx which plays an important role in lengthening of the outflow tract, and for the proper alignment of the aorta and pulmonary trunk with respect to the septal complex. Disruption of these processes can already be detected early, that is, before the neural crest cells reach the outflow tract (Keyte and Hutson, 2012). If cardiac neural crest cells are ablated experimentally, the myocardial cells from the second heart field may fail to be incorporated normally into the myocardium, causing abnormal looping of the heart (Yelbuz et al., 2002).

In addition to cardiac malformations, we often saw hypoplasia or aplasia of the upper beak, and failure of Meckel's cartilage to fuse with its contralateral partner. The co-occurrence of cardiac and craniofacial malformations in our study is consistent with the fact that the cranial neural crest contributes to the development of both the heart and the facial skeleton (Keyte and Hutson, 2012). The idea of a mechanistic link between cardiac and craniofacial development is embodied in the concept of the 'cardiocraniofacial module' (Keyte and Hutson, 2012). Furthermore an association of cardiac and craniofacial malformations is seen in clinical syndromes such as DiGeorge syndrome (chromosome 22q11.2 deletion syndrome) (McDonald-McGinn and Sullivan, 2011).

Our results show that 25 nm PS-NPs cause various cardiac and vascular defects in the chicken embryo. These defects include: excess cardiac jelly with a lack of epithelial mesenchymal transition, thin epicardium and myocardium, ventricular septal defect, persistent truncus arteriosus and supernumerary arteries. One of these defects alone, or a combination of defects, probably explain the abnormal cardiac function that we observed (lower heart rate and abnormal blood flow) in PS-NPs-treated embryos. We speculate that these cardiac effects could result in high mortality rate among PS-NPs-treated embryos. In Chapter 4, we will explore the potential cellular mechanisms of PS-NP toxicity to embryos.

References

Abd-Elgaliel, W. R. and Tung, C. H. (2012). A Cardiac Tissue-Specific Binding Agent of Troponin I. *Mol Biosyst* **8**, 2629-2632.

Anagnosti, L., Varvaresou, A., Pavlou, P., Protopapa, E. and Carayanni, V. (2021). Worldwide Actions against Plastic Pollution from Microbeads and Microplastics in Cosmetics Focusing on European Policies. Has the Issue Been Handled Effectively? *Marine Pollution Bulletin* **162**, 111883.

Bamforth, S. D., Braganca, J., Eloranta, J. J., Murdoch, J. N., Marques, F. I., Kranc, K. R., Farza, H., Henderson, D. J., Hurst, H. C. and Bhattacharya, S. (2001). Cardiac Malformations, Adrenal Agenesis, Neural Crest Defects and Exencephaly in Mice Lacking Cited2, a New Tfap2 Co-Activator. *Nat Genet* **29**, 469-474.

Bancroft, J. D. and Gamble, M. (2008). *Theory and Practice of Histological Techniques*: Elsevier Health Sciences.

Boehnke, N., Straehla, J. P., Safford, H. C., Kocak, M., Rees, M. G., Ronan, M., Rosenberg, D., Adelmann, C. H., Chivukula, R. R., Nabar, N., et al. (2022). Massively Parallel Pooled Screening Reveals Genomic Determinants of Nanoparticle Delivery. *Science* **377**, eabm5551.

Brewer, S., Jiang, X., Donaldson, S., Williams, T. and Sucov, H. M. (2002). Requirement for Ap-2alpha in Cardiac Outflow Tract Morphogenesis. *Mech Dev* **110**, 139-149.

Cotti, S., Huysseune, A., Koppe, W., Rücklin, M., Marone, F., Wölfel, E. M., Fiedler, I. A., Busse, B., Forlino, A. and Witten, P. E. (2020). More Bone with Less Minerals? The Effects of Dietary Phosphorus on the Post-Cranial Skeleton in Zebrafish. *International Journal of Molecular Sciences* **21**, 5429.

Cox, K. D., Covernton, G. A., Davies, H. L., Dower, J. F., Juanes, F. and Dudas, S. E. (2019). Human Consumption of Microplastics. *Environmental Science & Technology* **53**, 7068-7074.

de Bakker, M. A. G., Fowler, D. A., Oude, K. d., Dondorp, E. M., Navas, M. C. G., Horbanczuk, J. O., Sire, J.-Y., Szczerbińska, D. and Richardson, M. K. (2013). Digit Loss in Archosaur Evolution and the Interplay between Selection and Constraints. *Nature* **500**, 445-448.

Erhardt, S., Zheng, M., Zhao, X., Le, T. P., Findley, T. O. and Wang, J. (2021). The Cardiac Neural Crest Cells in Heart Development and Congenital Heart Defects. *J Cardiovasc Dev Dis* **8**.

European_Commission (2022). Commission Regulation (Eu) Amending Annex Xvii to Regulation (Ec) No 1907/2006 of the European Parliament and of the Council Concerning the Registration, Evaluation, Authorisation and Restriction of Chemicals (Reach) as Regards Synthetic Polymer Microparticles. pp. 12. Brussels.

Feng, M., Luo, J., Wan, Y., Zhang, J., Lu, C., Wang, M., Dai, L., Cao, X., Yang, X. and Wang, Y. (2022). Polystyrene Nanoplastic Exposure Induces Developmental Toxicity by Activating the Oxidative Stress Response and Base Excision Repair Pathway in Zebrafish (Danio Rerio). *ACS omega* **7**, 32153-32163.

Gittenberger-de Groot, A. C., Winter, E. M., Bartelings, M. M., Goumans, M. J., DeRuiter, M. C. and Poelmann, R. E. (2012). The Arterial and Cardiac Epicardium in Development, Disease and Repair. *Differentiation* **84**, 41-53.

Hutson, M. R. and Kirby, M. L. (2007). Model Systems for the Study of Heart Development and Disease. Cardiac Neural Crest and Conotruncal Malformations. *Semin Cell Dev Biol* **18**, 101-110.

Jamali, M., Rogerson, P. J., Wilton, S. and Skerjanc, I. S. (2001). Nkx2–5 Activity Is Essential for Cardiomyogenesis*. *Journal of Biological Chemistry* **276**, 42252-42258.

Jenner, L. C., Rotchell, J. M., Bennett, R. T., Cowen, M., Tentzeris, V. and Sadofsky, L. R. (2022). Detection of Microplastics in Human Lung Tissue Using Mftir Spectroscopy. *Sci Total Environ* **831**, 154907.

Keyte, A. and Hutson, M. R. (2012). The Neural Crest in Cardiac Congenital Anomalies. *Differentiation* **84**, 25-40.

Kirby, M. L. and Waldo, K. L. (1990). Role of Neural Crest in Congenital Heart Disease. *Circulation* **82**, 332-340.

Kirby, M. L. and Waldo, K. L. (1995). Neural Crest and Cardiovascular Patterning. *Circ.Res.* **77**, 211-215.

Koelmans, A. A., Nor, N. H. M., Hermsen, E., Kooi, M., Mintenig, S. M. and De France, J. (2019). Microplastics in Freshwaters and Drinking Water: Critical Review and Assessment of Data Quality. *Water research*.

Kögel, T., Bjorøy, Ø., Toto, B., Bienfait, A. M. and Sanden, M. (2020). Micro-and Nanoplastic Toxicity on Aquatic Life: Determining Factors. *Science of The Total Environment* **709**, 136050-136050.

Leslie, H. A., van Velzen, M. J. M., Brandsma, S. H., Vethaak, A. D., Garcia-Vallejo, J. J. and Lamoree, M. H. (2022). Discovery and Quantification of Plastic Particle Pollution in Human Blood. *Environ Int* **163**, 107199.

Mai, C. T., Isenburg, J. L., Canfield, M. A., Meyer, R. E., Correa, A., Alverson, C. J., Lupo, P. J., Riehle-Colarusso, T., Cho, S. J., Aggarwal, D., et al. (2019). National Population-Based Estimates for Major Birth Defects, 2010–2014. *Birth Defects Research* **111**, 1420-1435.

Malik, R., Zilberman, M. V., Tang, L., Miller, S. and Pandian, N. G. (2015). Ectopia Cordis with a Double Outlet Right Ventricle, Large Ventricular Septal Defect, Malposed Great Arteries and Left Ventricular Hypoplasia. *Echocardiography* **32**, 589-591.

Marone, F., Studer, A., Billich, H., Sala, L. and Stampanoni, M. (2017). Towards on-the-Fly Data Post-Processing for Real-Time Tomographic Imaging at Tomcat. *Advanced Structural and Chemical Imaging* **3**, 1-11.

McClelland, K. S., Ng, E. T. and Bowles, J. (2016). Agarose/Gelatin Immobilisation of Tissues or Embryo Segments for Orientated Paraffin Embedding and Sectioning. *Differentiation* **91**, 68-71.

McCulley, D. J. and Black, B. L. (2012). Chapter Nine - Transcription Factor Pathways and Congenital Heart Disease. In *Current Topics in Developmental Biology* (ed. B. G. Bruneau), pp. 253-277: Academic Press.

McDonald-McGinn, D. M. and Sullivan, K. E. (2011). Chromosome 22q11.2 Deletion Syndrome (Digeorge Syndrome/Velocardiofacial Syndrome). *Medicine (Baltimore)* **90**, 1-18.

Mitrano, D. M., Wick, P. and Nowack, B. (2021). Placing Nanoplastics in the Context of Global Plastic Pollution. *Nature Nanotechnology* **16**, 491-500.

Newbern, J., Zhong, J., Wickramasinghe, R. S., Li, X., Wu, Y., Samuels, I., Cherosky, N., Karlo, J. C., O'Loughlin, B., Wikenheiser, J., et al. (2008). Mouse and Human Phenotypes Indicate a Critical Conserved Role for Erk2 Signaling in Neural Crest Development. *Proc Natl Acad Sci U S A* **105**, 17115-17120.

Nie, J.-h., Shen, Y., Roshdy, M., Cheng, X., Wang, G. and Yang, X. (2021). Polystyrene Nanoplastics Exposure Caused Defective Neural Tube Morphogenesis through Caveolae-Mediated Endocytosis and Faulty Apoptosis. *Nanotoxicology*, 1-20.

Paffett-Lugassy, N., Singh, R., Nevis, K. R., Guner-Ataman, B., O'Loughlin, E., Jahangiri, L., Harvey, R. P., Burns, C. G. and Burns, C. E. (2013). Heart Field Origin of Great Vessel Precursors Relies on Nkx2.5-Mediated Vasculogenesis. *Nature Cell Biology* **15**, 1362-1369.

Paganin, D., Mayo, S. C., Gureyev, T. E., Miller, P. R. and Wilkins, S. W. (2002). Simultaneous Phase and Amplitude Extraction from a Single Defocused Image of a Homogeneous Object. *Journal of Microscopy* **206**, 33-40.

Pitt, J. A., Kozal, J. S., Jayasundara, N., Massarsky, A., Trevisan, R., Geitner, N., Wiesner, M., Levin, E. D. and Di Giulio, R. T. (2018). Uptake, Tissue Distribution, and Toxicity of Polystyrene Nanoparticles in Developing Zebrafish (*Danio Rerio*). *Aquatic Toxicology* **194**, 185-194.

Poelmann, R. E., Mikawa, T. and Gittenberger-de Groot, A. C. (1998). Neural Crest Cells in Outflow Tract Septation of the Embryonic Chicken Heart: Differentiation and Apoptosis. *Dev Dyn* **212**, 373-384.

Porras, D. and Brown, C. B. (2008). Temporal-Spatial Ablation of Neural Crest in the Mouse Results in Cardiovascular Defects. *Dev Dyn* **237**, 153-162.

Schwabl, P., Köppel, S., Königshofer, P., Bucsics, T., Trauner, M., Reiberger, T. and Liebmann, B. (2019). Detection of Various Microplastics in Human Stool: A Prospective Case Series. *Ann Intern Med* **171**, 453-457.

Stampanoni, M., Groso, A., Isenegger, A., Mikuljan, G., Chen, Q., Bertrand, A., Henein, S., Betemps, R., Frommherz, U. and Böhler, P. (2006). Trends in Synchrotron-Based Tomographic Imaging: The Sls Experience. In *Developments in X-ray Tomography V*, pp. 193-206: SPIE.

Sulukan, E., Şenol, O., Baran, A., Kankaynar, M., Yıldırım, S., Kızıltan, T., Bolat, İ. and Ceyhun, S. B. (2022). Nano-Sized Polystyrene Plastic Particles Affect Many Cancer-Related Biological Processes Even in the Next Generations; Zebrafish Modeling. *Science of The Total Environment* **838**, 156391.

Vighi, M., Bayo, J., Fernández-Piñas, F., Gago, J., Gómez, M., Hernández-Borges, J., Herrera, A., Landaburu, J., Muniategui-Lorenzo, S. and Muñoz, A.-R. (2021). Micro and Nano-Plastics in the Environment: Research Priorities for the near Future. *Reviews of Environmental Contamination and Toxicology Volume 257*, 163-218.

Waldo, K., Zdanowicz, M., Burch, J., Kumiski, D. H., Stadt, H. A., Godt, R. E., Creazzo, T. L. and Kirby, M. L. (1999). A Novel Role for Cardiac Neural Crest in Heart Development. *J Clin Invest* **103**, 1499-1507.

Waldo, K. L., Hutson, M. R., Stadt, H. A., Zdanowicz, M., Zdanowicz, J. and Kirby, M. L. (2005). Cardiac Neural Crest Is Necessary for Normal Addition of the Myocardium to the Arterial Pole from the Secondary Heart Field. *Dev Biol* **281**, 66-77.

Wan, J.-K., Chu, W.-L., Kok, Y.-Y. and Lee, C.-S. (2018). Distribution of Microplastics and Nanoplastics in Aquatic Ecosystems and Their Impacts on Aquatic Organisms, with Emphasis on Microalgae. *Reviews of Environmental Contamination and Toxicology Volume 246*, 133-158.

Xu, Q. and Wilkinson, D. G. (1998). In Situ Hybridization of Mrna with Hapten Labelled Probes. *In Situ Hybridisation: A Practical Approach*, 87-106.

Yelbuz, T. M., Waldo, K. L., Kumiski, D. H., Stadt, H. A., Wolfe, R. R., Leatherbury, L. and Kirby, M. L. (2002). Shortened Outflow Tract Leads to Altered Cardiac Looping after Neural Crest Ablation. *Circulation* **106**, 504-510.

Zhang, J., Wang, L. and Kannan, K. (2020). Microplastics in House Dust from 12 Countries and Associated Human Exposure. *Environment international* **134**, 105314.

Zhang, Y., Yin, K., Wang, D., Wang, Y., Lu, H., Zhao, H. and Xing, M. (2022). Polystyrene Microplastics-Induced Cardiotoxicity in Chickens Via the Ros-Driven Nf-Kb-Nlrp3-Gsdmd and Ampk-Pgc-1α Axes. *Science of The Total Environment* **840**, 156727.

Zhu, X., Wang, C., Duan, X., Liang, B., Genbo Xu, E. and Huang, Z. (2023). Micro- and Nanoplastics: A New Cardiovascular Risk Factor? *Environment International* **171**, 107662.

Chapter 4. Nanoplastics passive target neural crest cells in the chicken embryo

Meiru Wang[1,2], Carmen L. de Mooij[1], Gerda E.M. Lamers[1], Merijn A.G. de Bakker[1], Martina G. Vijver[3], Michael K. Richardson[1].*

1. Institute of Biology, Leiden University, Sylvius Laboratory, Sylviusweg 72, 2333 BE, Leiden, The Netherlands.
2. Naturalis Biodiversity Center, Darwinweg 2, 2333 CR, Leiden, The Netherlands.
3. Institute of Environmental Sciences, Leiden University (CML), Van Steenis Building, Einsteinweg 2, 2333 CC, Leiden, The Netherlands.

This chapter has been published as part of: Wang, M., Rücklin, M., Poelmann, R.E., de Mooij, C.L., Fokkema, M., Lamers, G.E.M., de Bakker, M.A.G., Chin, E., Bakos, L.J., Marone, F., Wisse, B.J., de Ruiter, M.C., Cheng, S., Nurhidayat, L., Vijver, M.G., Richardson, M.K. Nanoplastics causes extensive congenital malformations during embryonic development by passively targeting neural crest cells. *Environment International* **173**, 107865. https://doi.org/10.1016/j.envint.2023.107865.

Abstract

Plastic pollution is a major environmental concern. Plastics waste in the environment continuously degrades into microplastics and nanoplastics. It has been previously reported that polystyrene nanoparticles can cause neural tube defects in the developing chick embryos. The authors of that study suggested a mechanism whereby nanoplastics cause caveolae-mediated endocytosis in neural tube cells. In Chapters 2 and 3, we found that nanoplastics also cause defects in the eyes, tailbud, heart and vascular system of chicken embryos. However, the mechanism previously proposed, of neural tube damage, could not account for this wide spectrum of malformations. Therefore, in this Chapter, we look in more detail at the cellular mechanisms involved. We exposed stage 8 chicken embryos to 25 nm fluorescent polystyrene nanoparticles in ovo. We found that the nanoparticles became localized to cell masses in the dorsal middle line of the neural tube. Molecular markers identified these cell masses as neural crest cells that had failed to migrate to the periphery. TUNEL staining of nanoplastic-exposed embryos showed that nanoplastics caused death and impaired migration of those cells. When we added fluorescent 25 nm fluorescent polystyrene nanoparticles to primary chick neural crest cells, we found that they could enter the cells within 2 h. Further supporting our hypothesis that nanoplastics specifically disrupt neural crest development, most of the malformations seen in Chapter 2 and Chapter 3 are in organs that depend for their normal development on neural crest cells. Our results demonstrate that polystyrene nanoparticles cause developmental toxicity to chick embryos. Our findings suggest that nanoplastics may pose a health risk to the developing embryo. This is a matter of concern given the large and growing burden of nanoplastics in the environment, and the potential use of nanoplastics in human medicine as drug-delivery vehicles.

Introduction

Plastic as a material is widely used, because of its low cost and ease of production, its versatility and imperviousness to water (Copp et al., 2003). The other advantages of using plastics including high strength-to-weight ratio, ductility, corrosion resistance, bio-inertness, high thermal/electrical insulation and outstanding durability at a relatively low lifetime cost. For these reasons, plastics have enabled progression and changes in a variety of industries, from automotive and aerospace applications, right through to textiles and consumer products, construction and agriculture, and food packaging (Andrady et al., 2015). Its ability to guard against contamination makes plastic useful for example in sterile medical environments such as hospitals, or as food packaging. Nanoplastics are also being considered for therapeutic use in humans, including as drug-delivery systems (Boehnke et al., 2022). Its success in industry and society combined with the persistence of plastic have resulted in plastic waste and pollution being widespread and ubiquitous in today's environment (Andrady et al., 2015). Thus, there are many opportunities for humans to absorb microplastics and nanoplastics (MPs and NPs) by skin contact, food ingestion and even inhalation (Sana et al., 2020).

In Chapter 2, we showed that 25 nm plain polystyrene nanoplastics could cause neural tube defects in developing chick embryos. In humans, neural tube defects are severe congenital defects with high mortality (in the case of cranial defects), long-term disability and costly surgical repair (Oumer et al., 2021). The causes of neural tube defect can be genetic or non-genetic factors (e.g. lack of folic acid; (Copp et al., 2013) or a combination of these factors (Greene et al., 2009). We hypothesis that nanoplastics might represent a novel environmental factor for neural tube defects, based on the work that we (Wang et al., 2023) and others (Nie et al., 2021; Yan et al., 2020) have published showing nanoparticle-induced neural tube defects in the chick

embryo. As neural tube defects are caused by a failure of neurulation, I shall now discuss the various mechanisms involved in neural tube development (neurulation).

There are two types of neurulation during the development of chick embryo, namely, primary neurulation and secondary neurulation (Schoenwolf, 2018; Shimokita and Takahashi, 2011; van der Spuy et al., 2023). Primary neurulation is the rolling-up of the neural plate to form a hollow tube, whereas secondary neurulation is the formation of a solid neural keel which secondarily becomes hollow (Dady et al., 2014). We have observed neural tube defects related to both of these processes (Chapter 2). Therefore, it is likely that PS-NPs disrupt the primary and/or neurulation of developing chick embryos. It is still unclear the mechanism underlying the NTDs caused by PS-NPs exposure.

In addition to neural tube defects observed in PS-NPs treated chick embryos (Chapter 2), we also noticed, on histological sections, an anomalous clump of cells located in lumen of neural tube. We speculated that these were likely neural crest cells, based on their location. This hypothesis is strengthened by the fact that these cells express the neural crest marker TFAP2A (Chapter 3). Neural crest cells are an embryonic population of migratory stem cells (Achilleos and Trainor, 2012). In birds, neural crest cells arise from the margins of the neural ectoderm and become localized to the neural folds (Le Douarin, 2004). After the neural folds meet in the dorsal middle line, the neural crest cells start to detach from the ectoderm and migrate through the mesoderm into various tissue and organs (Le Douarin, 1999). These migratory cells differentiate into various cell types, contributing to the development and function of multiple organs (Kirby and Waldo, 1995; Martik and Bronner, 2021; Waldo et al., 1999).

In this research, we want to investigate the possible mechanism of how PS-NPs cause neural tube defects. We want to use *in situ* hybridization to identify the potential tissue or cell population which has been affect by PS-NPs. *In situ* hybridization is a tool for locating mRNA transcripts in whole specimens (‘wholemount *in situ*

hybridization') or sections (Wilkinson, 1998). this technique is widely used in biomedical research (Chu et al., 2019). We have selected several highly conserved genes as markers (Table 2) for the neural crest, according to the literature (Martik and Bronner, 2021), and then examined them using wholemount *in situ* hybridization. The aim of this chapter is to investigate the how polystyrene nanoparticles affect neurulation, and possibly the neural crest, casing malformations.

Materials and Methods

Sample collection and preparation

We used the same materials and techniques as described in detail in Chapter 2. Briefly, surviving embryos exposed to 25 nm plain nanoplastics were fixed in 2% PFA in PBS at 4 °C overnight. Fixed embryos were then rinsed in PBS and dehydrated through methanol series (25%, 50%, 70% and 100%) and stored at -20 °C in 100% methanol. All embryos were staged according to Hamburger and Hamilton (Hamburger and Hamilton, 1951).

RNA extraction and cDNA synthesis

The RNA was isolated from stage 13-16 chick embryos by TRIzol™ Reagent (Thermo Fisher Scientific, USA) in house followed by purification with RNeasy Mini Kit (50; Qiagen, Venlo, Netherlands). The concentration of purified RNA was measured by Nanodrop. To generate first strand cDNA, we performed two-step reverse transcription polymerase chain reaction (RT-PCR) using SuperScript III (Invitrogen™, USA). The cDNA was diluted 10 ×with DNA- and RNA-free water and stored at -20 °C (Sigma).

Probe synthesis

This protocol is as previously described by us (de Bakker et al., 2013). In brief, we isolated total RNA from an embryo using TRIzol (Invitrogen) and carried out reverse transcription using SuperScript III (Invitrogen). PCR was performed on these

templates using specific primers (Table 4-1; Table S4), and the PCR products were cloned in the TOPOTA-PCRII vector (Invitrogen™). The inserted amplicons were checked by a PCR with M13-pUC primers located on the TOPOTA-PCRII plasmid and checked on an agarose gel. When they were of the right size they were sent for Sanger sequencing (BaseClear B.V., Leiden). After checking the sequence by BLAST searching, the positive results were used as templates for making the digoxigenin labelled antisense RNA probes. See Table S4 for accession numbers.

Table 4-1. **Details of gene markers used for in situ hybridization.**

Gene	Expressed	Location expressed	Reference
FOXD3 (Forkhead box D3)	(pre-)migratory neural crest	Dorsal neural tube, neural folds and head mesenchyme	(Dottori et al., 2001; Fairchild et al., 2014)
SNAI2 (Snail family transcriptional repressor 2)	(pre-)migratory neural crest	Dorsal neural tube and paraxial mesoderm	(Jhingory et al., 2010)
WNT1(Wnt family member 1)	neural crest	Dorsal neural tube Rhombencephalon and mesencephalon	(Brown and Zervas, 2017; Galli et al., 2014)
SOX10 (SRY-box 10)	neural crest	Neural crest and central nervous system	(Cheng et al., 2000)
LMO4 (LIM domain only 4)	neural crest	Neural plate and neural crest	(Ferronha et al., 2013)
PAX3 (Paired box 3)	neural crest	Neural crest and somite	(Bothe and Dietrich, 2006; Goulding et al., 1994)
TFAP2A (Transcription factor AP-2 alpha)	neural crest	Neural plate and Neural crest, pharyngeal arches, ectoderm, cleft	(Poelmann et al., 2017; Wang et al., 2011)

Whole mount *in situ* hybridization

In this study, all gene names are according to Ensembl for *Homo sapiens* (https://www.ensembl.org/). This wholemount protocol is as previously described by us (de Bakker et al., 2021). In brief, embryos were fixed in 2% buffered depolymerized pPFA for 24 h at 4 °C. They were then washed 3 × with cold PBS and dehydrated through a graded methanol series (25%, 50%, 75% and 100%) and stored at -20 °C . Embryos were rehydrated through a graded methanol series, lightly digested with proteinase K (10 mg/mL in PBS) for 5 min and postfixed in 4% buffered pFA in PBS after several washes in PBST (PBS pH 7.2 with 0.1% Tween-20). This was followed by a prehybridization step at 60 °C for at least 3 h or until the embryo had sunk. The hybridization mixture consisted of: 50% formamide, 2% Boehringer blocking powder, 5 × SSC (from 20× standard sodium citrate buffer, 3M sodium chloride, 0.3M sodium citrate, pH 7), 1mg/mL total RNA, 50 µg/mL heparin, 0.1% Triton X-100, 0.1% CHAPS (3-[(3-cholamidopropyl) dimethylammonio]-1-propanesulfonate) and 5mM ethylenediaminetetraacetic acid (EDTA). After the prehybridization mix was removed, we added 400 ng/mL specific probe to fresh hybridization mixture preheated to 60 °C. The embryos were incubated in this mix at 60 °C overnight with slow shaking. The next day, the specific probe mixture was removed, collected and stored at -20 °C for re-use. Several stringent washes were done at 60 °C to remove non-specifically bound probe [2× SSC, 0.1% CHAPS, 50% formamide]; [2× SSC 0.1% CHAPS]; [0.2× SSC, 0.1% CHAPS]. After washing several times at room temperature with TBST (0.1M tris [tris (hydroxymethyl)aminomethane] buffered saline, pH 7.5, 0.1% Tween-20) the embryos were preincubated with heat-inactivated 10% sheep serum in TBST for 90 min at room temperature followed by overnight incubation with sheep anti-digoxigenin conjugated to alkaline phosphatase (Roche; 1:5,000 dilution in 10% sheep serum in TBST at 4 °C overnight).

The next day, the non-specifically bound antibodies were washed away by several washes with TBST of which the last one was overnight at 4 °C. The embryos were brought to a higher pH by washing 3x 10 min in NTT buffer (0.1M sodium chloride,

0.1M Tris/HCl, 0.1% Tween-20, pH 9.5). The enzyme reaction of alkaline phosphate with BM purple (Roche) as substrate results in a blue precipitate. The development of the stain was checked regularly and stopped by washing several times in TBST, removing the substrate and chromogens, and lowering the pH.

Wholemount TUNEL staining

This protocol has been described by us (de Bakker et al., 2021). In brief, embryos were collected and fixed as for *in situ* hybridization, rehydrated through a graded methanol series, and washed in TBST (0.1M tris-buffered saline containing 0.1% Tween). Next, they were pre-treated with proteinase K (10 mg/ml, 5 min at room temperature), washed in TBST, postfixed with 4% formaldehyde in PBST, washed in TBST followed by a wash in the TdT buffer (30 mMTris/HCl, 140 mM Na-cacodylate, 0.1% Triton pH 7.2). They were then preincubated in the reaction mix (70 nM digoxigenin-labeled dUTP, 400 nM ATP, and 1 U/mL terminal transferase in the enzyme buffer) at 4 °C without the cofactor CoCl2 which was added to the reaction mix (1mM end-concentration) after 1 h. With CoCl2 added, the embryos were incubated at room temperature overnight. The reaction was stopped by adding 200 mM EDTA (ethylenediaminetetraacetic acid), pH 7.0, ⅒ of the reaction volume. The digoxygenin-labelled nucleotides were localized with a standard anti-digoxigenin antibody conjugated to alkaline phosphatase procedure followed by staining with BM-purple.

TUNEL staining on paraffin sections

The following protocol has been described by us previously (de Bakker et al., 2021). The protocol was slightly modified by us. Briefly, chicken embryos were fixed and dehydrated as above were, rinsed in 100% ethanol followed by xylene, embedded in paraffin wax, sectioned at 7 µm and mounted on silane-coated slides (VWR International B.V, Amsterdam). The dewaxed slides were treated with 10 µg/mL proteinase K in PBS for 5 min, postfixed in 4% formaldehyde in PBS. The TUNEL reaction took place at 37 °C for 2 h in a similar reaction mix as above but with a

higher concentrations of digoxygenin-labeled dUTP (3.5 µM) and ATP (20 µM) and CoCl2 already added to the mix. The reaction was stopped by rinsing the slides in 20 mM EDTA in PBS. TUNEL-positive cells were localized with a standard anti-digoxigenin antibody conjugated to alkaline phosphatase followed by staining with BM-purple. As a counter stain we used 0.1% neutral red.

Vibratome sectioning

Embryos processed for wholemount *in situ* hybridization and TUNEL were stored in 1% pFA in PBS. They were soaked in a mixture of 30% BSA, 20% sucrose and 0.5% gelatin in PBS as the embedding mixture. The albumin/gelatin was made by dissolving 0.49 g of gelatin (Sigma Cat. No. G1890) in warm PBS (100 mL). The mixture was then cooled to room temperature and 30 g of bovine albumin (Sigma Cat. No. A-4503) added and allowed to dissolve (for several hours). Finally, 20 g sucrose was added. The embryos were then placed in 3 mL of fresh albumin/gelatin mixture in plastic embedding moulds and 240 µL of 10% glutaraldehyde was added as a hardener. The solidified cubes were trimmed and sectioned at 70 µm in Milli-Q® water and mounted on glass slides with 99.5% glycerol.

Localisation of fluorescent 25 nm PS-NPs *in ovo* and *in vitro*

Stage 8 Hamburger-Hamilton chicken embryos were exposed to PS-NPs as described in Chapter 2 under '*In ovo* embryo toxicity experiments' with the exception that, instead of plain PS-NPs, we used green fluorescent polystyrene nanoparticles (cat. number FGP25; 1% solid, 1.05 g/cm^3). The embryos were returned to the incubator and re-incubated for 2, 6 and 24 h. They were then removed from the egg and visualized as wholemounts by confocal microscopy (Zeiss Airyscan 900).

Chicken embryo neural crest cultures

For neural crest cultures, Hamburger-Hamilton 58 stage 14-15 embryos were removed from the egg, and rinsed with sterile calcium-magnesium free Dulbecco's PBS (CMF; Corning®, New York). The method of Cohen and Konigsberg was used

(Cohen and Konigsberg, 1975), slightly modified. In brief, a segment of the embryo body from the axial levels of the last 6-9 somites was cut out using tungsten needles and placed in 0.25% Trypsin-EDTA (Sigma-Aldrich, Zwijndrecht, Cat. No. T4049) on ice for 8-10 min, when the somites and neural tube appeared to be beginning to separate from the surrounding tissues. The segments were then transferred to DMEM (Sigma-Aldrich, Zwijndrecht, D0819) 15% foetal calf serum (Sigma-Aldrich, Zwijndrecht, Cat. No. F7524) and 1% antibiotic-antimycotic (Sigma-Aldrich, Zwijndrecht, Cat. No. A5955).

The tissue pieces were gently triturated with a blue Gilson pipette tip (with the tip cut off and the cut surface polished in a flame). Then, neural tubes and somites were plated into separate µ-Dish 35 mm high glass-bottom dishes (ibidi GmbH; Gräfelfing, Germany,) which we pre-coated with rat-tail collagen type-I (ibid Cat. No. 50201), according to the manufacturer's instructions. The µ-Dishes contained 1 mL culture medium (MEM, HEPES, GlutaMAX™ Supplement (42360, Gibco™ with 15% foetal calf serum and 1% antibiotic-antimycotic). Most of the medium was then aspirated leaving the tissue samples pressed against the substratum by surface tension. They were incubated for 4 h (in 5% CO_2, 37 ° C) until attached and then 1 ml culture medium was added. They were returned to the CO2 incubator and cultured overnight.

We exposed these 2 d cultures of chick neural crest to fluorescent PS-NPs (25 nm). This was done by aspirating the culture medium and replacing with 1 mL fresh culture medium containing PS-NPs at a final concentration 0.1 mg/mL. After incubating for 2 or 6 h at 37 ° C, in 5% CO_2, the culture medium containing PS-NPs was aspirated and the cultures rinsed 3 x with warm culture medium then stained with 5 µg/mL DAPI (4',6-diamidino-2-phenylindole; Invitrogen™) in culture medium for 20 min at 37 ° C. The cultures were rinsed with plain, fresh medium and observed as living cultures under a Zeiss Airyscan 900 confocal microscope fitted with warmed air chamber (37 °

C) to maintain the cultures. The warmed air chamber was an XL-LSM S1 123, connected to Heating Unit XL S and TempModule S (all from Zeiss).

Cryosections

Embryos were fixed with 4% pFA in PBS and then transferred to 30% sucrose solution in PBS (4 h, 4 °C). They were then transferred to OCT embedding matrix (Carl Roth, Karlsruhe) 1 h (4 °C) then transferred to fresh OCT in a plastic mould and snap-frozen in liquid nitrogen. Sections were cut at 25 µm using a Leica CM3050S cryostat and mounted on glass microscope slides. The slides were analyzed using Zeiss Axioplan 2 aka DIC.

Transmission electron microscopy

Primary trunk neural crest cultures were prepared as described above under 'Localisation of fluorescent 25 nm PS-NPs *in ovo* and *in vitro*'. They were cultured on Thermanox coverslips (24 mm ⌀; Thermo Fisher Scientific™) pre-coated with rat-tail collagen type-I, placed into µ-Dish 35 mm high glass-bottom dishes (ibidi GmbH; Gräfelfing, Germany,). The cultures were exposed to 0.1 mg/mL plain PS-NPs 25 nm (1 mL) for 1 h. Coverslips were carefully transferred to 6-well plates and fixed with 2% glutaraldehyde and 2% formaldehyde in sodium cacodylate buffer (0.1 M, pH 7.2) for 2 h. Samples were then incubated with 1% osmium tetroxide with 0.8% potassium ferrocyanide in water for 1 h. After rinsing, they were stained *en bloc* with 1% uranyl acetate in water. The staining of the samples was checked under a Zeiss Observe Z1 inverted fluorescence microscope before further process (Fig. S1). The samples were dehydrated through a graded ethanol series (70%, 90%, 100%, 1 h each). Finally, they were embedded in Agar 100 resin kit (cat. number R1031, Agar Scientific, Essex, UK) using propylene oxide as the intermediate reagent, and sectioned at 70 nm using a diamond knife. The sections were examined using a JEOL 1400+ electron microscope.

Results

Nanoplastics become localized to the dorsal middle of the neural tube

To track the distribution of PS-NPs, stage 8 chicken embryos were exposed *in ovo* to 50 µL (0.1 mg/mL) fluorescein-labelled 25 nm PS-NPs for 2, 6 and 24 h. Confocal imaging showed that that fluorescence became localized in cell masses in the dorsal midline of the neural tube (Fig. 4-1a-c). This corresponds to the region where neural crest cells develop. Labelled cell masses were also seen protruding into the lumen from the dorsal aspect of the neural tube, or lying free in the lumen (Fig. 4-1d).

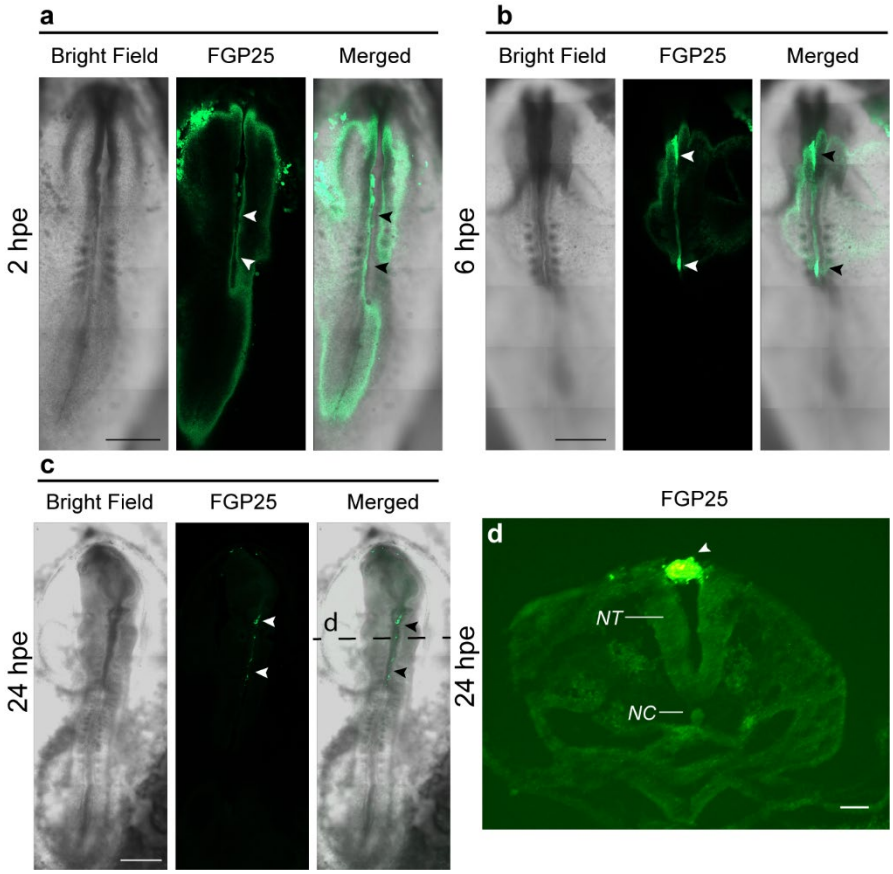

Fig. 4-1. **25 nm green fluorescent polystyrene nanoparticles adhere to the dorsal middle line and lying between the neural folds. a**-**c**, chick embryos exposed to fluorescent PS-NPs (FGP, green florescence) examined at 2, 6 and 24 h, respectively. *n* = 2 for all different time series. **a**, 2 hpe PS-NPs treated chick embryos, stage 8. **b**, 6 hpe PS-NPs treated chick embryos, stage 9. **c**, 24 hpe PS-NPs treated chick embryos, stage 13. In **a**-**c**, there is strong fluorescence *(Copp et al.)* associated with the dorsal midline of the neural tube (black and white arrowheads; note that the chicken embryos did not show autofluorescence). **d**, transverse cryosection (25 µm). There is strong fluorescence *(Copp et*

al.) in a cellular mass lying in between the neural folds (white arrowheads). Key, hpe, hours post-exposure. Note, NC, notochord, NT, neural tube. Scale bars, 500 µm in **a**-**c** and 50 µm in **d**.

Nanoplastics disrupt the development of neural crest cells

To confirm the neural crest identity of the affected cells, we studied the expression of a panel of neural crest markers, namely: WNT1, FOXD3, SNAI2 (SLUG, SNAIL2), LMO4, SOX10, PAX3 and TFAP2A (Table 4-1 and Table S4). In PS-NP treated embryos, we found that the cells remaining in the dorsal midline, or the margins of the open neural tube, express neural crest markers (Fig. 4-2, Fig. 4-3, and Fig. 4-4). These findings were consistent across all seven neural crest markers (Fig. 4-2, Fig. 4-3, and

Fig. 4-4).

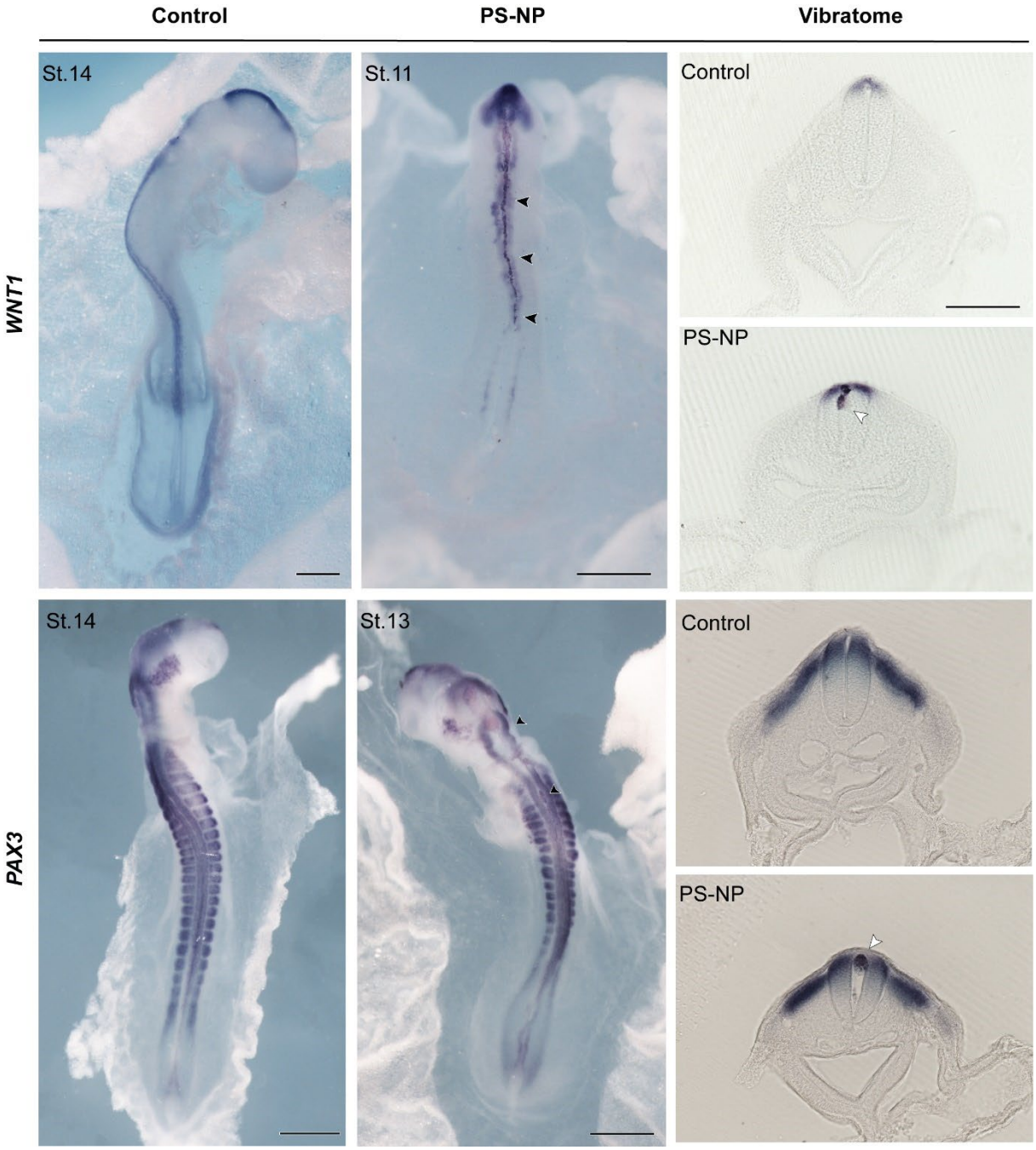

Fig. 4-2. **Cells disrupted by 25 nm PS-NPs express neural crest markers (*WNT1* and *PAX3*)**. Embryos were exposed at stage 8 to 50 µL plain PS-NPs (5 mg/mL) or Ringer's only. *n* = 3 for both control and PS-NP treated group of all genes. *Note*, all embryos are two days incubation; the treated embryos all showed developmental delay relative to the controls. Cellular debris of neural crest cells (black arrowheads). *Note*, White arrowheads in the treated embryos indicate putative neural crest cells. *Key*: hpe: hours post-exposure, PS-NP, embryos treated with polystyrene nanoparticles, 25 nm, 5 mg/mL. Scale bars, 500 µm in wholemount embryos, and 200 µm in vibratome transverse sections.

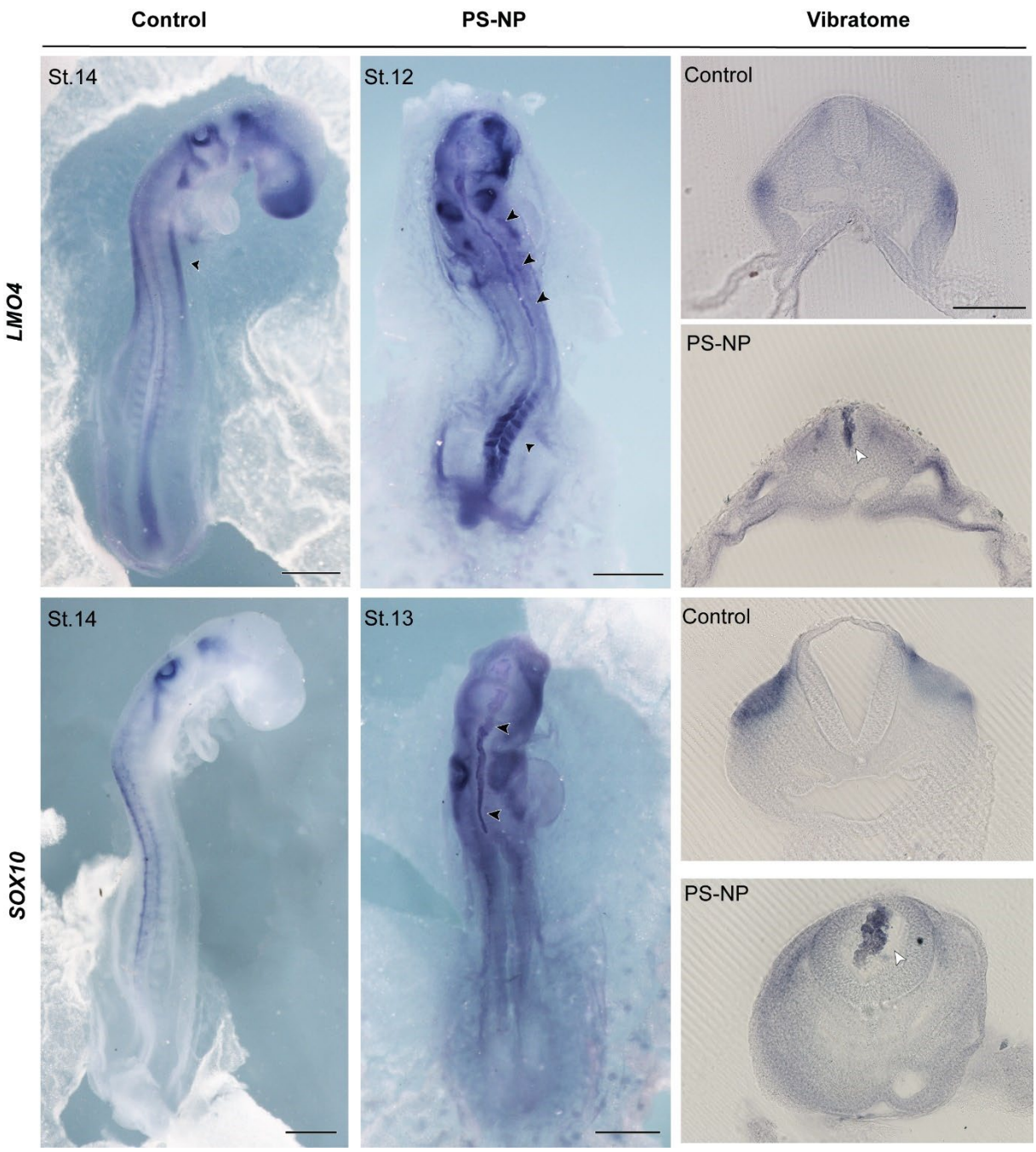

Fig. 4-3. **Cells disrupted by 25 nm PS-NPs express neural crest markers (*LMO4* and *SOX10*).** Embryos were exposed at stage 8 to 50 µL plain PS-NPs (5 mg/mL) or Ringer's only. *n* = 3 for both control and PS-NP treated group of all genes. *Note*, all embryos are two days incubation; the treated embryos all showed developmental delay relative to the controls. Cellular debris of neural crest cells (arrowheads). *Note*, White arrowheads in the treated embryos indicate putative neural crest cells. *Key*: hpe: hours post-exposure, PS-NP, embryos treated with polystyrene nanoparticles, 25 nm, 5 mg/mL. Scale bars, 500 µm in wholemount embryos, and 200 µm in vibratome transverse sections.

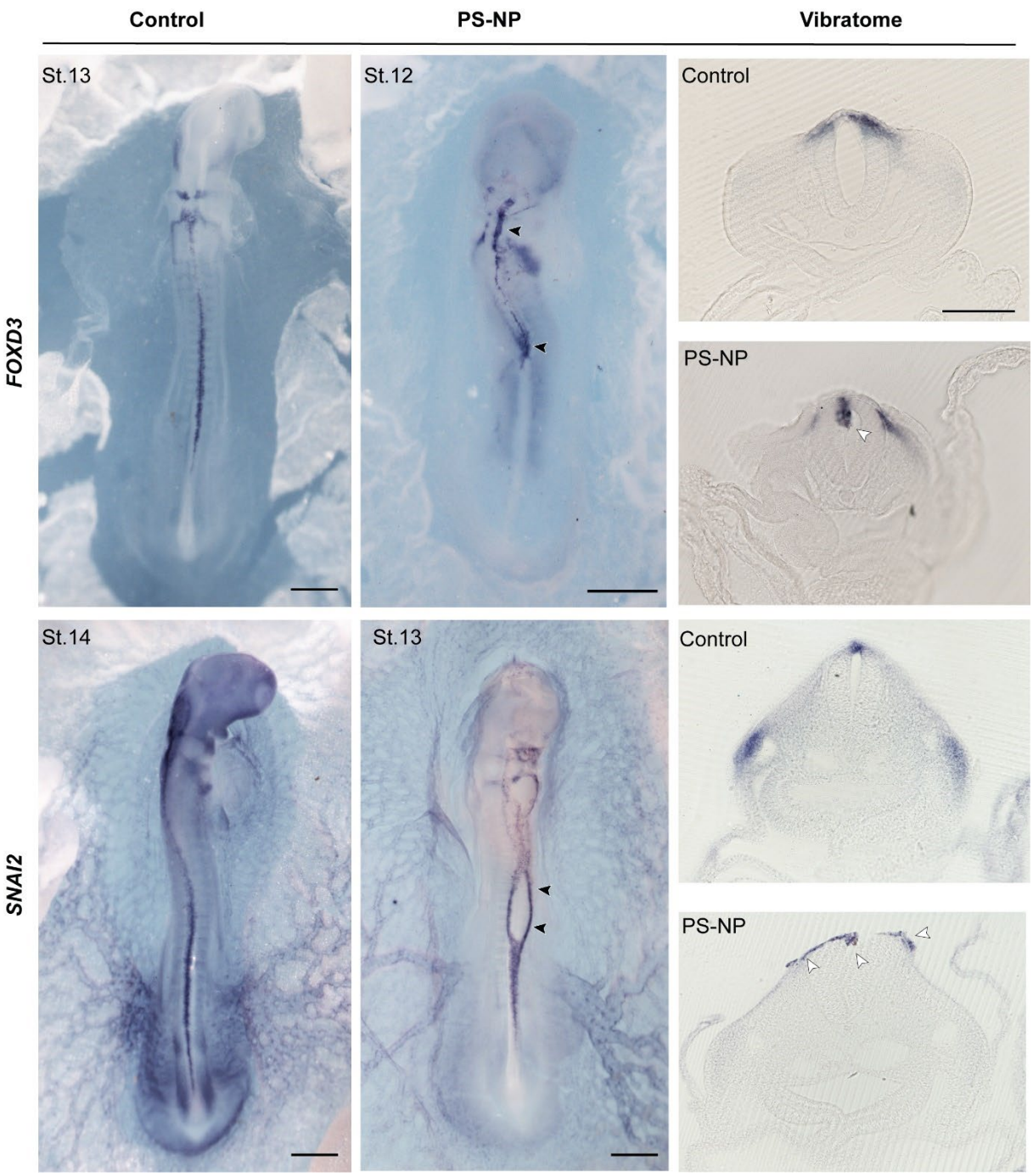

Fig. 4-4. **Cells disrupted by 25 nm PS-NPs express neural crest markers (*FOXD3* and *SNAI2*)**. Embryos were exposed at stage 8 to 50 µL plain PS-NPs (5 mg/mL) or Ringer's only. *n* = 3 for both control and PS-NP treated group of all genes. *Note*, all embryos are two days incubation; the treated embryos all showed developmental delay relative to the controls. Cellular debris of neural crest cells (black arrowheads). *Note,* White arrowheads in the treated embryos indicate putative neural crest cells. *Note*, In the FOXD3 *in situs*, the cells are clumped. In the SNAI2 *in situs*, there are putative neural crest cells that are margins of the neural tube defects. Scale bars, 500 µm in wholemount embryos, and 200 µm in vibratome transverse sections.

Nanoplastics can enter neural crest cells

To understand the interaction between PS-NPs and neural crest cells, we have exposed primary cultures of chicken embryo neural crest cells to PS-NPs (Fig. 4-5). We found that the cells showed an uptake of fluorescent PS-NPs within 2–6 h (Fig. 4-5d-f) as indicated by the appearance of fluorescence in the cytoplasm. Transmission electron microscopy of the cultured cells showed inclusions or lacunae that were consistent with PS-NPs in the cytoplasm (Fig. 4-6).

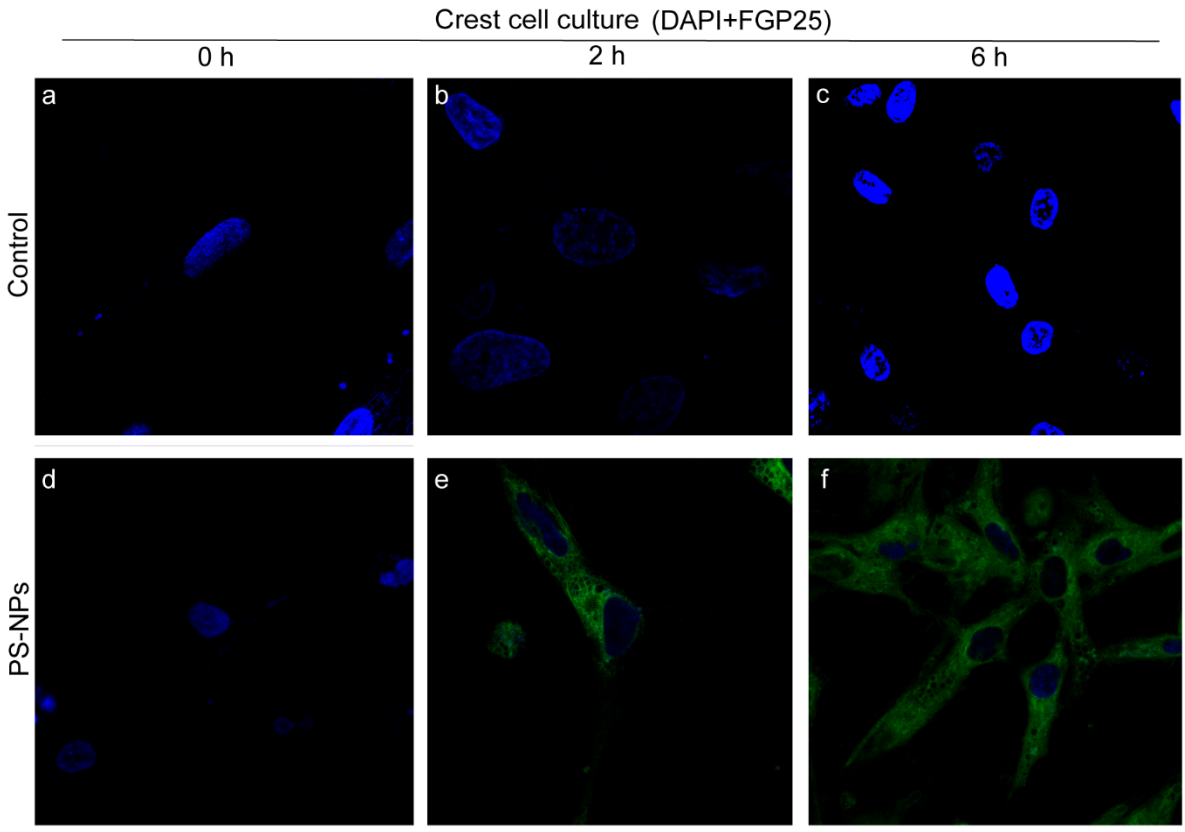

Fig. 4-5. **Fluorescent polystyrene nanoplastics (25 nm) become co-localized to primary neural crest cells *in vitro***. **a**-**c**, neural crest cells stain with DAPI (blue florescence) exposed in vitro to Ringer's solution and examined at 0, 2, and 6 h, respectively. **d**-**f**, neural crest cells stain with DAPI (blue florescence) exposed in vitro to fluorescent PS-NPs (green florescence) and examined at 0, 2, and 6 h, respectively.

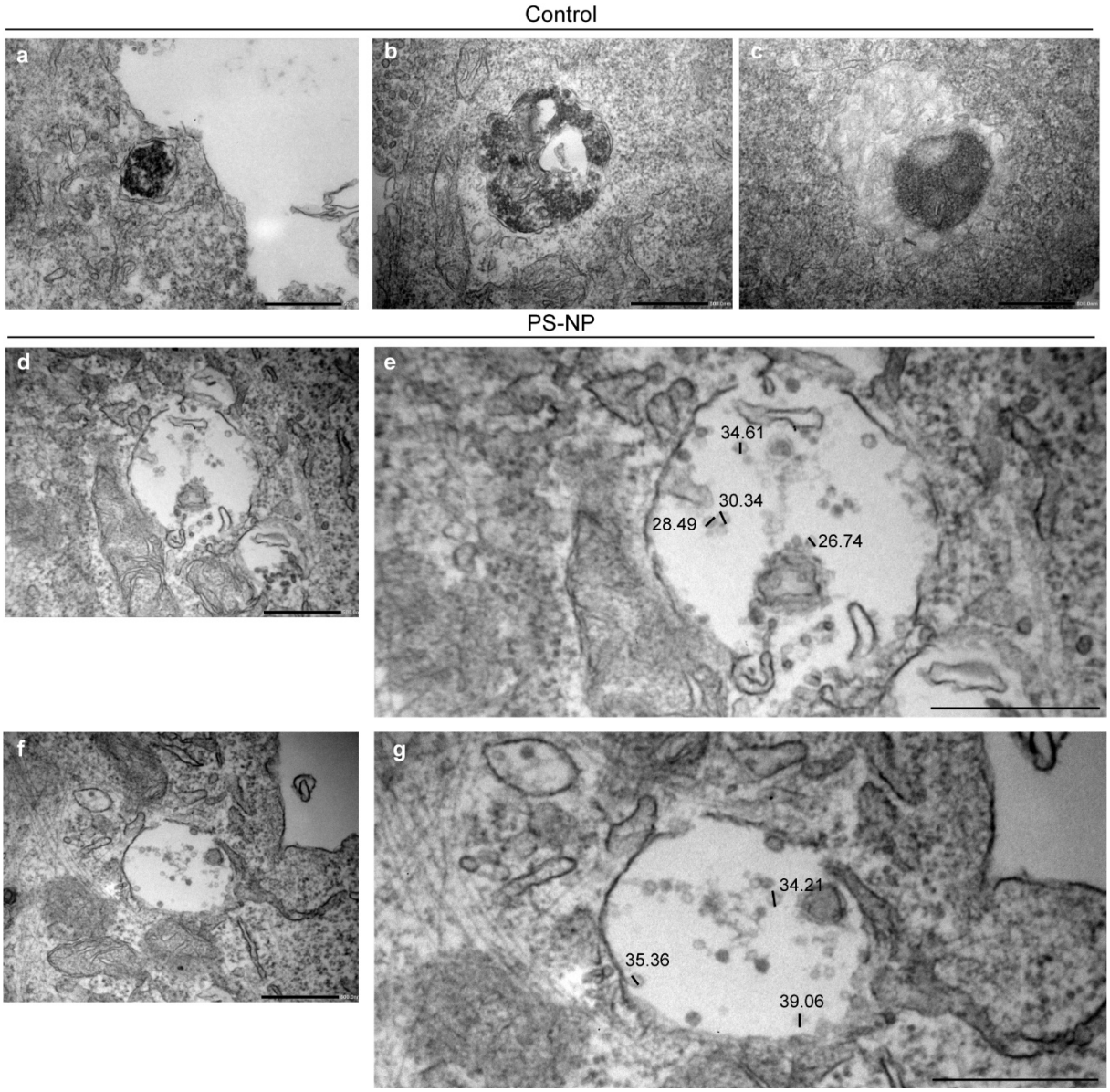

Fig. 4-6. **Transmission electron microscopy of 2 d chicken embryo neural crest cultures 1 h after exposure to PS-NPs (0.1 mg/mL) in culture medium**. **a**-**c**, controls (culture medium only); **d**-**g**, PS-NP-treated. In the treated cultures, spheres of 26.74—39.06 nm were observed. These near-perfect spheres lacked any sign of a membrane (biological membranes will appear dark because of the osmium tetroxide treatment). According to several reports in the literature (Domenech et al., 2021; Qiao et al., 2021), such spherical structures may represent nanoplastic particles. In any case, we present these findings as only tentative identification of PS-NPs. To make a positive identification of PS-NPs with TEM would require — for example — the use of PS-NPs with a gold core. *Note,* also that our confocal imaging studies do support the idea of uptake of PS-NPs by neural crest cells in Fig. 4-3). *Key*: scale bars, 500 nm.

Nanoplastics cause cell death in presumptive neural crest cells

We performed TUNEL assay on wholemount control and PS-NPs-treated embryo at 24 hpe. When we examined the dorsal aspect of the wholemount embryos, we saw

only a few, scattered cells positive for TUNEL label in control (Fig. 4-7a). Vibratome sections showed that these cells were located in the dorsal ectoderm and neural folds (Fig. 4-7d). In the PS-NP treated embryos, the numbers of TUNEL-positive cells were greatly increased (Fig. 4-7b and c). These labeled cells, like those in the control embryos, were visible in the dorsal ectoderm in vibratome sections, and surrounding the neural folds (Fig. 4-7e-g). In addition, clumps of TUNEL-positive cells were seen in the lumen of the neural tube (Fig. 4-7e-g). We observed similar results with TUNEL staining on paraffin sections, which showed clumps of putative dead cells in the lumen of the neural tube (Fig. 4-7h-k).

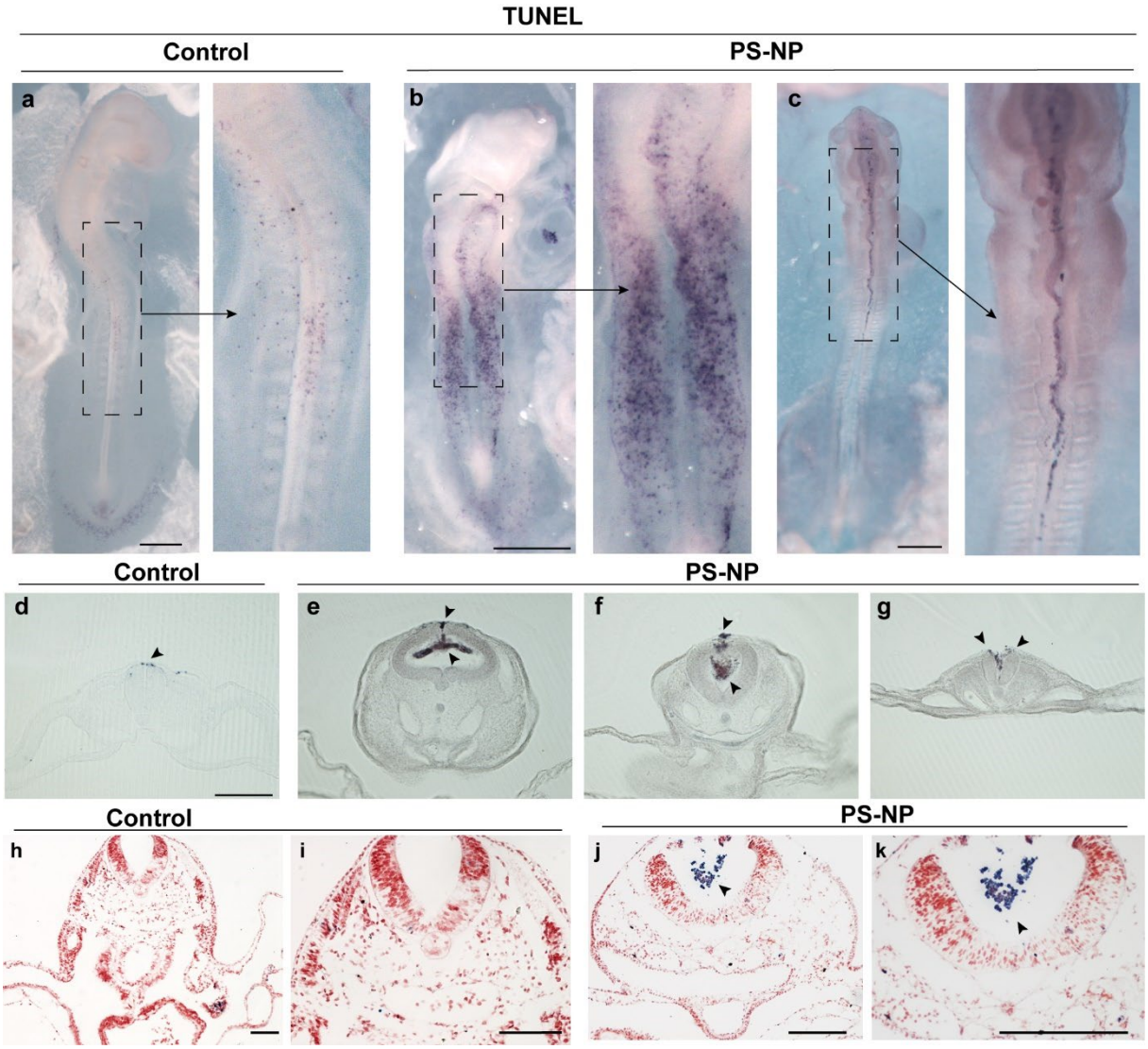

Fig. 4-7. **Exposure of stage 8 chicken embryos to plain polystyrene nanoparticles induces cell death in putative neural crest cells**. Figures show embryos 24 hpe. Wholemount TUNEL staining of control (**a**) and PS-NP-treated (**b** and **c**) chick embryos. *n* = 2 for control and *n* = 3 for PS-NP treated group. (**a**), stage 14, (**b**), stage 12, (**c**), stage 12 (Note all embryos are 2 d incubation, but **b** and **c** show a

developmental delay caused by PS-NP treatment. In **b** and **c**, note the extensive cell death, and dead cells in the dorsal midline. **d**-**g**, TUNEL staining on vibratome sections. *n* = 2 for both control and PS-NPs-treated chick embryos. **d**, control, stage 14. **f**-**g**, PS-NPs-treated, stage 12. PS-NPs treatment resulted in clumps of dead cells in the neural folds and in the neural tube lumen (black arrowhead). **h**-**k**, TUNEL staining on paraffin sections of control embryo (**h** and **i**), and PS-NPs treated embryo (Smits-van Prooije et al.), *n* = 2 for both groups. *Note*, massive cell death lying free in the lumen of neural tube (**j** and **k**). *Key*, 500 µm in **a**-**c**, 200 µm in **d**-**k**.

Discussion

It has been reported that 60 and 900 nm NPs can have harmful effects on the developing chick embryo (Nie et al., 2021). Those negative effects include neural tube defects and development delay (Nie et al., 2021). In our previous research (Chapters 2 and 3), we found a much wider spectrum defects, including defects in cardiovascular and craniofacial tissues, eyes, tail-bud, and vertebral column defects in the PS-NPs treated embryos. The previous study suggested that PS-NPs were taken up through caveolae-mediated endocytosis into nerve cells (Nie et al., 2021). After entering the cells, PS-NPs induce autophagy and apoptosis leading to neural tube defects (Nie et al., 2021). However, these suggested mechanisms could not easily account for the major malformations that we have described in Chapters 2 and 3. We agree that PS-NPs can damage cells in the location of the neural tube since we also observe dead cells surrounding the neural folds (this chapter). However, compared to the dead cells we saw in the lumen, very few cells in the neural tube itself were stained by the TUNEL protocol. Therefore, we explored mechanisms alternative to a simple effect of PS-NPs on the neural tube itself.

To explore this possibility, we first conducting experiments in which we tracked distribution of fluorescent PS-NPs in the chick embryo. We saw that many PS-NPs become localized to the dorsal middle line of the embryo, often attached to clumps of cells in the lumen of the neural tube. We noticed these abnormal clumps of cells in our previous experiments (Chapters 2 and 4). Normally, the lumen of the neural tube does not contain such clumps of cells. We speculate that these cell clusters might be neural crest cells because of their location. This would explain why we and the

previous authors observed neural tube defects: the normal migration of neural crest cells is thought to be essential to the neural tube closure (Copp et al., 2003; Ewart et al., 1997; Morris-Kay and Tan, 1987). Therefore, the neural tube defects we observed in our research may caused by the disruption of PS-NPs to the migration of neural crest cells.

To further examine the possible neural crest identity of the cells disrupted by PS-NPs, we examined the expression of six neural crest markers in PS-NPs-treated and control embryos at 24 hpe. Interestingly, we found that the expression of all neural crest markers – except SNAI2) – is consistent with our hypothesis that the abnormal cells in PS-NP treated embryos are putative neural crest cells. Interestingly, in this context, it has been reported that the exposure of developing chick embryos to zinc oxide nanoparticles leads to abnormal migration of cranial neural crest cells (Yan et al., 2020). Therefore it is possible that neural crest are sensitive to nanoparticles more generally.

In addition, the dysplasia we saw in the craniofacial tissue of PS-NPs-treated embryos (Chapter 3), could be explained by the same mechanism: disruption of neural crest cells. Cranial neural crest cells play a crucial role in head morphogenesis. This is because they migrate in prosencephalic and mesencephalic streams into the facial region (Martik and Bronner, 2021; Santagati and Rijli, 2003). Moreover, the exposure of chick embryos to high glucose concentrations, disrupts the migration of cranial neural crest cells, resulting in abnormalities of the facial skeleton (Wang et al., 2015).

In Chapters 2, 3 and 4, we have consistently detected microphthalmia at various stages among PS-NP-treated chick embryos. It has previously been shown that silver and gold nanoparticles can interfere with the development of the eyes in zebrafish (Kim et al., 2013; Lee et al., 2007). Those two studies (Kim et al., 2013; Lee et al., 2007) also suggest that metal nanoparticles disrupt the expression of genes related to eye development, or maybe even influence the development of the central nervous system.

We did not find that fluorescent PS-NPs adhere to, or accumulate in, the eyes of chicken embryos after exposure (this Chapter). Therefore, it is highly unlikely that our observed microphthalmia was caused by PS-NPs directly. Our alternative hypothesis is that the microphthalmia may be caused indirectly by the disruption of neural crest cells. It has previously been shown that neural crest cells are essential for eye development in chick embryos (Grocott et al., 2011). Migrating neural crest cells produce TGF-βs, that activate both SMAD3 and canonical WNT signaling, controlling PAX6 function and transcription (Grocott et al., 2011). Pax6 is a well known gene that play a crucial role in eye development in many species (Chow et al., 1999; Gehring, 1996; Hanson, 2003; Nishina et al., 1999; Onuma et al., 2002).

In Chapter 3, we studied the effects of nanoplastics on the chick embryo cardiovascular system. We also looked at the expression of TFAP2A, a gene expressed in neural crest cells. In this chapter, we have examined six additional neural crest cell markers. The results are consistent across the different stages studied (Chapters 3 and 4) and show that PS-NPs affect the migration of neural crest cells. Furthermore, TUNEL labelling suggests that at least some neural crest cells are damaged, and undergo cell death. Consequently, fewer neural crest cells are able to migrate through pharyngeal arches into heart, resulting in heart ventricle septum and cardiovascular defects (Kirby and Waldo, 1995; Waldo et al., 1999). Moreover, these results are consistent with previous studies of hear development in which the microsurgical ablation of neural crest results in various heart defects, including persistent truncus arteriosus, and ventricular septal defects (Hutson and Kirby, 2007).

Although most of the malformations observed after PS-NP exposure are consistent with neural crest disruption, the tailbud effects and caudal neural tube dysplasia cannot be explained as neural crest defects. In the chick embryo, the tailbud and caudal neural tube are in the caudal region of the embryo where the neural tube is formed by secondary neurulation. Secondary neurulation is the formation of the neural tube as a solid primordium without the folding up of a neural plate (Harrington

et al., 2009). Secondary neurulation therefore takes place process entirely under the surface ectoderm (Catala, 2021). This contrasts with primary neurulation where the neural plate develops two folds (neural folds) which elevate and finally fuse in the midline. During primary neurulation, neural crest cells develop at the margins of the neural plate, where the neural folds develop. The neural crest cells then undergo epithelial-to-mesenchymal transformation (EMT) (Rocha et al., 2020; Schoenwolf and Smith, 1990; Schoenwolf and Smith, 2000).

Because secondary neurulation takes place under (ventral to) the surface ectoderm, and the PS-NPs were dripped onto the dorsal side of the ectoderm, we have to explain how the PS-NPs come in contact with the neural tube forming by secondary neurulation, considering that the caudal neural tube is grossly dysplastic in several treated embryos (Figure 7 in **Chapter 2**). Furthermore, the chick embryo has not start secondary neurulation at stage 8 when we introduce the PS-NPs (Schoenwolf and Smith, 1990). To explain these facts, we suggest an alternative hypothesis whereby PS-NPs may adhere to surface mesenchymal populations in the primitive streak of the tailbud, and thereby entering the region of the developing neural tube via EMT (Bellairs, 1986; Shook and Keller, 2003). Another alternative hypothesis could be that PS-NPs may adhere to cells at the junction between primary and secondary neurulation (Dady et al., 2014). Junctional cells in this region undergo EMT and so it is possible that that PS-NPs may attach to these mesenchymal cells, interrupting their EMT (Dady et al., 2014).

Conclusions

We suggest that the mechanism of the malformations we have observed in our research is that PS-NPs passively target migration neural crest cells disrupting their migration and development. The PS-MPs may also disrupt other cell populations undergoing epithelial-mesenchymal transformation on the dorsal surface of the embryo, specifically the cells of the primitive streak. Finally, PS-NPs cause direct

effect on the caudal neural tube in the junctional area between primary and secondary neurulation. This results in neural tube dysplasia in the cadual region. Future work is needed to identify the molecular interactions that lead PS-NPs to adhere to cells undergoing epithelial-mesenchymal transformation. We also need to know whether these effects are specific to polystyrene plastic nanoparticles or to other types of nanomaterials more generally.

References

Achilleos, A. and Trainor, P. A. (2012). Neural Crest Stem Cells: Discovery, Properties and Potential for Therapy. *Cell Res* **22**, 288-304.

Andrady, A. L., Torikai, A., Redhwi, H. H., Pandey, K. K. and Gies, P. (2015). Consequences of Stratospheric Ozone Depletion and Climate Change on the Use of Materials. *Photochem Photobiol Sci* **14**, 170-184.

Bellairs, R. (1986). The Primitive Streak. *Anatomy and Embryology* **174**, 1-14.

Boehnke, N., Straehla, J. P., Safford, H. C., Kocak, M., Rees, M. G., Ronan, M., Rosenberg, D., Adelmann, C. H., Chivukula, R. R., Nabar, N., et al. (2022). Massively Parallel Pooled Screening Reveals Genomic Determinants of Nanoparticle Delivery. *Science* **377**, eabm5551.

Bothe, I. and Dietrich, S. (2006). The Molecular Setup of the Avian Head Mesoderm and Its Implication for Craniofacial Myogenesis. *Dev Dyn* **235**, 2845-2860.

Brown, S. and Zervas, M. (2017). Temporal Expression of Wnt1 Defines the Competency State and Terminal Identity of Progenitors in the Developing Cochlear Nucleus and Inferior Colliculus. *Front Neuroanat* **11**, 67.

Catala, M. (2021). Overview of Secondary Neurulation. *J Korean Neurosurg Soc* **64**, 346-358.

Cheng, Y.-C., Cheung, M., Abu-Elmagd, M. M., Orme, A. and Scotting, P. J. (2000). Chick Sox10, a Transcription Factor Expressed in Both Early Neural Crest Cells and Central Nervous System. *Developmental Brain Research* **121**, 233-241.

Chow, R. L., Altmann, C. R., Lang, R. A. and Hemmati-Brivanlou, A. (1999). Pax6 Induces Ectopic Eyes in a Vertebrate. *Development* **126**, 4213-4222.

Chu, Y. H., Hardin, H., Zhang, R., Guo, Z. and Lloyd, R. V. (2019). In Situ Hybridization: Introduction to Techniques, Applications and Pitfalls in the Performance and Interpretation of Assays. *Semin Diagn Pathol* **36**, 336-341.

Cohen, A. M. and Konigsberg, I. R. (1975). A Clonal Approach to the Problem of Neural Crest Determination. *Developmental Biology* **46**, 262-280.

Copp, A. J., Greene, N. D. and Murdoch, J. N. (2003). The Genetic Basis of Mammalian Neurulation. *Nat Rev Genet* **4**, 784-793.

Copp, A. J., Stanier, P. and Greene, N. D. (2013). Neural Tube Defects: Recent Advances, Unsolved Questions, and Controversies. *Lancet Neurol* **12**, 799-810.

Dady, A., Havis, E., Escriou, V., Catala, M. and Duband, J. L. (2014). Junctional Neurulation: A Unique Developmental Program Shaping a Discrete Region of the Spinal Cord Highly Susceptible to Neural Tube Defects. *J Neurosci* **34**, 13208-13221.

de Bakker, M. A. G., Fowler, D. A., Oude, K. d., Dondorp, E. M., Navas, M. C. G., Horbanczuk, J. O., Sire, J.-Y., Szczerbińska, D. and Richardson, M. K. (2013). Digit Loss in Archosaur Evolution and the Interplay between Selection and Constraints. *Nature* **500**, 445-448.

de Bakker, M. A. G., van der Vos, W., de Jager, K., Chung, W. Y., Fowler, D. A., Dondorp, E., Spiekman, S. N. F., Chew, K. Y., Xie, B., Jimenez, R., et al. (2021). Selection on Phalanx Development in the Evolution of the Bird Wing. *Mol Biol Evol* **38**, 4222-4237.

Domenech, J., de Britto, M., Velazquez, A., Pastor, S., Hernandez, A., Marcos, R. and Cortes, C. (2021). Long-Term Effects of Polystyrene Nanoplastics in Human Intestinal Caco-2 Cells. *Biomolecules* **11**.

Dottori, M., Gross, M. K., Labosky, P. and Goulding, M. (2001). The Winged-Helix Transcription Factor Foxd3 Suppresses Interneuron Differentiation and Promotes Neural Crest Cell Fate. *Development* **128**, 4127-4138.

Ewart, J. L., Cohen, M. F., Meyer, R. A., Huang, G. Y., Wessels, A., Gourdie, R. G., Chin, A. J., Park, S. M., Lazatin, B. O., Villabon, S., et al. (1997). Heart and Neural Tube Defects in Transgenic Mice Overexpressing the Cx43 Gap Junction Gene. *Development* **124**, 1281-1292.

Fairchild, C. L., Conway, J. P., Schiffmacher, A. T., Taneyhill, L. A. and Gammill, L. S. (2014). Foxd3 Regulates Cranial Neural Crest Emt Via Downregulation of Tetraspanin18 Independent of Its Functions During Neural Crest Formation. *Mech Dev* **132**, 1-12.

Ferronha, T., Rabadán, M. A., Gil-Guiñon, E., Le Dréau, G., de Torres, C. and Martí, E. (2013). Lmo4 Is an Essential Cofactor in the Snail2-Mediated Epithelial-to-Mesenchymal Transition of Neuroblastoma and Neural Crest Cells. *J Neurosci* **33**, 2773-2783.

Galli, L. M., Munji, R. N., Chapman, S. C., Easton, A., Li, L., Onguka, O., Ramahi, J. S., Suriben, R., Szabo, L. A., Teng, C., et al. (2014). Frizzled10 Mediates Wnt1 and Wnt3a Signaling in the Dorsal Spinal Cord of the Developing Chick Embryo. *Dev Dyn* **243**, 833-843.

Gehring, W. J. (1996). The Master Control Gene for Morphogenesis and Evolution of the Eye. *Genes Cells* **1**, 11-15.

Goulding, M., Lumsden, A. and Paquette, A. J. (1994). Regulation of Pax-3 Expression in the Dermomyotome and Its Role in Muscle Development. *Development* **120**, 957-971.

Greene, N. D., Stanier, P. and Copp, A. J. (2009). Genetics of Human Neural Tube Defects. *Hum Mol Genet* **18**, R113-129.

Grocott, T., Johnson, S., Bailey, A. P. and Streit, A. (2011). Neural Crest Cells Organize the Eye Via Tgf-B and Canonical Wnt Signalling. *Nature Communications* **2**, 265.

Hamburger, V. and Hamilton, H. L. (1951). A Series of Normal Stages in the Development of the Chick Embryo. *J Morphol* **88**, 49-92.

Hanson, I. M. (2003). Pax6 and Congenital Eye Malformations. *Pediatr Res* **54**, 791-796.

Harrington, M. J., Hong, E. and Brewster, R. (2009). Comparative Analysis of Neurulation: First Impressions Do Not Count. *Mol Reprod Dev* **76**, 954-965.

Hutson, M. R. and Kirby, M. L. (2007). Model Systems for the Study of Heart Development and Disease: Cardiac Neural Crest and Conotruncal Malformations. *Seminars in Cell & Developmental Biology* **18**, 101-110.

Jhingory, S., Wu, C. Y. and Taneyhill, L. A. (2010). Novel Insight into the Function and Regulation of Alphan-Catenin by Snail2 During Chick Neural Crest Cell Migration. *Dev Biol* **344**, 896-910.

Kim, K. T., Zaikova, T., Hutchison, J. E. and Tanguay, R. L. (2013). Gold Nanoparticles Disrupt Zebrafish Eye Development and Pigmentation. *Toxicol Sci* **133**, 275-288.

Kirby, M. L. and Waldo, K. L. (1995). Neural Crest and Cardiovascular Patterning. *Circ Res* **77**, 211-215.

Le Douarin, N. M. (2004). The Avian Embryo as a Model to Study the Development of the Neural Crest: A Long and Still Ongoing Story. *Mechanisms of Development* **121**, 1089-1102.

Le Douarin, N. M. K., C (1999). *The Neural Crest.*: Cambridge University Press.

Lee, K. J., Nallathamby, P. D., Browning, L. M., Osgood, C. J. and Xu, X. H. (2007). In Vivo Imaging of Transport and Biocompatibility of Single Silver Nanoparticles in Early Development of Zebrafish Embryos. *ACS Nano* **1**, 133-143.

Martik, M. L. and Bronner, M. E. (2021). Riding the Crest to Get a Head: Neural Crest Evolution in Vertebrates. *Nat Rev Neurosci* **22**, 616-626.

Morris-Kay, G. and Tan, S.-S. (1987). Mapping Cranial Neural Crest Cell Migration Pathways in Mammalian Embryos. *Trends in Genetics* **3**, 257-261.

Nie, J. H., Shen, Y., Roshdy, M., Cheng, X., Wang, G. and Yang, X. (2021). Polystyrene Nanoplastics Exposure Caused Defective Neural Tube Morphogenesis through Caveolae-Mediated Endocytosis and Faulty Apoptosis. *Nanotoxicology* **15**, 885-904.

Nishina, S., Kohsaka, S., Yamaguchi, Y., Handa, H., Kawakami, A., Fujisawa, H. and Azuma, N. (1999). Pax6 Expression in the Developing Human Eye. *Br J Ophthalmol* **83**, 723-727.

Onuma, Y., Takahashi, S., Asashima, M., Kurata, S. and Gehring, W. J. (2002). Conservation of Pax 6 Function and Upstream Activation by Notch Signaling in Eye Development of Frogs and Flies. *Proc Natl Acad Sci USA* **99**, 2020-2025.

Oumer, M., Tazebew, A. and Silamsaw, M. (2021). Birth Prevalence of Neural Tube Defects and Associated Risk Factors in Africa: A Systematic Review and Meta-Analysis. *BMC Pediatr* **21**, 190.

Poelmann, R. E., Gittenberger-de Groot, A. C., Biermans, M. W. M., Dolfing, A. I., Jagessar, A., van Hattum, S., Hoogenboom, A., Wisse, L. J., Vicente-Steijn, R., de Bakker, M. A. G., et al. (2017). Outflow Tract Septation and the Aortic Arch System in Reptiles: Lessons for Understanding the Mammalian Heart. *Evodevo* **8**, 9.

Qiao, J., Chen, R., Wang, M., Bai, R., Cui, X., Liu, Y., Wu, C. and Chen, C. (2021). Perturbation of Gut Microbiota Plays an Important Role in Micro/Nanoplastics-Induced Gut Barrier Dysfunction. *Nanoscale* **13**, 8806-8816.

Rocha, M., Beiriger, A., Kushkowski, E. E., Miyashita, T., Singh, N., Venkataraman, V. and Prince, V. E. (2020). From Head to Tail: Regionalization of the Neural Crest. *Development* **147**, dev193888.

Sana, S. S., Dogiparthi, L. K., Gangadhar, L., Chakravorty, A. and Abhishek, N. (2020). Effects of Microplastics and Nanoplastics on Marine Environment and Human Health. *Environ Sci Pollut Res Int* **27**, 44743-44756.

Santagati, F. and Rijli, F. M. (2003). Cranial Neural Crest and the Building of the Vertebrate Head. *Nat Rev Neurosci* **4**, 806-818.

Schoenwolf, G. C. (2018). Contributions of the Chick Embryo and Experimental Embryology to Understanding the Cellular Mechanisms of Neurulation. *Int J Dev Biol* **62**, 49-55.

Schoenwolf, G. C. and Smith, J. L. (1990). Mechanisms of Neurulation: Traditional Viewpoint and Recent Advances. *Development* **109**, 243-270.

Schoenwolf, G. C. and Smith, J. L. (2000). Mechanisms of Neurulation. *Developmental Biology Protocols: Volume II*, 125-134.

Shimokita, E. and Takahashi, Y. (2011). Secondary Neurulation: Fate-Mapping and Gene Manipulation of the Neural Tube in Tail Bud. *Dev Growth Differ* **53**, 401-410.

Shook, D. and Keller, R. (2003). Mechanisms, Mechanics and Function of Epithelial–Mesenchymal Transitions in Early Development. *Mechanisms of Development* **120**, 1351-1383.

Smits-van Prooije, A. E., Poelmann, R. E., Gesink, A. F., van Groeningen, M. J. and Vermeij-Keers, C. (1986). The Cell Surface Coat in Neurulating Mouse and Rat Embryos, Studied with Lectins. *Anat Embryol (Berl)* **175**, 111-117.

van der Spuy, M., Wang, J. X., Kociszewska, D. and White, M. D. (2023). The Cellular Dynamics of Neural Tube Formation. *Biochem Soc Trans* **51**, 343-352.

Waldo, K., Zdanowicz, M., Burch, J., Kumiski, D. H., Stadt, H. A., Godt, R. E., Creazzo, T. L. and Kirby, M. L. (1999). A Novel Role for Cardiac Neural Crest in Heart Development. *J Clin Invest* **103**, 1499-1507.

Wang, M., Rucklin, M., Poelmann, R. E., de Mooij, C. L., Fokkema, M., Lamers, G. E. M., de Bakker, M. A. G., Chin, E., Bakos, L. J., Marone, F., et al. (2023). Nanoplastics Causes Extensive Congenital Malformations During Embryonic Development by Passively Targeting Neural Crest Cells. *Environ Int* **173**, 107865.

Wang, W. D., Melville, D. B., Montero-Balaguer, M., Hatzopoulos, A. K. and Knapik, E. W. (2011). Tfap2a and Foxd3 Regulate Early Steps in the Development of the Neural Crest Progenitor Population. *Dev Biol* **360**, 173-185.

Wang, X. Y., Li, S., Wang, G., Ma, Z. L., Chuai, M., Cao, L. and Yang, X. (2015). High Glucose Environment Inhibits Cranial Neural Crest Survival by Activating Excessive Autophagy in the Chick Embryo. *Sci Rep* **5**, 18321.

Wilkinson, D. G. (1998). *In Situ Hybridization: A Practical Approach.*: OUP Oxford.

Yan, Y., Wang, G., Huang, J., Zhang, Y., Cheng, X., Chuai, M., Brand-Saberi, B., Chen, G., Jiang, X. and Yang, X. (2020). Zinc Oxide Nanoparticles Exposure-Induced Oxidative Stress Restricts Cranial Neural Crest Development During Chicken Embryogenesis. *Ecotoxicol Environ Saf* **194**, 110415.

Supporting Information

File S1. Supplementary Figure. LB Agar plates tests of PS-NP sterility.

File S2. Statistical analysis of malformation and mortality data on size response.

File S3. Statistical analysis of malformation and mortality data on dose response.

Movies S1. Control chicken embryo, exposed at stage 8 to vehicle only (Ringer's solution), and imaged with MicroCT at 24 hpe.

(Link: https://www.sciencedirect.com/science/article/pii/S0160412023001381r exposure; rotating view.)

Movies S2. Experimental (treated) chicken embryo, exposed at stage 8 to 50 of 25 nm PS-NPS, 5 mg/mL, and imaged with MicroCT 24 h after exposure; rotating view.

(Link: https://www.sciencedirect.com/science/article/pii/S0160412023001381)

Movies S3. Another experimental (treated) chicken embryo imaged with MicroCT.

(Link: https://www.sciencedirect.com/science/article/pii/S0160412023001381)

Table S1. Table of malformations that have been seen at 24 hpe.

Table S2. Table of malformations that have been seen at 4 dpe.

Table S3. Table of malformations that have been seen at 8 dpe.

Table S4. Primers used for PCR.

Fig. S1. Bright field microscopic images of 2 d chicken embryo neural crest cultures 1 h after exposure to PS-NPs (0.1 mg/mL) in culture medium or culture medium only (controls).

File S1. LB Agar plate streaking to confirm the sterility of PS-NPs used in this study. No colonies were observed in any of the plates after overnight incubation at 37 °C. (**a**) 25 nm plain nanoplastics, (**b**) 100 nm plain nanoplastics, (**c**) 500 nm plain nanoplastics.

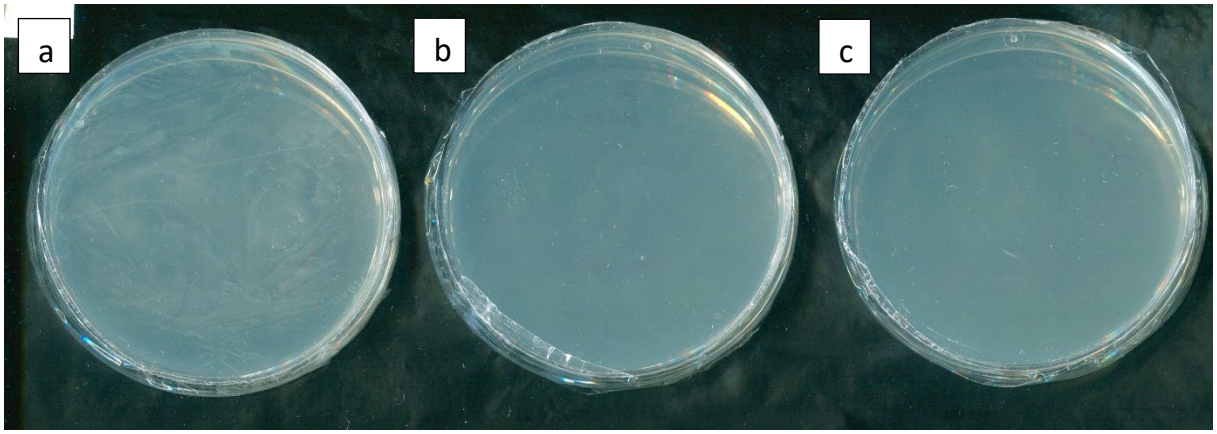

File S2. **Statistical analysis of malformation and mortality data on size response.**

Effects of Polystyrene Size

Method

All computations were performed in **R** version 4.1.3 (R Core Team, 2021). We computed the relative amount of particles as $100 \times \frac{\text{concentration}}{\text{particle size}}$.

We computed χ^2 tests from 2x2 contingency tables to evaluate the difference in death and malformedness between zero and non-zero size, relative amount and concentration of particles. We computed p-values based on both the asymptotic distribution of χ^2 statistics, as well as on Monte Carlo simulation with 2000 simulation replications (Hope, 1968).

Results

The raw data are depicted in Figure 1, where outcomes are plotted against particle size, and Figure 2, where outcomes are plotted against the relative amount of particles. For particle size, we observe highest probabilities of malformedness and death for size 25 nm. There is also a clear increasing probability of malformedness and death if the amount of particles increases. The increasing probability of malformedness and death could be a combined effect of particle size and/or the amount of particles, which cannot be disentangled in the current experiments: Because concentration was kept constant, the amount of particles automatically decreases if particle size increases.

Figure 1

Observed proportions of death and malformedness as a function of particle size.

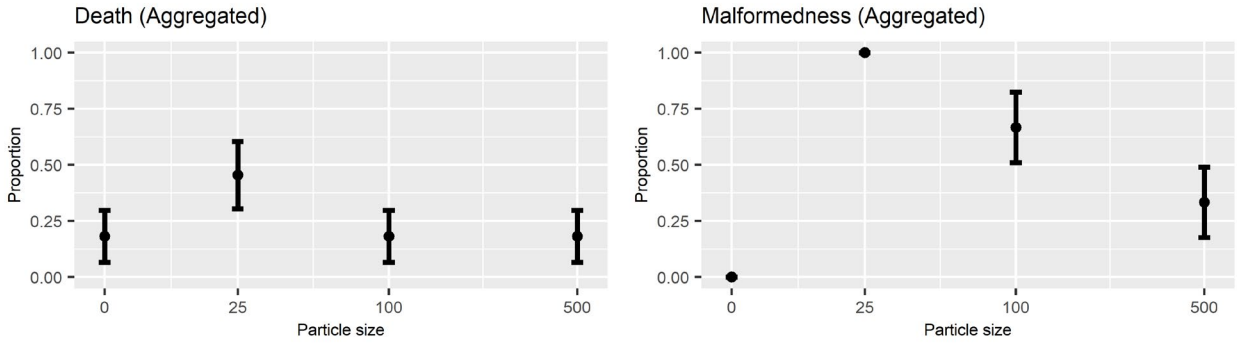

Note. Error bars represent estimated proportions $\pm$ 1 standard error, computed as $\sqrt{\frac{\hat{p}(1-\hat{p})}{n}}$.

Figure 2

Observed proportions of death and malformedness as a function of relative amount of particles.

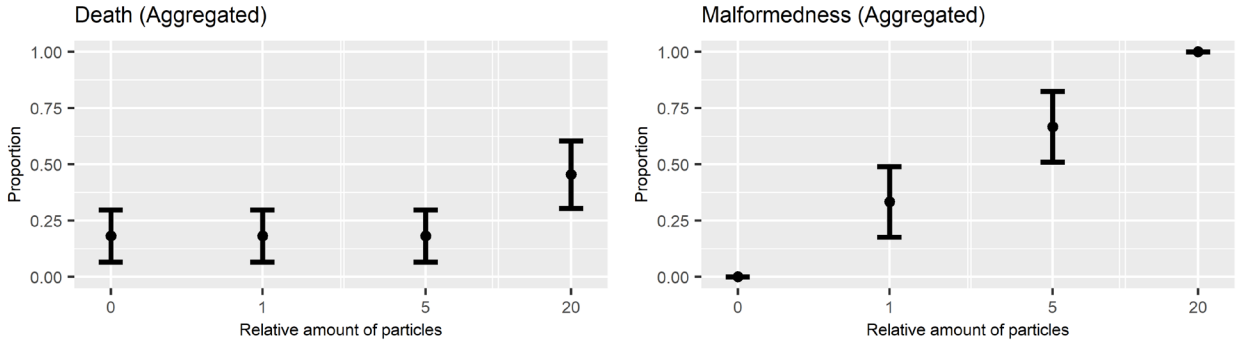

Note. Error bars represent estimated proportions $\pm$ 1 standard error, computed as $\sqrt{\frac{\hat{p}(1-\hat{p})}{n}}$.

We ran χ^2 tests to compare rates of malformedness and death between zero and non-zero particle sizes (with zero particle size equaling a relative amount of zero). χ^2 tests indicated a significant effect of particle size on the probability of malformedness: $X^2(1) = 7.946$; $p = 0.005$; Monte-Carlo $X^2 = 10.313$; $p = 0.003$. No significant effect of particle size on the probability of death was found: $X^2(1) = 0.04$; $p = 0.841$; Monte-Carlo $X^2 = 0.364$; $p = 0.688$.

Raw data

Table 1 presents the raw data on which these analyses were based.

Table 1

Raw data from the experiments.

experiment	size	concentration	relative amount	# normal	# malformed	# dead	# alive	# total	prop. dead	prop. malformed
size	0	0	0	9	0	2	9	11	0.182	0.000
size	25	5	20	0	6	5	6	11	0.455	1.000
size	100	5	5	3	6	2	9	11	0.182	0.667
size	500	5	1	6	3	2	9	11	0.182	0.333

References

Hope, A. C. (1968). A simplified monte carlo significance test procedure. *Journal of the Royal Statistical Society: Series B (Methodological)*, *30*(3), 582–598. https://doi.org/10.1111/j.2517-6161.1968.tb00759.x

R Core Team. (2021). *R: A language and environment for statistical computing*. R Foundation for Statistical Computing. https://www.R-project.org/

File S3. **Statistical analysis of malformation and mortality data on dose response.**

Effects of Polystyrene Concentration

Method

All computations were performed in **R** [version 4.1.3; R Core Team (2021)], using package **drc** [version 3.0.1; Ritz et al. (2015)].

We first computed χ^2 tests from 2x2 contingency tables to evaluate the difference in death and malfermedness between zero and non-zero size, relative amount and concentration of particles. We computed p-values based on both the asymptotic distribution of χ^2 statistics, as well as on Monte Carlo simulation with 2000 simulation replications (Hope, 1968).

We fitted dose-response curves using package **drc** (Ritz et al., 2015), which estimates log-logistic models (i.e., a logistic model with a parameter-dependent link function) using maximum likelihood. We used the 2- and 4-parameter models:

$$f(x) = c + \frac{d - c}{1 + \exp(b(\log(x) - \log(e)))}$$

where x is the dose and $f(x)$ gives the predicted probability of death. Parameter b reflects the effect of dose on the response, with a negative value indicating a positive effect (on death or malformedness, in the current study). Parameter c is a lower limit, and parameter d is an upper limit, both of which can be freely estimated, or fixed to a-priori known constants. If c is fixed to a value of zero and d is fixed to a value of 1, they can be dropped from the equation which yields the 2-parameter model:

$$f(x) = \frac{1}{1 + \exp(b(\log(x) - \log(e)))}$$

To evaluate model fit, we used a Pearson χ^2 goodness-of-fit test, and interpreted a high p-value to indicate acceptable model fit.

Results

Figure 1

Observed proportions of death and malformedness as a function of particle concentration.

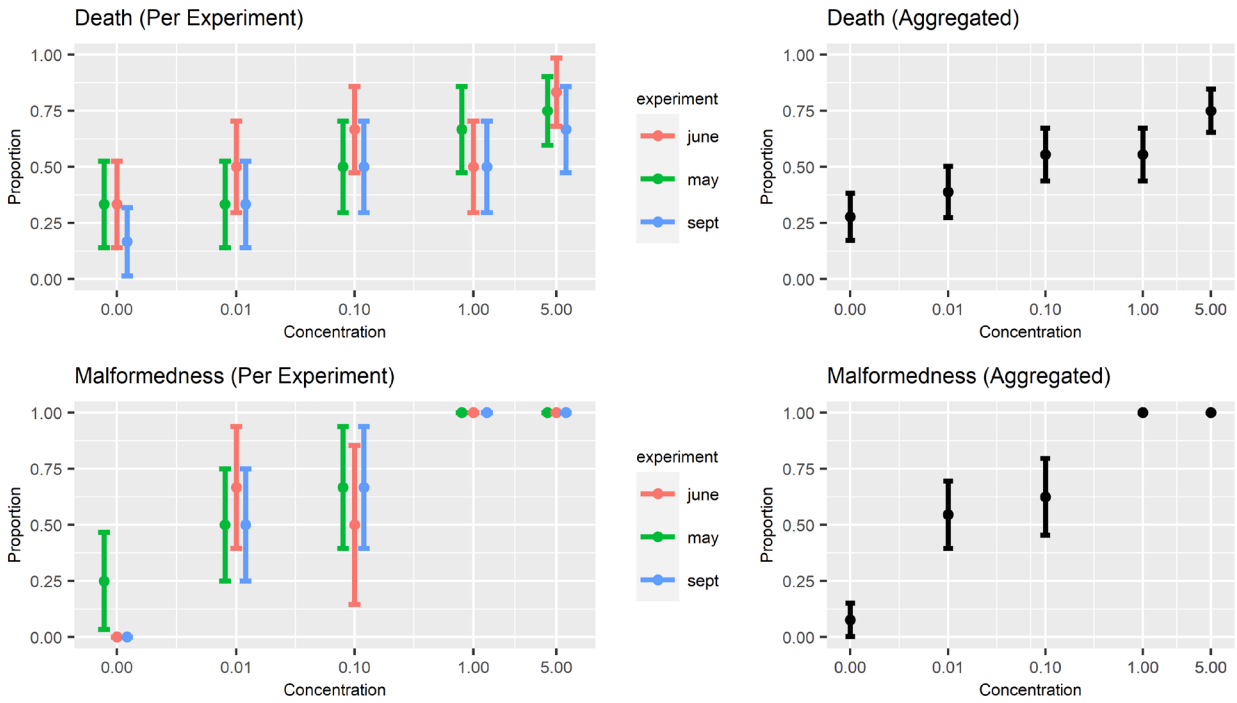

Note. Error bars represent estimated proportions $\pm$ 1 standard error, computed as $\sqrt{\frac{\hat{p}(1-\hat{p})}{n}}$.

The raw data are depicted in Figure 1, where outcomes are plotted against the concentration of particles. The plots indicate an increasing probability of malformedness and death if concentration increases.

We ran χ^2 tests to compare rates of malformedness and death between zero and non-zero concentrations. The χ^2 tests indicated a significant effect of concentration on the probability of malformedness: $X^2(1) = 14.345$; $p < 0.001$; Monte-Carlo $X^2 = 16.962$; $p < 0.001$. The χ^2 tests indicated a significant effect of concentration on the probability of death only according to the Monte-Carlo test: $X^2(1) = 3.775$; $p = 0.052$; Monte-Carlo $X^2 = 4.866$; $p = 0.036$.

Table 1

Parameter estimates for the effect of concentration on malformedness.

	Estimate	Std. error	t-value	p-value
b	-0.606	0.268	-2.261	0.024
e	0.011	0.010	1.088	0.276

Figure 2

Fitted dose-response curve for the effect of concentration on malformedness (2-parameter log-logistic model).

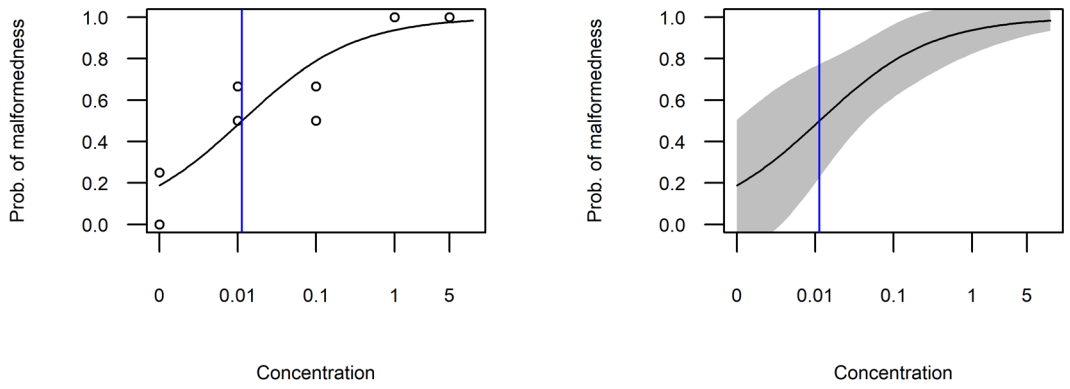

Note. The left plot shows observed datapoints, indicated by dots. The right plot depicts a 95% confidence interval. Blue vertical lines indicate the estimated concentration which would lead to malformedness in 50% of the population.

Next we fitted log-logistic models. Figure 1 indicated that the lower limit of the probability of malformedness is equal to zero, and the upper limit is equal to 1; we thus fitted a 2-parameter log-logistic model for malformedness. Table 1 shows the resulting parameter estimates; the negative and significant value of b indicates a significant effect of concentration on malformedness. Figure 2 shows the fitted dose-response curve. The model showed acceptable model fit: $X^2(10) = 2.63$: $p = 0.989$.

Table 2

Parameter estimates for the effect of concentration on death.

	Estimate	Std. error	t-value	p-value
b	-0.338	0.286	-1.180	0.238
c	0.276	0.104	2.648	0.008
d	0.949	0.553	1.715	0.086
e	0.721	3.781	0.191	0.849

Figure 3

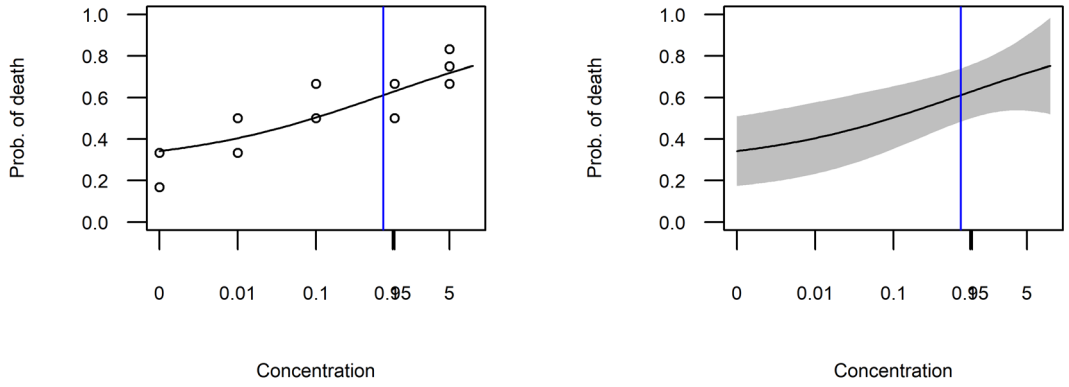

Fitted dose-response curve for the effect of concentration on death (4-parameter log-logistic model).

Note. The left plot shows observed datapoints, indicated by dots. The right plot depicts a 95% confidence interval. Blue vertical lines indicate the estimated LD50.

Figure 3 suggested the lower and upper limits on the probability of death were not equal to 0 and 1, respectively. We fitted a 4-parameter log-logistic model, in which the lower and upper limits are freely estimated; parameter estimates are presented in Table 2. The model showed acceptable model fit: $X^2(11) = 3.097$: $p = 0.989$. The

fitted dose-response curve is depicted in Figure 3. We performed a likelihood ratio test, which tests the null hypothesis of no effect against the 4-parameter dose-response model, which indicated a significant effect of concentration on death: $X^2(3) = 9.476$; $p = 0.024$

Raw data

Table 6 presents the raw data on which these analyses were based.

Table

Raw data from the experiments.

	experiment	size	concentration	# normal	# malformed	# dead	# alive	# total	prop. dead	prop. malformed
5	may	0	0.00	3	1	2	4	6	0.333	0.250
6	may	25	0.04	2	2	2	4	6	0.333	0.500
7	may	25	0.40	1	2	3	3	6	0.500	0.667
8	may	25	4.00	0	2	4	2	6	0.667	1.000
9	may	25	20.00	0	2	6	2	8	0.750	1.000
10	june	0	0.00	4	0	2	4	6	0.333	0.000
11	june	25	0.04	1	2	3	3	6	0.500	0.667
12	june	25	0.40	1	1	4	2	6	0.667	0.500
13	june	25	4.00	0	3	3	3	6	0.500	1.000
14	june	25	20.00	0	1	5	1	6	0.833	1.000
15	sept	0	0.00	5	0	1	5	6	0.167	0.000
16	sept	25	0.04	2	2	2	4	6	0.333	0.500
17	sept	25	0.40	1	2	3	3	6	0.500	0.667
18	sept	25	4.00	0	3	3	3	6	0.500	1.000
19	sept	25	20.00	0	2	4	2	6	0.667	1.000

References

Hope, A. C. (1968). A simplified monte carlo significance test procedure. *Journal of the Royal Statistical Society: Series B (Methodological)*, *30*(3), 582–598. https://doi.org/10.1111/j.2517-6161.1968.tb00759.x

R Core Team. (2021). *R: A language and environment for statistical computing*. R Foundation for Statistical Computing. https://www.R-project.org/

Ritz, C., Baty, F., Streibig, J. C., & Gerhard, D. (2015). Dose-response analysis using R. *PLOS ONE*, *10*(e0146021, 12). https://doi.org/10.1371/journal.pone.0146021

Table S1. **Table of malformations that have been seen at 24 hpe.**

Embryos analysed for phenotypic effects 28 h after treatment with 5mg/mL plain PS-NPs. In the column 'Concentration PS-NPs', 0 mg/mL = Ringer's only controls. HH, Hamburger & Hamilton, 1951 stages.

Embryo number	Concentration of PS-NPs (mg/ml)	Mortality: alive, 0; dead, 1	Gross assessment of phenotype: normal, 0; abnormal, 1	No. somite pairs	Stage (HH)	Phenotype judgement Normal(0)/Abnormal(1)	Neural tube defect location		
							head	trunk	caudal
1	5	1	1						
2	5	0	1	7	9	1	1	1	1
3	5	1	1						
4	5	0	1	13	11	1	1	1	
5	5	1	1						
6	5	0	1	12	11	1	1	1	1
7	5	1	1						
8	5	1	1						
9	5	1	1						
10	5	0	1	13	11	1	1	1	
11	0	1							
12	0	0	0	25	15	0			
13	0	0	0	26	15	0			
14	0	0	0	23	15	0			
15	0	0	0	22	14	0			
16	0	0	0	22	14	0			
17	0	0	0	24	15	0			
18	0	0	0	22	14	0			
19	0	0	0	26	15	0			
20	0	1							
21	5	1							
22	5	0	1	13	11	1	1	1	1
23	5	1							
24	5	0	1	22	14	1	1		
25	5	1							
26	5	0	1			1	1		
27	5	1							
28	5	0	1	n.d	11	1	1	1	1
29	5	1							
30	5	1							

31	0	0	0	19	13				
32	0	1							
33	0	0	0	20	13				
34	0	1							
35	0	0	0	19	13				
36	0	0	0	22	14				
37	0	0	0	17	12				
38	0	0	0	19	13				
39	0	0	0	22	14				
40	0	0	0	20	13				
41	5	0	1	20	13	1		1	
42	5	1							
43	5	1							
44	5	0	1	18	12	1		1	
45	5	0	1	16	12	1	1	1	1
46	5	0	1	15	11	1	1	1	
47	5	0	1	18	12	1	1	1	
48	5	1							
49	5	1							
50	5	1							
51	0	0	0	25	15				
52	0	0	0	22	14				
53	0	0	0	22	14				
54	0	0	0	17	12				
55	0	0	0	22	14				
56	0	0	0	21	13				
57	0	1							
58	0	0	0	15	11				
59	0	1							
60	0	0	0	20	13				
61	5	0	1	18	12	1	1	1	
62	5	0	1	16	12	1	1	1	1
63	5	1							
64	5	1							
65	5	1							
66	5	0	1	17	12	0			
67	5	0	1	17	12	0			
68	5	0	1	19	13	1	1	1	
69	5	0	1	18	12	1		1	
70	5	1							
71	0	0	0	22	14	0			

72	0	0	0	24	15	0			
73	0	1							
74	0	0	0	21	13	0			
75	0	0	0	20	13	0			
76	0	0	0	20	13	0			
77	0	0	0	21	13	0			
78	0	0	0	22	14	0			
79	0	0	0	21	13	0			
80	0	0	0	23	14	0			
81	5	0	1	20	13	0	0	0	0
82	5	1							
83	5	1							
84	5	0	1	18	12	1			1
85	5	1							
86	5	1							
87	5	0	1	20	13	1	1		
88	5	0	0	21	13	1	1		
89	5	0	1	17	12	1	0	1	0
90	5	0	1	17	12	1	1		1
91	0	0	0	20	13	0			
92	0	0	0	20	13	0			
93	0	1							
94	0	0	0	20	13	0			
95	0	0	0	22	14	0			
96	0	0	0	25	15	0			
97	0	0	0	23	14	0			
98	0	0	0	20	13	0			
99	0	0	0	22	14	0			
100	0	0	0	22	14	0			

Table S2. **Table of malformations that have been seen at 4 dpe.**

Embryos analysed for phenotypic effects 4 d after treatment with 5mg/mL plain PS-NPs. In the column 'Concentration PS-NPs', 0 mg/ml = Ringer's only controls.

Embryo number	Concentration of PS-NPs (mg/ml)	Mortality: alive, 0; dead, 1	gross assessment of phenotype: normal, 0; abnormal, 1	Neural tube defect			tail	microphthalmia		
				head	trunk	caudal		left eye	right eye	torsion /flexure
1	0	0	0							
2	0	1								
3	0	0	0							
4	0	0	0							
5	0	1								
6	0	0	1	0						1
7	0.01	0	0							
8	0.01	0	1			1	1			
9	0.01	1								
10	0.01	0	0							
11	0.01	1								
12	0.01	0	1	1		1				1
13	0.1	0	0							
14	0.1	1								
15	0.1	0	1	1		1	1	1		
16	0.1	0	1	1		1	1	1	1	1
17	0.1	1								
18	0.1	1								
19	1	1								
20	1	0	1			1		1	1	
21	1	1								
22	1	1								
23	1	0	1			1				1
24	1	1								
25	5	0	1	1						1

26	5	1									
27	5	1									
28	5	1									
29	5	1									
30	5	0	1			1					1
31	5	1									
32	5	1	0								
33	0	0	0								
34	0	1									
35	0	0	0								
36	0	1									
37	0	0	0								
38	0	0	0								
39	0.01	1									
40	0.01	1									
41	0.01	1									
42	0.01	0	1					1			
43	0.01	0	1						1	1	1
44	0.01	0	0								
45	0.1	0	0								1
46	0.1	0	0								
47	0.1	1									
48	0.1	1									
49	0.1	1									
50	0.1	1									
51	1	0	1	1						1	
52	1	1									
53	1	0									
54	1	1									
55	1	0	1	1	1	1	1	1	1	1	
56	1	1									
57	5	1									
58	5	1									
59	5	0	1	1							1
60	5	1									
61	5	1									
62	5	1									
63	0	1									
64	0	0	1	1							
65	0	0	0								
66	0	0	0								

67	0	0	0						
68	0	0	0						
69	0.01	1							
70	0.01	1							
71	0.01	0	0						
72	0.01	0	1						1
73	0.01	0							
74	0.01	0	1						1
75	0.1	1							
76	0.1	1							
77	0.1	0	1						1
78	0.1	0							
79	0.1	1							
80	0.1	0	1	1					
81	1	1							
82	1	0	1						1
83	1	0	1					1	1
84	1	0	1						1
85	1	1							
86	1	1							
87	5	0	1	1					1
88	5	1							
89	5	1							
90	5	1							
91	5	1							
92	5	0	1	1	1	1	1		

Table S3. **Table of malformations seen at 8 dpe.**

				Neural tube defect			Microphthalmia		Cardiac Malformations (normal,0; abnormal,1)								Comments
Embryo number	**Concentration of PS-NPs (mg/mL)**	**Analysis approach**	**gross assessment of phenotype: normal, 0; abnormal, 1**	**Head**	**Trunk**	**Tail**	**Left**	**Right**	**Craniofacial dysplasia (CD), Cleft Primary Palate (CPP)**	**Vertebral/Axial malformations**	**Failure of ventral side closure**	**Thymic disruption**	**Ventricular septal defect**	**Abnormal pharyngeal arch arteries**	**Persistent truncus arteriosus**	**Aortopulmonary Septal Defect**	
1	0	Alcian blue, H&E	0	0	0	0	0	0	0	0	0	0	0	0	0	0	
2	0	Alcian blue, H&E	0	0	0	0	0	0	0	0	0	0	0	0	0	0	
3	0	Alcian blue, H&E	0	0	0	0	0	0	0	0	0	0	0	0	0	0	
4	0	Alcian blue, H&E	0	0	0	0	0	0	0	0	0	0	0	0	0	0	
5	5	Alcian blue, H&E	1	1	0	n.d	1	1	1(CD)	1	1	1	n,d	n.d	1	n.d	Sample was destroyed while embedding
6	5	Alcian blue, H&E	1	1	1	n.d	0	1	1(CPP)	1	1	1	0	1 (persistent pharyngeal	0	0	Persist 4th arch

													arch artery)				
7	5	Alcian blue, H&E	1	0	0	n.d	0	0	0	1	0	1	1(DORV)	0	0	1	Significant pericardial blebbing, OFTs fail to spiral, common IFT complex
8	5	Alcian blue	1	1	1	n.d	1	1	1(CPP)	1	1	n.d	n.d	n.d	n.d	n.d	Phocomelia and severe microphthalmia
9	5	Alcian blue	1	1	1	n.d	1	1	1(CD)	1	1	n.d	n.d	n.d	n.d	n.d	
10	5	Alcian blue	1	1	n.d	n.d	0	1	1(CD+CPP)	1	1	n.d	n.d	n.d	n.d	n.d	severe facial clefting
11	0	Synchrotron	0	0	0	0	0	0	0	0	0	0	0	0	0	0	
12	5	Synchrotron	1	n.d	n.d	n.d	n.d	n.d	n.d	n.d	n.d	n.d	1	1(2 extra pharyngeal arch arteries)	0	0	
13	5	Synchrotron	1	n.d	n.d	n.d	n.d	n.d	n.d	n.d	n.d	n.d	1	0	0	1	Pericardial blebbing
14	0	Synchrotron	0	0	0	0	0	0	0	0	0	0	0	0	0	0	
15	5	Synchrotron	1	n.d	n.d	n.d	n.d	n.d	n.d	n.d	n.d	n.d	0	0	0	0	
16	5	Synchrotron	1	n.d	n.d	n.d	n.d	n.d	n.d	n.d	n.d	n.d	0	0	0	0	

Table S4. **Primers used for PCR.**

Gene	Forward Primers	Reverse Primer	Accession NCBI Reference Sequence
FOXD3 (Forkhead box D3)	CGAAGAGCAGCCTGGTGAAGC	CGATGATGTTGGTAGGCACGCT	NM_204951.3
SNAI2 (Snail family transcriptional repressor 2)	CCACGCTCCTTCCTGGTC	CCAGGTAAACATTGACTGCATGA	CR407272
WNT1(Wnt family member 1)	TCTGATCCGACAGAACCCCG	GTCCCCATCTTCCCGCTGTA	NM_001396681.1
SOX10 (SRY-box 10)	GCAGCCTTCACAGGGTTTG	CCCTTCTCGCTTGGAGTCAG	NM_204792.2
LMO4 (LIM domain only 4)	CTACACCAAGAGCGGCATGA	AGTCTCCCATTAGCCCAGGT	NM_204112.2
PAX3 (Paired box 3)	TCGGGAAGAACTCGCACAAA	GCGAGACCGGAAAATAACACC	NM_001397759.1
TFAP2A (Transcription factor AP-2 alpha)	CCAAGTCTAACAACAACGCC	TTTCGGTGCTTCTCCTCTTT	NM_205094.2

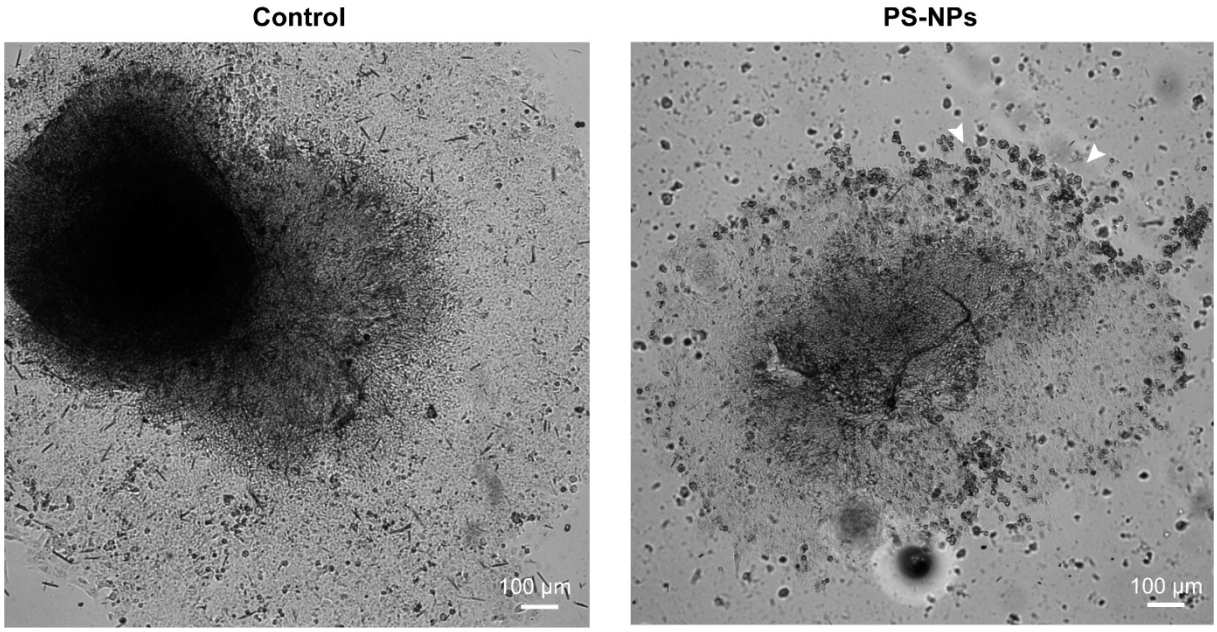

Fig. S1. Bright field microscopic images of 2 d chicken embryo neural crest cultures 1 h after exposure to PS-NPs (0.1 mg/mL) in culture medium or culture medium only (controls). Note the dead cells (white arrowheads) in the PS-NP treated culture.

Chapter 5. Summary, discussion and perspective

Meiru Wang[1,2], Martina G. Vijver[3], Michael K. Richardson[1].*

1. Institute of Biology, Leiden University, Sylvius Laboratory, Sylviusweg 72, 2333 BE, Leiden, The Netherlands.

2. Naturalis Biodiversity Center, Darwinweg 2, 2333 CR, Leiden, The Netherlands.

3. Institute of Environmental Sciences, Leiden University (CML), Van Steenis Building, Einsteinweg 2, 2333 CC, Leiden, The Netherlands.

Manuscript in preparation.

Summary

Plastics are used as the main material for fabricating every-day items which have brought great convenience to our lives. On the downside, however, 60% of plastics end up dumped in landfills or as plastic waste in the environment (Geyer et al., 2017). This waste slowly releases fragments called small plastic particles which can be divided into microplastics and nanoplastics (MPs and NPs) according to their size. Small plastic particles have become ubiquitous in the environment where they pose potential dangers to wildlife and to humans (Allen et al., 2022; Zolotova et al., 2022).

MPs and NPs have been demonstrated to transfer from mother to offspring in zebrafish (Pitt et al., 2018). Furthermore, they are even found to be able to transfer through food webs (Chae et al., 2018; Kim et al., 2022). MPs and NPs are suspected to be a potential health risk to humans due to toxicity to cell cultures (Aguilar-Guzmán et al., 2022; Cortés et al., 2020; Gopinath et al., 2021; Ramsperger et al., 2020), and the fact that they have been detected in multiple human tissues body fluids (Jenner et al., 2022; Leslie et al., 2022; Ragusa et al., 2021; Zhao et al., 2023). Indirect evidence of potential toxicity to humans is the fact that small plastic particles are toxic in several whole animal models (Yin et al., 2021; Yong et al., 2020). For example, the toxicity of MPs and NPs has been widely studied in aquatic animals including *Daphnia magna* (Abdolahpur Monikh et al., 2020; Kelpsiene et al., 2020) the zebrafish (Lee et al., 2022; Torres-Ruiz et al., 2021) and the Pacific Oyster (Cole and Galloway, 2015). However, little is known about their potential risk to warm-blooded vertebrates.

In **Chapter 1**, we have summarized the currently findings about MPs and NPs, and their potential risk to humans. Additionally, we have reviewed the literature on using the chick embryo as a model for testing toxic agents for their specific toxicity towards embryonic development. Indeed chick embryos have already been used for several toxicity studies of nanoparticles, particularly metal and carbon particles.

In **Chapter 2**, I have shown that PS-NPs can cause neural tube defects in the head, trunk, tail, or a combination of these regions in the chick embryo. Neural tube defects represent a failure of neural tube closure (Greene and Copp, 2014), leading to increased morbidity and mortality (Copp and Greene, 2010; Madrid et al., 2023). We suggest that this failure of closure is due to toxic effects of PS-NPs on the neural crest — a population of neuroectodermal cells adjacent to the fusion zone of the closing neural tube (Creuzet, 2009; Green et al., 2015; Le Douarin et al., 2012; Le Douarin and Kalcheim, 1999; Martik and Bronner, 2021; Waldo et al., 1998). This model (which we summarize in Fig. 5-1) is consistent with a study showing that the neural crest is essential for neural tube closure, at least in the cranial region (Creuzet, 2009; Creuzet et al., 2006; Wang et al., 2023).

Next, in **Chapter 3**, we have provided the first evidence that exposure of chick embryos to PS-NPs can cause heart malformations. Specifically, we have detected cardiovascular malformations including ventricular septal defect, supernumerary arteries, persistent truncus arteriosus, abnormal blood vessels and excess cardiac jelly. In addition, we have shown that PS-NPs cause impaired cardiac function. These findings make sense in the light of previous reports that neural crest cells play an essential role of the cardiovascular development (Le Douarin and Kalcheim, 1999). For example, after neural crest cells were ablated surgically, the resulting embryo phenotype displayed cardiovascular abnormalities (Keyte and Hutson, 2012; Kirby and Waldo, 1995; Waldo et al., 1999).

In addition to the cardiovascular malformations described in **Chapter 3**, we have also noticed craniofacial defects in treated embryos. These defects include malformation (hypoplasia or aplasia) of the upper beak, and failure of Meckel's cartilage to fuse with its contralateral partner. These malformations, like others mentioned above may also be explained by the results of NPs affecting neural crest cells. This is because neural crest cells play an essential role in craniofacial development (Martik and Bronner, 2021).

Our finding of both cardiovascular and craniofacial defects is consistent with the concept of a 'cardiocraniofacial module' (Gans and Northcutt, 1983; Keyte and Hutson, 2012; Martik and Bronner, 2021) which is dependent on neural crest cells for its normal development. Interestingly, it was previously shown that the exposure of chicken embryos to metal nanoparticles (zinc oxide) causes craniofacial abnormalities, which was suggested to result from disruption of neural crest development (Yan et al., 2020). We should be cautious in interpreting those findings because many types of metal nanoparticles shed ions, and so the toxicity of zinc oxide nanoparticles observed in that study is not necessarily mediated by the same mechanisms nanoplastic toxicity. It should also be noted that craniofacial defects that we observed here are not necessarily a reflection of abnormal neural crest development.

In a few NP treated embryos, the tailbud was hypoplastic or aplastic; one embryo showed agenesis of the tail and phocomelia of the hindlimbs (**Chapters 2** and **3**). We suggest that these effects reflect an effect of PS-NPs on surface-exposed mesenchymal populations in the primitive streak of the tailbud. During gastrulation, and the process of ingression, the dorsal surface epithelium undergoes an epithelial-mesenchymal transition with local loss of the basal lamina (Bellairs, 1986; Shook and Keller, 2003). This process is still active at the stage when we introduced the PS-NPs to the egg (Knezevic et al., 1998).

Another potential source of mesenchymal cells in the caudal region, that might be affected by PS-NP exposure, is the junction between regions of primary and secondary neurulation (Dady et al., 2014). This process starts around stage 8 (Dady et al., 2014). Binding of the PS-NPs to these junctional mesenchymal cells could explain the gross dysplasia of the neural tube in the caudal region of some embryos (**Chapters 2** and **3**). We exposed embryos to PS-NPs at stage 8. Both gastrulation and neurulation are still active at this stage (Keibel and Abraham, 1900).

In **Chapter 4**, our experiments, with fluorescent PS-NPs added to live embryos, show strong labelling in the neural crest, but little or none in any other tissues (**Chapter 4**, Fig. 4-1). Furthermore, we find that that fluorescence is seen in the cytoplasm within 2 h and is still there at 6 h. However, these experiments should be interpreted with caution because: single 25 nm particles are too small to be directly visualized with optical microscopes; and it is possible that the fluorescence we saw was partly due to leakage of the fluorochrome from the particles. In any case, it is evident that strong fluorescence is specifically found in neural crest cells.

Our TUNEL-labelling experiments showed enhanced cell death in both the dorsal midline of the neural tube (**Chapter 4**, Fig. 4-7), and in ectopic clumps of cells in the neural tube lumen that we identified as neural crest cells with neural crest markers (**Chapter4**, Fig. 4-2 to 4). The same markers also identify a population of neural crest cells in the dorsal midline of PS-NP treated embryos that have failed to migrate. We also see evidence of reduced neural crest cell migration into the pharyngeal arches when using TFAP2A expression as a marker of migrating cardiac crest cells (**Chapter 3**, Fig.3-6).

Together, these data suggest that neural crest cells are damaged or undergo cell death after binding PS-NPs and fail to migrate (Fig. 5-1; (Wang et al., 2023). Candidate mechanisms of PS-NPs cell-damage include the denaturation of proteins (Gopinath et al., 2019; Hollóczki and Gehrke, 2019), and the accumulation of PS-NPs in the cytoplasm, after being taken up by endocytosis, and then resisting degradation by lysosomal enzymes (Nie et al., 2021). Our hypothesis, that PS-NPs inhibit neural crest migration, is consistent with experiments on other migratory cell types. For example, it has been shown that PS-NPs supress the migration and dispersion of aggregated CT26 murine carcinoma cells *in vitro* (Beaune et al., 2019).

Our study shows that PS-NPs have harmful effects on early chicken embryos, producing a range of malformations. We find that the toxicity of PS-NPs is due to their ‘targeting’ a specific subpopulation of embryonic cells. The targeting is passive,

in the sense that PS-NPs appear to strongly bind to neural crest cells and not to other cells. The fact that NPs cause multi-system malformations is of great concern; given the extensive environmental exposure of humans to small plastic particles, the reported presence of small plastic particles in human tissues, and the current development of a new generations of nanomedicines intended for human therapeutic use.

In the future, it will be important to explore the underlying mechanism of the selective binding of nanoplastics to neural crest cells. One hypothesis is that nanoplastics bind to specific cell adhesion molecules, known to be expressed by neural crest cells, such as cadherin 6B. Cadherin 6B is associated with epithelial mesenchymal transformation in both embryonic cells and some cancer cells. If this hypothesis is confirmed, the finding would contribute to both our understanding of the embryonic toxicity of nanoplastics and possibly also to cancer research.

Discussion and perspective

Our data show that 25 nm PS-NPs selectively attach to neural crest cells, and possibly other cell populations undergoing epithelial-mesenchymal transformation on the dorsal surface of the embryo. By contrast, PS-NPs show little or no attachment to intact embryonic epithelia. It is possible that this reflects the differential expression of adhesion molecules on different cell populations on the surface of the embryo. For example, sugar residues in the cell coat of neural crest cells in mouse and rat embryos differ considerably from neurectoderm and epithelial ectoderm (Smits-van Prooije et al., 1986). Furthermore the cell adhesion molecule cadherin 6B is differentially expressed on pre-migratory crest cells and cadherin 7 is expressed on migratory crest cells (Taneyhill and Schiffmacher, 2017). Note that the switch between the expression of different cadherin molecules (the ‘cadherin switch’) accompanies the segregation of the neural crest lineage from the neurectoderm (Dady et al., 2012). Our hypothesis is that PS-NPs may interact with the cadherins

during neurulation, possibly changing the protein structure and functions (Hollóczki and Gehrke, 2019; Kihara et al., 2021). The interaction of proteins with nanoplastics is the basis of the 'corona' which is sometimes observed on nanoparticles exposed to proteins .

The concentration of nanoparticles used in this study (5 mg/mL) is higher than that reported, for example, in human blood. (Leslie et al., 2022). However, it should be remembered that PS-NPs and other nanomedicines are likely to be used in high concentrations. Furthermore, it has been shown that nanoplastics can be transmitted to offspring in several animal models (Pitt et al., 2018; Zhao et al., 2017); if this applies to humans, then we might expect a cumulative increase in particles in human tissues over the generations.

The highly selective effect of PS-NPs on embryonic neural crest cells may mean that they are capable of disrupting development even in low levels exposures. Furthermore, detecting nanoplastics in the environment and in human tissues, is extremely difficult, and the associated analytics are in their infancy. As a result, it is likely that human exposure to PS-NPs has been substantially underestimated. Finally, it is worth remembering that even if society stops now with all plastic pollution, the weathered nanoplastic debris levels from existing plastics in the environment will still increase. In the future, we will need more information about the teratogenicity of nanoplastics — and possibly of nanomaterials in general.

Our study shows that PS-NPs cause effects on development that closely resemble those produced by a surgical ablation of the neural crest (Bockman et al., 1987; Hutson and Kirby, 2007; Kirby, 1999; Kirby et al., 1989; Kirby et al., 1985). This means that nanoplastics can have catastrophic effects on development by 'targeting' a specific subpopulation of embryonic cells. The targeting is passive, in the sense that PS-NPs may simply show strong binding to certain cell-surface molecules on neural crest cells. In any case, the highly selective effect of PS-NPs on certain exposed embryonic cell populations may mean that they are capable of disrupting

development even in low-level exposures. The production of malformations by NPs are of concern, given the extensive environmental exposure of humans to small plastic particles (Anagnosti et al., 2021; Cox et al., 2019; Koelmans et al., 2019; Vighi et al., 2021; Zhang et al., 2020), the reported presence of small plastic particles in human tissues (Jenner et al., 2022; Leslie et al., 2022; Ragusa et al., 2021), and the current development of a new generations of nanomedicines intended for human therapeutic use (Boehnke et al., 2022). In summary, we believe that PS-NPs of primary or secondary origin pose a potential danger to living embryos of humans and other vertebrates. Because of this, the increasing burden of environmental nanoplastics is a matter for concern.

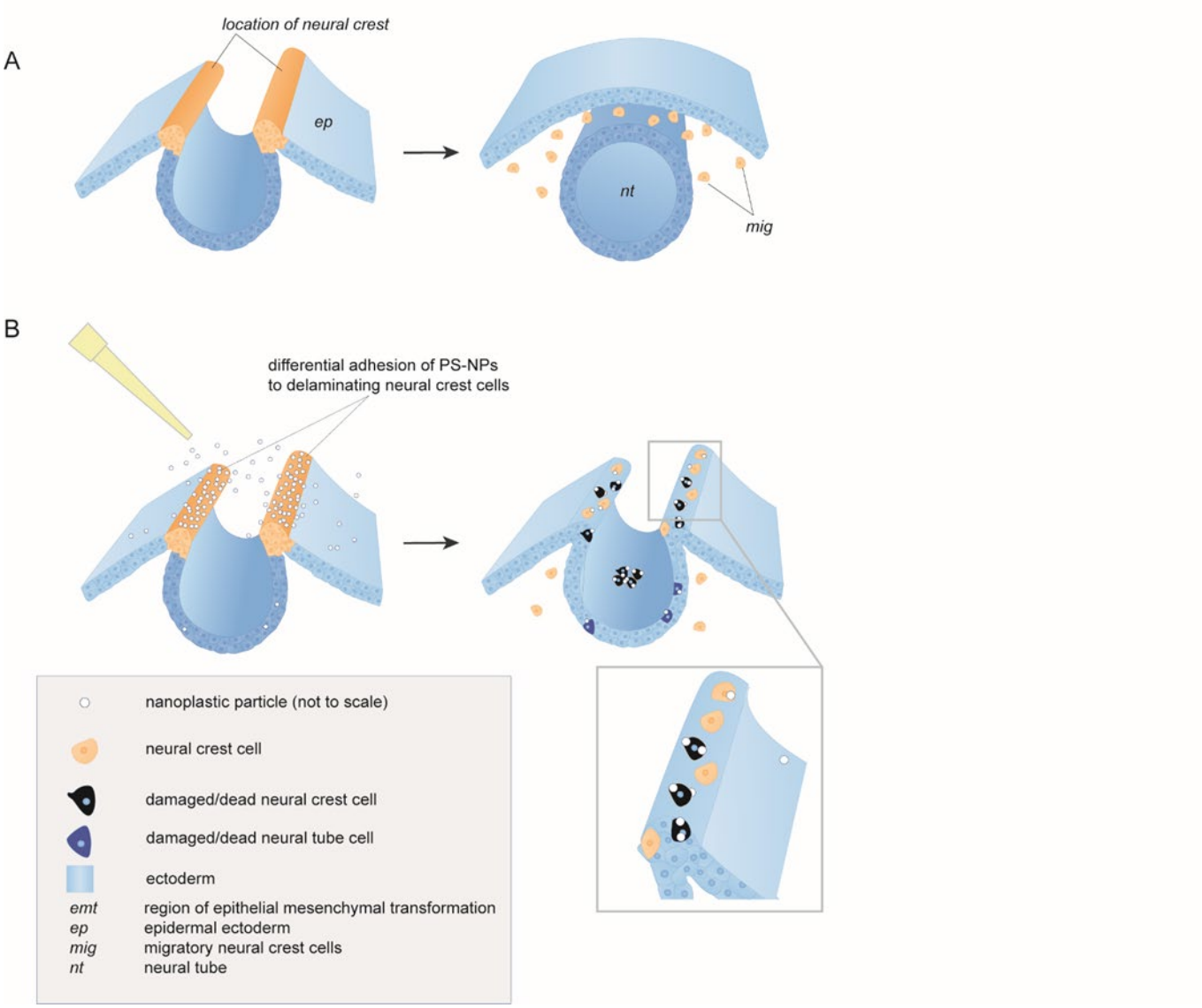

Fig. 5-1. **Our hypothesis of PS-NP-induced developmental toxicity, based on disruption of neural crest development. A**, normal development of the neural tube and neural crest. **B**, development of the neural tube and crest after exposure of the embryo to 25 nm PS-NPs. We hypothesize that the nanoparticles adhere selectively to the neural crest cells undergoing epithelial-mesenchymal transition, and induce cell death in at least a subpopulation of those neural crest cells. This reduces the number of normal neural crest cells, disrupts their migration and interferes with the normal closure of the neural tube. It also often leaves a clump of putative neural crest cells in the lumen of the neural tube (or the neural groove, in the case of a neural tube defect). We suggest that these events lead to neural tube defects, microphthalmia, craniofacial and cardiac malformations. Note that we saw some evidence of very limited cell death in the neural tube induced by PS-NPs (as shown in this figure).

References

Abdolahpur Monikh, F., Vijver, M. G., Guo, Z., Zhang, P., Darbha, G. K. and Peijnenburg, W. J. G. M. (2020). Metal Sorption onto Nanoscale Plastic Debris and Trojan Horse Effects in Daphnia Magna: Role of Dissolved Organic Matter. *Water Research* **186**, 116410.

Aguilar-Guzmán, J. C., Bejtka, K., Fontana, M., Valsami-Jones, E., Villezcas, A. M., Vazquez-Duhalt, R. and Rodríguez-Hernández, A. G. (2022). Polyethylene Terephthalate Nanoparticles Effect on Raw 264.7 Macrophage Cells. *Microplastics and Nanoplastics* **2**, 9.

Allen, D., Allen, S., Abbasi, S., Baker, A., Bergmann, M., Brahney, J., Butler, T., Duce, R. A., Eckhardt, S., Evangeliou, N., et al. (2022). Microplastics and Nanoplastics in the Marine-Atmosphere Environment. *Nature Reviews Earth & Environment* **3**, 393-405.

Anagnosti, L., Varvaresou, A., Pavlou, P., Protopapa, E. and Carayanni, V. (2021). Worldwide Actions against Plastic Pollution from Microbeads and Microplastics in Cosmetics Focusing on European Policies. Has the Issue Been Handled Effectively? *Marine Pollution Bulletin* **162**, 111883.

Beaune, G., Nagarajan, U., Brochard-Wyart, F. and Winnik, F. M. (2019). Polymeric Nanoparticles Limit the Collective Migration of Cellular Aggregates. *Langmuir* **35**, 7396-7404.

Bellairs, R. (1986). The Primitive Streak. *Anat Embryol (Berl)* **174**, 1-14.

Bockman, D. E., Redmond, M. E., Waldo, K., Davis, H. and Kirby, M. L. (1987). Effect of Neural Crest Ablation on Development of the Heart and Arch Arteries in the Chick. *Am.J.Anat.* **180**, 332-341.

Boehnke, N., Straehla, J. P., Safford, H. C., Kocak, M., Rees, M. G., Ronan, M., Rosenberg, D., Adelmann, C. H., Chivukula, R. R., Nabar, N., et al. (2022). Massively Parallel Pooled Screening Reveals Genomic Determinants of Nanoparticle Delivery. *Science* **377**, eabm5551.

Chae, Y., Kim, D., Kim, S. W. and An, Y.-J. (2018). Trophic Transfer and Individual Impact of Nano-Sized Polystyrene in a Four-Species Freshwater Food Chain. *Scientific reports* **8**, 284.

Cole, M. and Galloway, T. S. (2015). Ingestion of Nanoplastics and Microplastics by Pacific Oyster Larvae. *Environmental Science & Technology* **49**, 14625-14632.

Copp, A. J. and Greene, N. D. (2010). Genetics and Development of Neural Tube Defects. *J Pathol* **220**, 217-230.

Cortés, C., Domenech, J., Salazar, M., Pastor, S., Marcos, R. and Hernández, A. (2020). Nanoplastics as a Potential Environmental Health Factor: Effects of Polystyrene Nanoparticles on Human Intestinal Epithelial Caco-2 Cells. *Environmental Science: Nano* **7**, 272-285.

Cox, K. D., Covernton, G. A., Davies, H. L., Dower, J. F., Juanes, F. and Dudas, S. E. (2019). Human Consumption of Microplastics. *Environmental Science & Technology* **53**, 7068-7074.

Creuzet, S. E. (2009). Regulation of Pre-Otic Brain Development by the Cephalic Neural Crest. *Proceedings of the National Academy of Sciences* **106**, 15774-15779.

Creuzet, S. E., Martinez, S. and Le Douarin, N. M. (2006). The Cephalic Neural Crest Exerts a Critical Effect on Forebrain and Midbrain Development. *Proc Natl Acad Sci USA* **103**, 14033-14038.

Dady, A., Blavet, C. and Duband, J. L. (2012). Timing and Kinetics of E- to N-Cadherin Switch During Neurulation in the Avian Embryo. *Dev Dyn* **241**, 1333-1349.

Dady, A., Havis, E., Escriou, V., Catala, M. and Duband, J. L. (2014). Junctional Neurulation: A Unique Developmental Program Shaping a Discrete Region of the Spinal Cord Highly Susceptible to Neural Tube Defects. *J Neurosci* **34**, 13208-13221.

Gans, C. and Northcutt, R. G. (1983). Neural Crest and the Origin of Vertebrates: A New Head. *Science* **220**, 268-273.

Geyer, R., Jambeck, J. R. and Law, K. L. (2017). Production, Use, and Fate of All Plastics Ever Made. *Sci Adv* **3**, e1700782.

Gopinath, P. M., Saranya, V., Vijayakumar, S., Mythili Meera, M., Ruprekha, S., Kunal, R., Pranay, A., Thomas, J., Mukherjee, A. and Chandrasekaran, N. (2019). Assessment on Interactive Prospectives of Nanoplastics with Plasma Proteins and the Toxicological Impacts of Virgin, Coronated and Environmentally Released-Nanoplastics. *Scientific Reports* **9**, 8860.

Gopinath, P. M., Twayana, K. S., Ravanan, P., John, T., Mukherjee, A., Jenkins, D. F. and Chandrasekaran, N. (2021). Prospects on the Nano-Plastic Particles Internalization and Induction of Cellular Response in Human Keratinocytes. *Particle and Fibre Toxicology* **18**, 35.

Green, S. A., Simoes-Costa, M. and Bronner, M. E. (2015). Evolution of Vertebrates as Viewed from the Crest. *Nature* **520**, 474-482.

Greene, N. D. and Copp, A. J. (2014). Neural Tube Defects. *Annu Rev Neurosci* **37**, 221-242.

Hollóczki, O. and Gehrke, S. (2019). Nanoplastics Can Change the Secondary Structure of Proteins. *Scientific Reports* **9**, 16013.

Hutson, M. R. and Kirby, M. L. (2007). Model Systems for the Study of Heart Development and Disease. Cardiac Neural Crest and Conotruncal Malformations. *Semin Cell Dev Biol* **18**, 101-110.

Jenner, L. C., Rotchell, J. M., Bennett, R. T., Cowen, M., Tentzeris, V. and Sadofsky, L. R. (2022). Detection of Microplastics in Human Lung Tissue Using Muftir Spectroscopy. *Sci Total Environ* **831**, 154907.

Keibel, F. and Abraham, K. (1900). Normentafeln Zur Entwicklungsgeschichte Des Huhnes (Gallus Domesticus). In *Normentafeln zur Entwicklungsgeschichte der Wirbelthiere.* (ed F. Keibel), pp. 132p. Jena: Fischer.

Kelpsiene, E., Torstensson, O., Ekvall, M. T., Hansson, L.-A. and Cedervall, T. (2020). Long-Term Exposure to Nanoplastics Reduces Life-Time in Daphnia Magna. *Scientific Reports* **10**, 5979.

Keyte, A. and Hutson, M. R. (2012). The Neural Crest in Cardiac Congenital Anomalies. *Differentiation* **84**, 25-40.

Kihara, S., Ashenden, A., Kaur, M., Glasson, J., Ghosh, S., van der Heijden, N., Brooks, A. E., Mata, J. P., Holt, S. and Domigan, L. J. (2021). Cellular Interactions with Polystyrene Nanoplastics—the Role of Particle Size and Protein Corona. *Biointerphases* **16**, 041001.

Kim, L., Cui, R., Il Kwak, J. and An, Y.-J. (2022). Trophic Transfer of Nanoplastics through a Microalgae–Crustacean–Small Yellow Croaker Food Chain: Inhibition of Digestive Enzyme Activity in Fish. *Journal of Hazardous Materials* **440**, 129715.

Kirby, M. L. (1999). 11 - Contribution of Neural Crest to Heart and Vessel Morphology. In *Heart Development* (ed. R. P. Harvey & N. Rosenthal), pp. 179-193. San Diego: Academic Press.

Kirby, M. L., Creazzo, T. L. and Christiansen, J. L. (1989). Chronotropic Responses of Chick Atria to Field Stimulation after Various Neural Crest Ablations. *Circ.Res.* **65**, 1547-1554.

Kirby, M. L., Tumage, K. L. and Hays, B. M. (1985). Characterization of Conotruncal Malformations Following Ablation of Cardiac Neural Crest. *Anatomical Records* **213**, 87-87.

Kirby, M. L. and Waldo, K. L. (1995). Neural Crest and Cardiovascular Patterning. *Circ.Res.* **77**, 211-215.

Knezevic, V., De Santo, R. and Mackem, S. (1998). Continuing Organizer Function During Chick Tail Development. *Development* **125**, 1791-1801.

Koelmans, A. A., Nor, N. H. M., Hermsen, E., Kooi, M., Mintenig, S. M. and De France, J. (2019). Microplastics in Freshwaters and Drinking Water: Critical Review and Assessment of Data Quality. *Water research*.

Le Douarin, N. M., Couly, G. and Creuzet, S. E. (2012). The Neural Crest Is a Powerful Regulator of Pre-Otic Brain Development. *Dev Biol* **366**, 74-82.

Le Douarin, N. M. and Kalcheim, C. (1999). *The Neural Crest*. Cambridge: Cambridge University Press.

Lee, W. S., Kim, H., Sim, Y., Kang, T. and Jeong, J. (2022). Fluorescent Polypropylene Nanoplastics for Studying Uptake, Biodistribution, and Excretion in Zebrafish Embryos. *ACS Omega* **7**, 2467-2473.

Leslie, H. A., van Velzen, M. J. M., Brandsma, S. H., Vethaak, A. D., Garcia-Vallejo, J. J. and Lamoree, M. H. (2022). Discovery and Quantification of Plastic Particle Pollution in Human Blood. *Environ Int* **163**, 107199.

Madrid, L., Vyas, K. J., Kancherla, V., Leulseged, H., Suchdev, P. S., Bassat, Q., Sow, S. O., El Arifeen, S., Madhi, S. A., Onyango, D., et al. (2023). Neural Tube Defects as a Cause of Death among Stillbirths, Infants, and Children Younger Than 5 Years in Sub-Saharan Africa and Southeast Asia: An Analysis of the Champs Network. *The Lancet Global Health*.

Martik, M. L. and Bronner, M. E. (2021). Riding the Crest to Get a Head: Neural Crest Evolution in Vertebrates. *Nature Reviews Neuroscience* **22**, 616-626.

Nie, J.-h., Shen, Y., Roshdy, M., Cheng, X., Wang, G. and Yang, X. (2021). Polystyrene Nanoplastics Exposure Caused Defective Neural Tube Morphogenesis through Caveolae-Mediated Endocytosis and Faulty Apoptosis. *Nanotoxicology*, 1-20.

Pitt, J. A., Trevisan, R., Massarsky, A., Kozal, J. S., Levin, E. D. and Di Giulio, R. T. (2018). Maternal Transfer of Nanoplastics to Offspring in Zebrafish (Danio Rerio): A Case Study with Nanopolystyrene. *Sci Total Environ* **643**, 324-334.

Ragusa, A., Svelato, A., Santacroce, C., Catalano, P., Notarstefano, V., Carnevali, O., Papa, F., Rongioletti, M. C. A., Baiocco, F., Draghi, S., et al. (2021). Plasticenta: First Evidence of Microplastics in Human Placenta. *Environ Int* **146**, 106274.

Ramsperger, A., Narayana, V. K. B., Gross, W., Mohanraj, J., Thelakkat, M., Greiner, A., Schmalz, H., Kress, H. and Laforsch, C. (2020). Environmental Exposure Enhances the Internalization of Microplastic Particles into Cells. *Science Advances* **6**, eabd1211.

Shook, D. and Keller, R. (2003). Mechanisms, Mechanics and Function of Epithelial-Mesenchymal Transitions in Early Development. *Mech Dev* **120**, 1351-1383.

Smits-van Prooije, A. E., Poelmann, R. E., Gesink, A. F., van Groeningen, M. J. and Vermeij-Keers, C. (1986). The Cell Surface Coat in Neurulating Mouse and Rat Embryos, Studied with Lectins. *Anat Embryol (Berl)* **175**, 111-117.

Taneyhill, L. A. and Schiffmacher, A. T. (2017). Should I Stay or Should I Go? Cadherin Function and Regulation in the Neural Crest. *Genesis* **55**.

Torres-Ruiz, M., De la Vieja, A., de Alba Gonzalez, M., Esteban Lopez, M., Castaño Calvo, A. and Cañas Portilla, A. I. (2021). Toxicity of Nanoplastics for Zebrafish Embryos, What We Know and Where to Go Next. *Science of The Total Environment* **797**, 149125.

Vighi, M., Bayo, J., Fernández-Piñas, F., Gago, J., Gómez, M., Hernández-Borges, J., Herrera, A., Landaburu, J., Muniategui-Lorenzo, S. and Muñoz, A.-R. (2021). Micro and Nano-Plastics in the Environment: Research Priorities for the near Future. *Reviews of Environmental Contamination and Toxicology Volume 257*, 163-218.

Waldo, K., Miyagawa-Tomita, S., Kumiski, D. and Kirby, M. L. (1998). Cardiac Neural Crest Cells Provide New Insight into Septation of the Cardiac Outflow Tract: Aortic Sac to Ventricular Septal Closure. *Dev.Biol.* **196**, 129-144.

Waldo, K., Zdanowicz, M., Burch, J., Kumiski, D. H., Stadt, H. A., Godt, R. E., Creazzo, T. L. and Kirby, M. L. (1999). A Novel Role for Cardiac Neural Crest in Heart Development. *J Clin Invest* **103**, 1499-1507.

Wang, M., Rücklin, M., Poelmann, R. E., de Mooij, C. L., Fokkema, M., Lamers, G. E. M., de Bakker, M. A. G., Chin, E., Bakos, L. J., Marone, F., et al. (2023). Nanoplastics Causes Extensive Congenital Malformations During Embryonic Development by Passively Targeting Neural Crest Cells. *Environment International* **173**, 107865.

Yan, Y., Wang, G., Huang, J., Zhang, Y., Cheng, X., Chuai, M., Brand-Saberi, B., Chen, G., Jiang, X. and Yang, X. (2020). Zinc Oxide Nanoparticles Exposure-Induced Oxidative Stress Restricts Cranial Neural Crest Development During Chicken Embryogenesis. *Ecotoxicol Environ Saf* **194**, 110415.

Yin, K., Wang, Y., Zhao, H., Wang, D., Guo, M., Mu, M., Liu, Y., Nie, X., Li, B., Li, J., et al. (2021). A Comparative Review of Microplastics and Nanoplastics: Toxicity Hazards on Digestive, Reproductive and Nervous System. *Science of The Total Environment* **774**, 145758.

Yong, C. Q. Y., Valiyaveettil, S. and Tang, B. L. (2020). Toxicity of Microplastics and Nanoplastics in Mammalian Systems. *International Journal of Environmental Research and Public Health* **17**, 1509.

Zhang, J., Wang, L. and Kannan, K. (2020). Microplastics in House Dust from 12 Countries and Associated Human Exposure. *Environment International* **134**, 105314.

Zhao, L., Qu, M., Wong, G. and Wang, D. (2017). Transgenerational Toxicity of Nanopolystyrene Particles in the Range of Mg L− 1 in the Nematode Caenorhabditis Elegans. *Environmental Science: Nano* **4**, 2356-2366.

Zhao, Q., Zhu, L., Weng, J., Jin, Z., Cao, Y., Jiang, H. and Zhang, Z. (2023). Detection and Characterization of Microplastics in the Human Testis and Semen. *Science of The Total Environment* **877**, 162713.

Zolotova, N., Kosyreva, A., Dzhalilova, D., Fokichev, N. and Makarova, O. (2022). Harmful Effects of the Microplastic Pollution on Animal Health: A Literature Review. *PeerJ* **10**, e13503.

Nederlandse Samenvatting

Plastic producten hebben ons dagelijks leven veel voordelen opgeleverd. Helaas wordt 60% van het plastic op vuilnisbelten gestort of komt als plastic afval in het milieu terecht (Geyer et al. 2017). Dit afval laat langzaam kleine plastic deeltjes vrij, die op basis van hun grootte worden onderverdeeld in microplastics en nanoplastics (MP's en NP's). Deze micro- en nanoplastic deeltjes zijn alomtegenwoordig in het milieu en vormen een potentieel gevaar voor dieren en mensen (Allen et al. 2022; Zolotova et al. 2022).

Van MP's en NP's is aangetoond dat ze in zebravissen worden overgedragen van moeder naar haar larven (Pitt et al. 2018). Bovendien kunnen ze zich zelfs via voedselwebben verspreiden (Chae et al. 2018; Kim et al. 2022). Van MP’s en NP's wordt vermoed dat ze een potentieel gezondheidsrisico kunnen vormen voor de mens vanwege de toxiciteit in celculturen (Aguilar-Guzmán et al. 2022; Cortés et al. 2020; Gopinath et al. 2021; Ramsperger et al. 2020), en het feit dat ze gedetecteerd zijn in lichaamsvloeistoffen van meerdere menselijke weefsels (Jenner et al. 2022; Leslie et al. 2022; Ragusa et al. 2021; Zhao et al. 2023). Indirect bewijs van mogelijke toxiciteit voor mensen is het feit dat kleine plastic deeltjes giftig zijn in verschillende diermodellen (Yin et al. 2021; Yong et al. 2020). De toxiciteit van MP's en NP's is bijvoorbeeld uitgebreid bestudeerd bij waterdieren, waaronder Daphnia magna (Abdolahpur Monikh et al. 2020; Kelpsiene et al. 2020) de zebravis (Danio rerio) (Lee et al. 2022; Torres-Ruiz et al. 2021) en de Japanse oester (Crassostrea gigas) (Cole en Galloway 2015). Er is echter weinig bekend over het potentiële risico voor warmbloedige gewervelde dieren.

In **Hoofdstuk 1** hebben we de huidige kennis over MP's en NP's en hun potentiële risico voor de mens samengevat. Daarnaast hebben we in de literatuur gezocht naar het gebruik van het kippenembryo als model voor het testen van toxische stoffen en dan vooral het effect op de embryonale ontwikkeling. Kippenembryo's zijn inderdaad

al gebruikt voor verschillende toxiciteitsstudies van nanodeeltjes, met name metaal- en koolstofdeeltjes.

In **Hoofdstuk 2** heb ik laten zien dat PS-NP's (polystyreen-nanoplastics) neurale buis defecten kunnen veroorzaken in de kop, romp, staart of een combinatie van deze gebieden in het kippenembryo. De neurale buis defecten worden veroorzaakt door het falen van de van de neurale buis sluiting (Greene en Copp 2014), wat leidt tot verhoogde morbiditeit en mortaliteit (Copp en Greene 2010; Madrid et al. 2023). Wij suggereren het falen van deze sluiting te wijten is aan toxische effecten van PS-NP's op de neurale lijst cellen - een populatie van neuro-ectodermale cellen grenzend aan de fusiezone van de sluitende neurale buis (Creuzet 2009; Green et al. 2015; Le Douarin et al. 2012; Le Douarin en Kalcheim 1999; Martik en Bronner 2021; Waldo et al. 1998). Dit model (dat we samenvatten in Fig. 1) komt overeen met een studie die aantoont dat de neurale lijst essentieel is voor het sluiten van de neurale buis, althans in het craniale gebied (Creuzet 2009; Creuzet et al. 2006; Wang et al. 2023).

Vervolgens hebben we in **Hoofdstuk 3** het eerste bewijs geleverd dat blootstelling van kippenembryo's aan PS-NP's hartafwijkingen kunnen veroorzaken. We hebben met name cardiovasculaire misvormingen gedetecteerd, waaronder ventriculair septumdefect, overtollige slagaders, blijvende truncus arteriosus, abnormale bloedvaten en overtollige cardiale gelei. Bovendien hebben we aangetoond dat PS-NP's een verminderde hartfunctie veroorzaken. Deze bevindingen zijn logisch in het licht van eerdere rapporten dat neurale lijstcellen een essentiële rol spelen bij de cardiovasculaire ontwikkeling (Le Douarin en Kalcheim 1999). Nadat bijvoorbeeld neurale lijstcellen chirurgisch waren verwijderd, vertoonde het resulterende embryofenotype cardiovasculaire afwijkingen (Keyte en Hutson 2012; Kirby en Waldo 1995; Waldo et al. 1999).

Naast de cardiovasculaire misvormingen beschreven in **Hoofdstuk 3**, hebben we ook craniofaciale defecten opgemerkt in de behandelde embryo's. Deze defecten omvatten misvorming (hypoplasie of aplasie) van de bovensnavel en het falen van

Meckel's kraakbeen om te fuseren met zijn contralaterale partner. Deze misvormingen kunnen, net als de andere hierboven, ook worden verklaard door het effect van NP's op de neurale lijstcellen. Dit komt doordat neurale lijstcellen een essentiële rol spelen bij de craniofaciale ontwikkeling (Martik en Bronner 2021).

De waarneming van zowel cardiovasculaire als craniofaciale defecten komen overeen met het concept van een 'cardiocraniofaciale module' (Gans en Northcutt 1983; Keyte en Hutson 2012; Martik en Bronner 2021) die voor zijn normale ontwikkeling afhankelijk is van de neurale lijstcellen. Opmerkelijk is dat eerder is aangetoond dat de blootstelling van kippenembryo's aan metalen nanodeeltjes (zinkoxide) craniofaciale afwijkingen veroorzaken, waarvan gesuggereerd werd dat ze het gevolg zijn van een verstoorde ontwikkeling van de neurale lijstcellen (Yan et al. 2020). We moeten voorzichtig zijn met het interpreteren van bovenstaande bevindingen, omdat veel soorten metalen nanodeeltjes ionen afgeven, en dus wordt de toxiciteit van zinkoxide-nanodeeltjes die in deze studie werd waargenomen niet noodzakelijkerwijs gemedieerd door dezelfde nanoplastische toxiciteit mechanismen. We merken ook op dat craniofaciale defecten die we hier hebben waargenomen niet noodzakelijkerwijs een weerspiegeling zijn van abnormale ontwikkeling van de neurale lijstcellen.

Bij enkele met NP behandelde embryo's was de staartknop hypoplastisch of aplastisch; één embryo vertoonde agenesie van de staart en phocomelia van de achterpoten (**Hoofdstuk 2 en 3**). We suggereren dat deze afwijkingen het effect zijn van PS-NP's die hechten aan de blootgestelde mesenchymale populaties aan het oppervlak van de primitieve streep van de staartknop. Tijdens gastrulatie en het proces van ingressie ondergaat het epitheel van het dorsale oppervlak een epitheel-mesenchymale overgang met plaatselijk verlies van de basale lamina (Bellairs 1986; Shook en Keller 2003). Dit proces is nog steeds actief tijdens het stadium waarin we de PS-NP's in het ei introduceerden (Knezevic et al. 1998).

Een andere potentiële bron van mesenchymale cellen in het caudale gebied, die kan worden beïnvloed door blootstelling aan PS-NP, is de overgang van primaire naar secundaire neurulatie, dit proces begint rond stadium 8 (Dady et al. 2014). Binding van de PS-NP's aan deze overgangs mesenchymcellen zou de grove dysplasie van de neurale buis in het caudale gebied van sommige embryo's kunnen verklaren (**Hoofdstuk 2 en 3**). We hebben embryo's blootgesteld aan PS-NP's in stadium 8. Zowel gastrulatie als neurulatie zijn nog steeds actief in dit stadium (Keibel en Abraham 1900).

In **Hoofdstuk 4** tonen onze experimenten, met fluorescerende PS-NP's toegevoegd aan levende embryo's, een sterke labelling in de neurale lijst, maar weinig of geen in andere weefsels (**Hoofdstuk 4**, Fig.4-1). Bovendien vinden we dat die fluorescentie binnen 2 uur in het cytoplasma wordt gezien en er na 6 uur nog steeds is. Deze experimenten moeten echter met de nodige voorzichtigheid worden geïnterpreteerd, omdat: afzonderlijke deeltjes van 25 nm te klein zijn om direct met optische microscopen te worden gevisualiseerd; en het is mogelijk dat de fluorescentie die we zagen gedeeltelijk te wijten was aan lekkage van het fluorochroom van de deeltjes. Het is in ieder geval duidelijk dat sterke fluorescentie specifiek wordt aangetroffen in neurale lijstcellen.

Onze TUNEL-labelexperimenten lieten verhoogde celdood zien in zowel de dorsale middellijn van de neurale buis (**Hoofdstuk 4**, Fig.4-7), als in ectopische klompjes cellen in het lumen van de neurale buis die we identificeerden als neurale lijstcellen met neurale lijst markers (**Hoofdstuk 4**, Fig.4-2 tot 4). Dezelfde markers identificeren ook een populatie van neurale lijstcellen in de dorsale middellijn van met PS-NP behandelde embryo's die niet zijn gemigreerd. We zien ook bewijs van verminderde migratie van neurale lijstcellen naar de pharyngale bogen wanneer TFAP2A-expressie wordt gebruikt als een marker voor migrerende cardiale neurale lijstcellen (**Hoofdstuk 3**, Fig.3-6).

Samen suggereren deze gegevens dat neurale lijstcellen na binding van PS-NP's beschadigd raken of celdood ondergaan en niet migreren (Fig. 5-1; (Wang et al. 2023). Kandidaat-mechanismen van PS-NP's celbeschadiging zijn: de denaturatie van eiwitten (Gopinath et al. 2019; Hollóczki en Gehrke 2019), en de accumulatie van PS-NP's in het cytoplasma, nadat ze zijn opgenomen door endocytose, en vervolgens weerstand bieden aan afbraak door lysosomale enzymen (Nie et al. 2021). Onze hypothese, dat PS-NP's de migratie van de neurale lijst remmen, komt overeen met experimenten met andere migrerende celtypen. Er is bijvoorbeeld aangetoond dat PS-NP's de migratie en verspreiding van geaggregeerde CT26-muizencarcinoomcellen in vitro onderdrukken (Beaune et al. 2019).

Uit ons onderzoek blijkt dat PS-NP's schadelijke effecten kunnen hebben op vroege kippenembryo's, waarbij ze een verscheidenheid van misvormingen veroorzaken. Uit onze resultaten blijkt dat de toxiciteit van PS-NP's te wijten is aan het feit dat ze zich richten op een specifieke subpopulatie van embryonale cellen. Deze doelgerichtheid is passief, in de zin dat PS-NP's sterk lijken te binden aan neurale lijstcellen en niet aan andere cellen. Het feit dat NP’s misvormingen in meerdere systemen veroorzaken is zorgwekkend; vooral gezien de uitgebreide blootstelling van mensen aan kleine plastic deeltjes in het milieu, de gerapporteerde aanwezigheid van kleine plastic deeltjes in menselijke weefsels en de huidige ontwikkeling van een nieuwe generatie nano-geneesmiddelen bedoeld voor medische therapieën.

In de toekomst zal het belangrijk zijn om het onderliggende mechanisme van de selectieve binding van nanoplastics aan neurale lijstcellen te onderzoeken. Eén hypothese is dat nanoplastics zich binden aan specifieke celadhesiemoleculen waarvan bekend is dat ze tot expressie worden gebracht door neurale lijst cellen, zoals cadherine 6B. Cadherine 6B wordt geassocieerd met epitheliale mesenchymale transformatie in zowel embryonale cellen als sommige kankercellen. Als deze hypothese wordt bevestigd, zou de bevinding bijdragen aan zowel ons begrip van de embryonale toxiciteit van nanoplastics als mogelijk ook aan het kankeronderzoek.

Curriculum vitae

Meiru Wang (王美儒) was born on 27th June, 1993 in the city of Changchun, Jilin Province, China. She completed her bachelor's degree in agriculture at the Dalian Ocean University, Dalian City, Liaoning Province, China. Because of her general interest in fish, she chose to focus on studying the nutrient composition of muscle from cultured and juvenile specimens of the River Beluga (*Huso dauricus*), a sturgeon, in the Key Laboratory of Hydrobiology in Dalian City, Liaoning Province, for her bachelor thesis and internship.

Meiru went on to conduct her master's study in the same field, also at Dalian Ocean University, starting in September, 2016. She chose to explore the seasonal and geographical variations of sediment from the Biliu Reservior, Liaoning Province, China, using 16s rDNA sequencing, for her master's thesis.

After her long and productive journey through Dalian Ocean university, Meiru was awarded a Chinese Scholarship Council (CSC) Ph.D. scholarship to study at the Institute of Biology, Leiden University under the supervision of prof. dr. Michael. K. Richardson, and the co-supervision of prof. dr. Martina G. Vijver. Her PhD project was entitled "Developmental effects of polystyrene nanoparticles in the chicken embryo".

List of publications

- **Wang, M**., Rücklin, M., Poelmann, R.E., de Mooij, C.L., Fokkema, M., Lamers, G.E.M., de Bakker, M.A.G., Chin, E., Bakos, L.J., Marone, F., Wisse, B.J., de Ruiter, M.C., Cheng, S., Nurhidayat, L., Vijver, M.G., Richardson, M.K. Nanoplastics causes extensive congenital malformations during embryonic development by passively targeting neural crest cells. *Environment International* 173, 107865.
- **Wang, M**., Zhao, W., Wei, J., Wang, S., & Xie, X. (2019). Acute effects of UVB radiation on the survival, growth, development, and reproduction of *Daphniopsis tibetana* Sars (Crustacea: Cladocera). *Environmental Science and Pollution Research*, *26*, 10916-10925.
- **Wang, M.**, Zhao, W., Wei, J., Li, C., Shi, Z., Chen, W. & Wang, H. (2019). Comparison of nutritional components in the muscle of cultured and wild juvenile fish of *Huso dauricus*. *Journal of Economic Animal*, 23, 139-143.
- **Wang, M**., Zhao, W., Jia, X., Wei, J., & Wang, S. (2018). Eco-toxicology effect on *Moina mongolica* Daday exposed to Cd^{2+}, Pb^{2+}, and Hg^{2+} by the food chain. *Environmental Science and Pollution Research*, 25, 16024-16036.
- Wei, J., Zhao, W., Wang, S., **Wang, M**., Wang, X., Ji, S., & An, H. (2018). Effect of temperature, salinity, and body length on the energy budget of *Daphniopsis tibetana* Sars (Cladocera: Daphniidae). *Journal of Oceanology and Limnology*, 36, 1812-1824.